2015

Development of mass spectrometry-based methods for the analysis of lipid isomers

Rachel Kozlowski
University of Wollongong

UNIVERSITY OF WOLLONGONG

Department of Chemistry

Development of Mass Spectrometry-based Methods for the Analysis of Lipid Isomers

Rachel Kozlowski

B.Sc., McGill University, 2006
M.Sc., University of Victoria, 2011

This thesis is presented as part of the requirements for the award of the Degree of
DOCTOR OF PHILOSOPHY
of the
University of Wollongong

March 2015

ABSTRACT

Glycerophospholipids, or phospholipids, are important biochemical components of many biological organisms. They are involved in many biochemical processes including signal transduction, serving as enzyme substrates for lipoprotein metabolism and serving as ligands for receptors and precursors of essential biomolecules; they are also intracellular traffickers of cholesterol as well as modulators of the immune system. Likely to fulfill these diverse functional roles, not only do phospholipids contain a variety of head groups attached to a glycerol backbone but even more diversity exists within the fatty acyl chain(s) that are attached to the same glycerol backbone. These differences can be very subtle as is the case with phospholipid *sn*-positional isomers or double bond positional isomers, where the position of the acyl chain(s) attached to the glycerol backbone or the double bond position(s) within these acyl chains can vary only slightly but have vastly different biochemical consequences. Despite this, little is known about the abundances, let alone the biochemical or evolutionary reasons for the existence of these phospholipid isomers in different biological tissues. This paucity of information exists, in part due to the lack of methods that are both specific and sensitive enough to be used to detect and quantify these phospholipid isomers [and others], especially in complex biological extracts. To this end, this thesis describes the development of a number of new analytical workflows that combine ozone-induced dissociation with analytical separations and direct desorption/ionization technologies for the rapid identification of isomeric lipids. The methods developed and described herein have combined liquid chromatography (LC) and desorption electrospray ionization (DESI) with ozonolysis and collision induced dissociation (CID) to develop LC-OzID, LC-CID/OzID and DESI-CID/OzID. This LC-OzID method has proven successful for the separation, identification and, to an extent, the quantification, of a number of phospholipid double bond positional isomers in complex biological samples. In a similar way, the LC-CID/OzID method described herein has proven successful for the separation and identification and to an extent, quantification, of several phospholipid *sn*-positional isomers. DESI-CID/OzID has proven a successful

technique for the rapid identification and detection of relative differences in phospholipid *sn*-positional isomer composition in complex biological extracts spotted on a surface but also sampled directly from tissue. Experimental results from DESI-CID/OzID experiments also support the likelihood that both complementary phospholipid *sn*-positional isomers are always present but at varied ratios in different tissues. Preliminary imaging data using DESI-CID/OzID demonstrate the great potential of this technique for imaging variations in phospholipid *sn*-positional isomer composition across different regions of a biological tissue.

ACKNOWLEDGEMENTS

To Todd Mitchell and Stephen Blanksby, thanks for being supportive of some of my many ideas. You were both good mentors to me in different ways, thanks for bestowing upon me some of your bounty of expertise. I always thought you made a great couple.

To the University of Wollongong, thanks for the scholarship you gave me, which vastly improved my knowledge of Australian wines.

To my lover, Martin Paine, who promised me he would never die and that he would marry me one day. Thanks for always being honest with me, and loving me even when it's difficult.

To the bookshelf gods, may this sacrifice be sufficiently pleasing to you so that this tome may come to collect many millimetres of dust on your sacred shelves for generations to come.

To all you non-believers, so long, and thanks for all the fish.

ABBREVIATIONS

CID	Collision-induced dissociation
DESI	Desorption electrospray ionization
ESI	Electrospray ionization
GC	Gas chromatography
HILIC	Hydrophilic interaction chromatography
HPLC	High-performance liquid chromatography
LC	Liquid chromatography
MALDI	Matrix assisted laser desorption ionization
MS	Mass spectrometry
MS/MS	Tandem mass spectrometry
MS^n	Tandem mass spectrometry
m/z	Mass-to-charge ratio
NP	Normal phase
OzID	Ozone-induced dissociation
PC	Phosphatidylcholine
sn	Stereospecific number
TIC	Total ion chromatogram
TLC	Thin layer chromatography
XIC	Extracted ion chromatogram

TABLE OF CONTENTS

LIST OF FIGURES

LIST OF TABLES

LIST OF SCHEMES

1 INTRODUCTION

1.1 Importance of Phospholipid Structure to Biochemical Function

Lipids in the average diet are primarily composed of triglycerides (TG) but also contain *ca.* 10% phospholipid content, which is largely comprised of phosphatidylcholine (PC) and phosphatidylethanolamine (PE). Shown in Figure 1.1, are the general structures of PC, PE and the five other major phospholipid classes, organized by headgroup: phosphatidylinositol (PI); phosphatidylserine (PS); phosphatidylglycerol (PG); phosphatidic acid (PA); and sphingomyelin (SM).

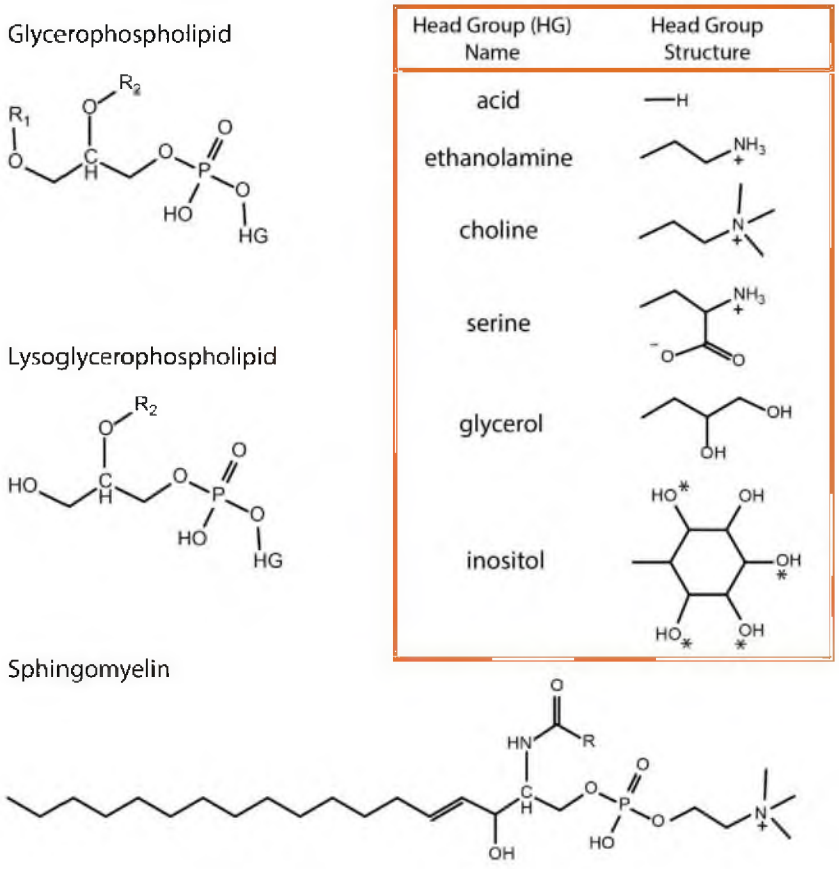

Figure 1.1 General Structures of Major Phospholipid Classes.

The general structure of major phospholipid classes. Phospholipids consist of a polar, hydrophilic head group, one or two hydrophobic acyl chain tail(s) and either a glycerol backbone, for glycerophospholipids, or a sphingosine backbone, in the case of sphingomyelin. The sites of acyl chain attachment are indicated by an R group – either R or R_1 and R_2 if two acyl chains are present. These acyl chain R groups usually

consist of a chain of carbon atoms that are either ester-linked or ether-linked to the glycerol backbone and may or may not include double bonds. In cases where two acyl chains are present, R_1 and R_2 can either represent the same acyl chain or different acyl chains. *Additional phosphate group(s) may be located at these locations of the inositol head group. This figure was adapted from a previous publication.[1]

Phospholipids are complex lipids that contain a headgroup, linked by a phosphate ester, in addition to one (lysophospholipid) or two (diacylphospholipid) acyl chains attached to a glycerol backbone. Thus they contain both a hydrophobic tail region and a hydrophilic head region. These structural characteristics are essential for their role as components of cell membranes – as they arrange into phospholipid bilayers with their hydrophobic tails facing each other and their hydrophilic head groups facing outwards towards the intra- and extra-cellular aqueous environments. Phospholipids also play an important role in nutrition and signal transduction for the maintenance and metabolic regulation of living cells.[2] For example, they serve as ligands for receptors, enzyme substrates for lipoprotein metabolism, second messengers in signal transduction, precursors of essential biomolecules, intracellular traffickers of cholesterol as well as modulators of the immune system.[3, 4] Individual phospholipid classes have also been associated with distinct biological effects. In studies in rabbits and rats, PC has been shown to enhance secretion of bile cholesterol and reduce both lymphatic cholesterol absorption and hepatic fatty acid synthesis.[5-7] Also in rats, PE and its head group base, ethanolamine, were linked to increased excretion of neutral steroids, such as cholesterol, in fecal matter, resulting in a cholesterol-lowering effect.[8, 9] In both rabbits and humans, phosphatidylinositol was shown to increase levels of beneficial high density lipoprotein (HDL)-cholesterol.[10, 11] Not only have distinct phospholipid classes been associated with important biological functions but so have individual phospholipids within a class.[12] Such examples have led to a renewed interest in more fully elucidating the molecular structure of lipids in complex biological extracts and the evolution of a structural hierarchy classification. An example of the different levels of structural definition for a single given phospholipid structure (1-hexadecanoyl-2-(5Z, 8Z, 11Z, 14Z-eicoosatetraenoyl)-*sn*-glycero-3-phospho-*L*-serine)

is shown in Figure 1.2. Naming conventions at each level of structural description were taken from the IUPAC IUBMB Joint Commission on Biochemical Nomenclature and the suggestions of Fahy *et al.* and Liebisch *et al.*[13, 14]

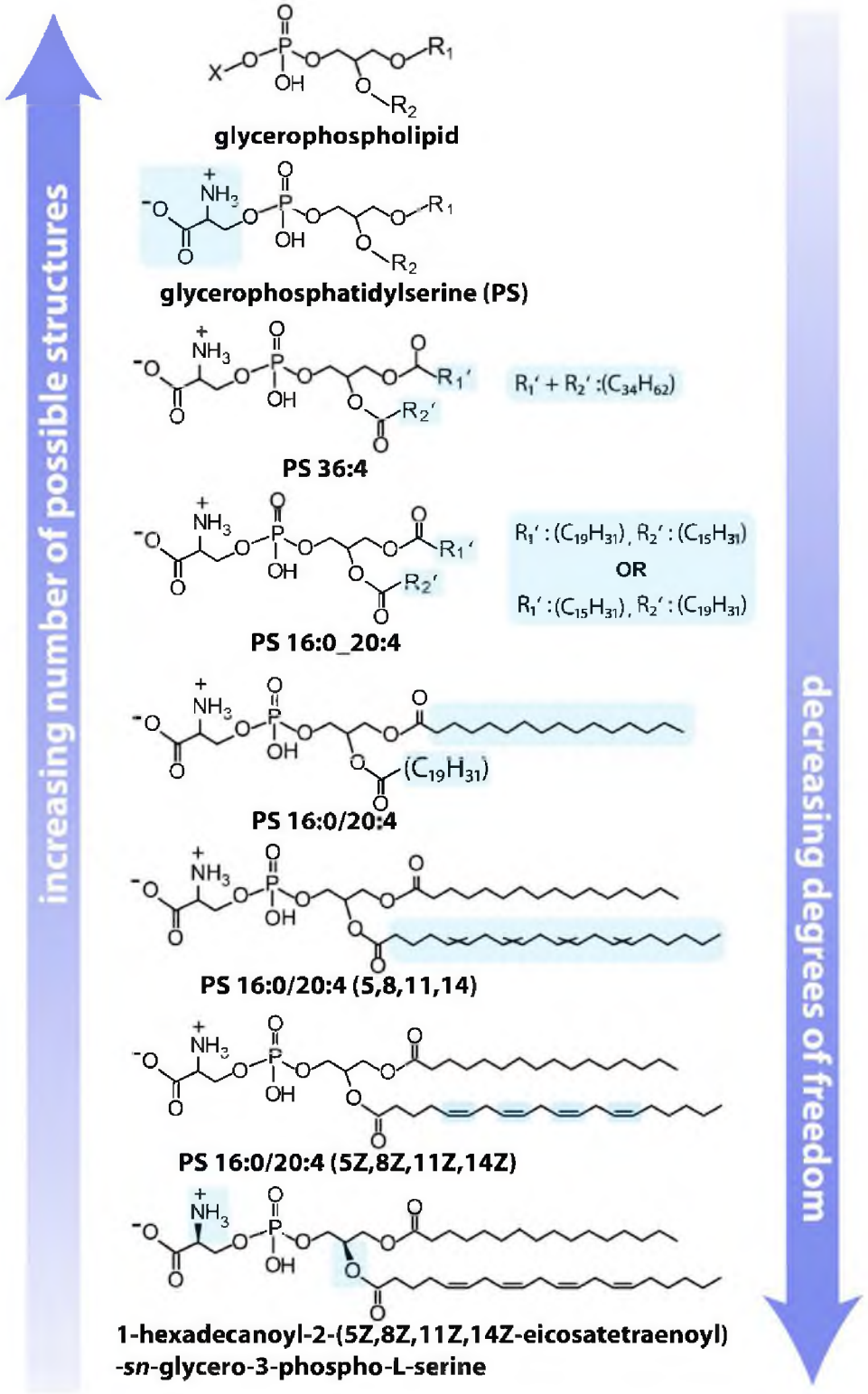

Figure 1.2 Phospholipid Structural Hierarchy

The structure of 1-hexadecanoyl-2-(5*Z*,8*Z*,11*Z*,14*Z*-eicoosatetraenoyl)-*sn*-glycero-3-phospho-*L*-serine and the structural classification groups relevant to it are shown.

Under each of these structural classes is the name for the level of known structure taken either from recommendation of IUPAC or from Liebisch *et al.*[13, 15] if only a partial structure is known. The portions of the phospholipid structure that have changed from one structural class level to the next are highlighted in blue.

As increased structural information is obtained from different analytical technologies, the molecular structure of phospholipids can be more explicitly defined and thus further classified according to the hierarchy of nomenclature shown in Figure 1.2. Moving from top to bottom of this figure, increased structural information obtained decreases the number of possible structures. Within a phospholipid headgroup class, phospholipids may be further grouped according to the sum composition of all fatty acids attached. For instance, within the glycerophosphatidylserine class (PS), this can be described as PS 36:4 - containing any combination of fatty acids with a combined total of 36 carbons and 4 double bonds. One possible fatty acid combination of PS 36:4, is PS 16:0_20:4 where the acyl chains comprise a 16-carbon saturated and a 20-carbon polyunsaturated substituent. The regiospecificity of the attachment of 16:0 and 20:4 chains to the glycerol backbone can then be defined. Thus, PS 16:0/20:4 is a sub-class of PS 16:0_20:4 meaning that 16:0 and 20:4 are found at the *sn*-1 and *sn*-2 position of the glycerol backbone, respectively, with the headgroup assumed to be at the *sn*-3 position. It should be noted, however, that without information about the absolute stereochemistry of the chiral centre on the glycerol backbone, the assumption that the headgroup is at the *sn*-3 position may not be correct. Knowledge of the double bond positions within the unsaturated acyl chain, enables the lipid to be described as PS 16:0/20:4 (5,8,11,14) – where the double bonds are said to be located at the 5th, 8th, 11th and 14th carbon (as counted from the ester end) of the fatty acid. Alternatively, the double bond position may be labelled by counting from the methyl end and placing the number of the first carbon involved in the double bond within brackets directly preceded by "*n*-" such that PS 16:0/20:4 (5,8,11,14) and PS 16:0/20:4 (*n*-6,*n*-9,*n*-12,*n*-15) would be structurally equivalent. The latter nomenclature will be used in Chapters 2 – 4 of this text and is otherwise noted elsewhere. The next possible level of molecular description is PS 16:0/20:4 (5*Z*,8*Z*,11*Z*,14*Z*) that explicitly

assigns the stereochemical configuration of all four double bonds as *cis* in this case. Lastly, the stereochemistries of the chiral centres present in the phospholipid are defined in the final sub-class, 1-hexadecanoyl-2-(5*Z*,8*Z*,11*Z*,14*Z*-eicosatetraenoyl)-*sn*-glycero-3-phospho-*L*-serine , which describes a single, unique molecular species.

These structural naming conventions arose from a growing need to more accurately identify specific levels of structural detail in order to incrementally strengthen the correlations between the phospholipid structural compositional differences and differences in other sample properties and the resultant conclusions.[16] This need is especially important when attempting to pinpoint biochemical differences and/or biological effects arising from subtle structural differences in a small subset of phospholipids - such as the position(s) of the acyl chain(s) on the glycerol backbone or the position(s) of the double bond(s) along the acyl chain(s). These seemingly minor structural differences have already been linked to detectable physicochemical and functional differences in biological systems as discussed further in Chapters 2 - 4.

Lipids with similar structures, indeed even isomers, that share identical elemental composition, have been associated with vastly different physiological outcomes. For instance, it is generally believed that fatty acid precursors with the final double bond at the *n*-6 position (often referred to as ω-6) are associated with chronic inflammatory effects while ω-3 fatty acid precursors are associated with resolving (anti-inflammatory) effects. These functional differences arise from subtle structural distinctions between lipid isomers that can be difficult to detect by modern analytical methods and are discussed in more detail in chapters 2 – 4. The structure of a biomolecule, *e.g.* a phospholipid, can provide significant insight into its biochemical function. It is therefore important to work towards complete structural elucidation in order to understand the distinct roles of very similar, yet structurally distinct, phospholipid isomers. Of concern to the studies outlined herein are double bond positional isomers and *sn*-positional isomers of phospholipids. Examples of each are shown in Figure 1.3.

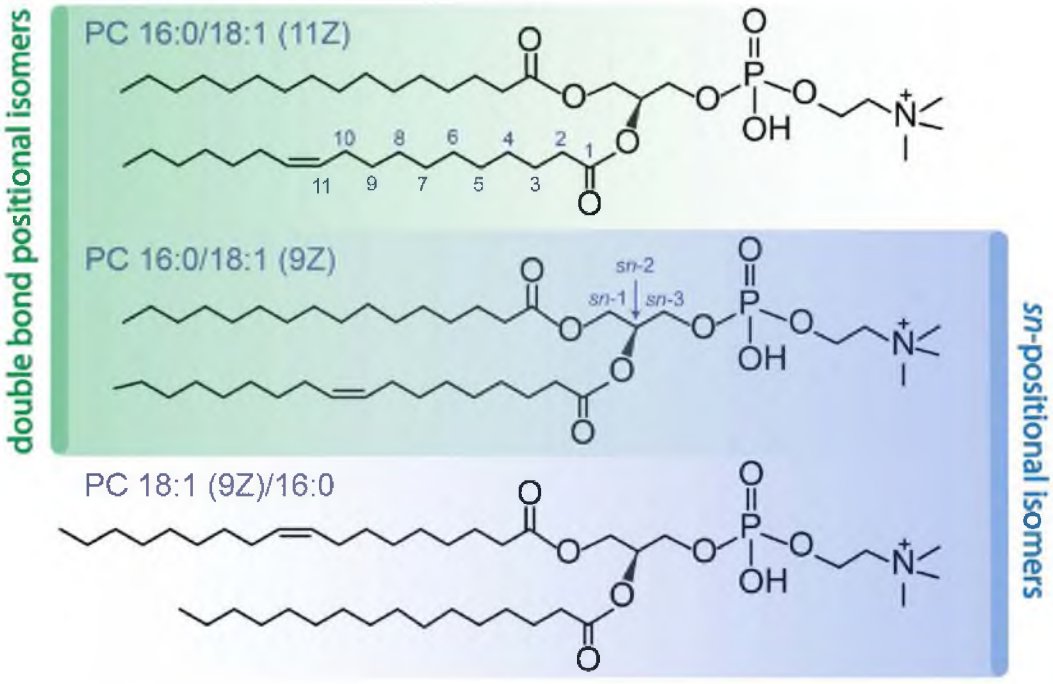

Figure 1.3 Phospholipid double bond positional isomers and *sn*-positional isomers.

The structures of a set of phospholipid double bond positional isomers and phospholipid *sn*-positional isomers are shown. Highlighted in green, the top and middle structures represent a pair of phospholipid double bond positional isomers. The topmost structure has a single double bond [named as being] at the 11th carbon (although, technically speaking, this double bond involves both the 11th and the 12th carbon) in the 18:1 acyl chain at the *sn*-2 position. For the middle structure, PC 16:0/18:1, the difference is the position of the double bond, named as belonging to the 9th carbon atom in the 18:1 acyl chain at the *sn*-2 position. Alongside the top structure, PC 16:0/18:1 (11Z), the carbon numbers of the acyl chain at the *sn*-2 position are labelled. For the middle structure, PC 16:0/18:1 (9Z), the *sn*-positions of the glycerol backbone are labelled. The middle and bottom structures, highlighted in blue, are an example of a pair of phospholipid *sn*-positional isomers. In the middle structure, the 18:1 (9Z) acyl chain is located at the *sn*-2 position and the acyl chain, 16:0, is located at the *sn*-1 position. For the bottom structure, this order is reversed so that the 18:1 (9Z) acyl chain is located at the *sn*-1 position while the 16:0 acyl chain is at the *sn*-2 position.

The top and middle phospholipid structures of Figure 1.3 are examples of a pair of phospholipid double bond positional isomers. At the top of this figure, PC 16:0/18:1 (11*Z*) is shown and in the middle, PC 16:0/18:1 (9*Z*). The difference in these two structures is the location of the double bond along the acyl chain - located between the 11th and 12th carbon and the 9th and 10th carbon, respectively. The carbon atoms

are labelled, in this way, on PC 16:0/18:1 (11*Z*) in Figure 1.3. The middle and bottom structure, PC 16:0/18:1 (9*Z*) and PC 18:1 (9*Z*)/16:0, respectively, are an example of a pair of *sn*-positional isomers. The stereochemical numbering of the carbon atoms of the glycerol backbone is presented on the middle phospholipid structure, PC 16:0/18:1 (9*Z*).

As more phospholipid structural detail is obtained, more confident conclusions about their functions may be ascertained. In order to better understand the different biological functions associated with specific phospholipid structural features, it is first important to develop technologies with the power to accurately identify (and quantify) these distinct phospholipid isomers in complex biological samples. This need has stemmed from the ever-growing pool of scientific research correlating phospholipid structural differences to biological differences and/or functional differences.[17] A deeper understanding of the importance of meeting the growing need for improved structural identification methods for phospholipids can be gained through a historical examination of phospholipid structural analysis.

1.2 Identification of Phospholipids

1.2.1 Elucidation of the General Structure of the First Phospholipid

Shortly after its discovery by Theodore Gobley, "lecithine" was defined in the mid 19th century as a phosphorus substance found within blood, chicken egg yolks and carp eggs that yielded oleic acid, margaric acid and phosphoglyceride upon decomposition with acid.[18] By the early 20th century, lecithin had developed a reputation as a "peculiar complex body" found in many biological tissues including vegetables, brain, nerve, blood, lymph, milk and pus, but most readily prepared from egg yolk.[19] Based on the widespread distribution of lecithin in many different biological samples as well as its occurrence in milk, it was assumed that lecithin played an important role in the body, and so the structure of lecithin quickly became a topic of interest for decades to follow.[19] Initially, elemental analyses of lecithins were performed in addition to testing the products of acid hydrolysis and/or saponification of phosphatides for functional groups. However, important structural details, for instance the way glycerol was bound to either two oleic, stearic or

palmitic acids within the molecule and the bonding of the phosphate or headgroup was unknown. In addition, the main elements of choline had been identified, but the connectivity of the three methyl groups and the hydroxyl group to the nitrogen was not known.[19] Approximately 10 years later, a structure for lecithin was proposed by Maclean showing the appropriate connectivity of acyl chains and a phosphoric acid "radicle" on a glycerol backbone with what was thought to be choline shown attached to the phosphoric acid.[20] However, the proposed structure of the headgroup attached to the phosphoric acid was not as we know it today – it was thought to contain an additional hydroxyl group bound to the nitrogen; it was also thought that the phosphocholine headgroup could be located at either the 2nd or 3rd carbon of the glycerol backbone.[20] The study of pure lecithin was extremely difficult prior to the advent of gas chromatography (GC) in the 1940's. Promptly following the discovery of lecithin though, distinctions were already being made between lecithin and a similar fatty compound containing nitrogen and phosphorus, named kephalin or cephalin, usually found together with lecithin but with decreased solubility in alcohol.[21] Discoveries of new, but similar compounds rapidly followed. In fact, after the discovery of both aminoethanol and serine in cephalin from brain, Folch and Schneider hypothesized that the brain may contain two types of cephalins, one containing ethanolamine and the other serine.[21, 22] In response to the discovery of these structurally-related compounds containing phosphorus and nitrogen, the term "phosphatides" was suggested to describe this group of compounds.[19] By the 1940's, the term "phospholipid" had been introduced in reference to lipids containing phosphorus, including lecithin, cephalin, sphingomyelin and glycerophosphoric acid.[23] While the discovery of new, related lipids and progress towards appropriate nomenclature was fast underway, progress towards the acceptance of the current general structure of lecithin was slow. The currently-accepted general structure of phosphatidylcholine had been proposed twice, once by the mid 1920's by Grün and Limpächer and later in the mid 1930's by Fischgold and Chain.[24, 25] However, this "endo-salt form" of lecithin, shown in Figure 1.4 (a), was not generally accepted - the competing "open formula" structure, shown in Figure 1.4 (b), was supported into the early 1950's by theoretical and experimental elemental composition data proposed

by Baer and Kates, contributing to the wide acceptance of the incorrect "open formula" structure that contained an additional oxygen and two additional protons for almost half a century.[26, 27]

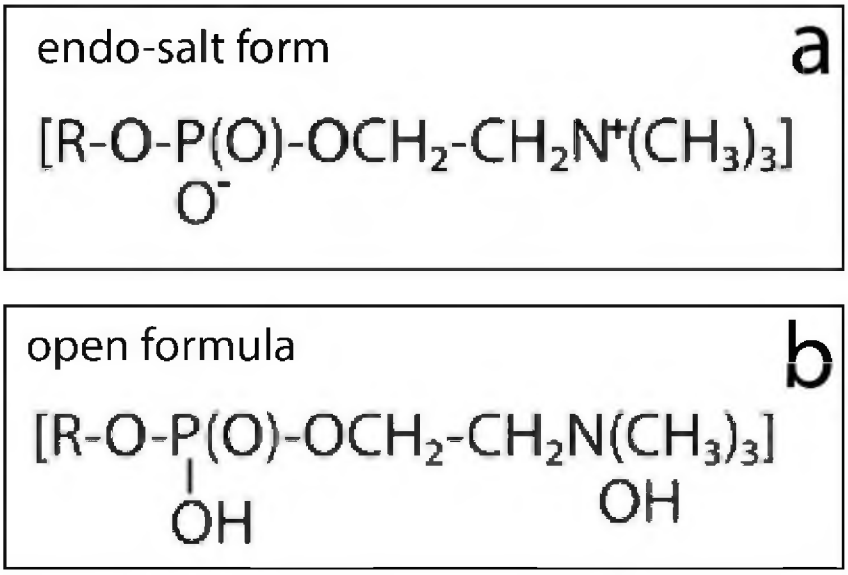

Figure 1.4 Phospholipid general structures proposed in the early 20th century.

The "endo-salt form" and the "open formula" for two proposed general structures of the phospholipid are shown in (a) and (b) respectively. This figure was created using information provided by previous publications.[26, 28]

In 1950, Baer showed that head group migration during hydrolysis may result in misleading data that would seem to support the phosphocholine headgroup position at either the 2nd or 3rd carbon of the glycerol backbone.[28] In doing so, he refuted the data existing at the time in support of the existence of phosphatidylcholines in nature containing a head group at the *sn*-2 position (β-lecithins).[28] By the mid 1960's the currently-accepted general structure of phosphatidylcholine had gained wide acceptance in the scientific community.[28-30] This general structure of phosphatidylcholine was further supported in 1979 by the publication of the first crystal structure of a lecithin dihydrate, 1,2-dimyristoyl-*sn*-glycero-3-phosphorylcholine.[31]

1.2.2 Classical Methods for Structural Analysis of Phospholipids

In the late 19th century, lecithin was thought to be a single molecule. Several years later, after a broader array of biological samples were tested, that view had expanded to include several possible structures of lecithin due to the discovery of several other fatty acid chains within lecithin. However, at this time, the extent of acyl chain variation within naturally-occurring phosphatidylcholines was unknown. Early in the 20th century, analysis of the fatty acid composition of lecithin in biological samples was nonspecific. That is, it was conducted by releasing all fatty acids from the parent compounds by either base hydrolysis (saponification) or acid hydrolysis and subsequent reaction of these released fatty acids with bromine and/or iodine.[32-34] The degree of unsaturation was determined by calculating the amount, in grams, of iodine that would react with 100 g of fatty acid (a quantity known as the iodine number) as well as calculating the percentage of bromine in bromine derivatives of fatty acids; bromine derivatives were then separated by successive steps of solubilization and/or precipitation in ether and petroleum to provide more specific information about the fatty acid structures.[33-35] The naturally-occurring polyunsaturated fatty acids corresponding to each bromine derivative could then be identified and their abundance estimated. In this way, newly-discovered fatty acids like arachidonic acid, 20:4, were identified in the lecithin of biological tissues of cow heart, hog brain and sheep brain.[33, 35] However, the diversity, let alone the stereochemistry, of fatty acids within lecithins remained largely uncharacterized at that time.

1.2.3 Lecithinase and Structural Analysis of Phospholipids

Progress began to unveil the structural diversity of phospholipids around the same time as the general structure of lecithin was being elucidated, with a discovery that was made while Kyes was working in the Ehrlich lab. Kyes found that a combination of lecithin and cobra venom, namely lecithid of venom, had haemolytic properties.[36, 37] This cobra venom could also be inactivated by heating for 30 mins at 100 °C.[37] This active component of cobra venom later came to be known as lecithinase. Kyes's discovery would soon unlock the door to fatty acyl

stereochemistry and diversity in phospholipids. He also pointed out that the solubility of this cobra lecithid in organic solvent differed from that of both lecithin and cobra venom, thereby confirming that cobra lecithid was a separate compound.[37] Shortly thereafter, Manwaring suggested that this lecithid was a partial hydrolysis product of lecithin and experiments conducted by Willstätter and Lüdecke, showed that lecithid of venom differed from lecithin by a single unsaturated fatty acid, and thus, lecithid was later known as lysolecithin.[32, 38] Prior to the 1960's, the action of the active component of snake venom, lecithinase A (later known as phospholipase A, then phospholipase A_2 (PLA_2)) was commonly believed to release unsaturated fatty acids from lecithins containing a mixture of saturated and unsaturated fatty acids.[39] However, both di-unsaturated and di-saturated lecithins were found to produce 1 mole each of fatty acid and lysolecithin by hydrolysis with lecithinase A, which led to the conclusion that the action of lecithinase A must be specific for one particular fatty acid position, either α' or β (*i.e.*, *sn*-1 or *sn*-2 respectively), of lecithin.[39] Whilst the general structure of lecithin was under debate, so was the specificity of snake venom lecithinase in 1960.[40] That would soon change when several experiments conducted in the early 1960's by Van Deenen and De Hass showed that lecithinase A from snake venom hydrolyzed fatty acids at the β-position (*sn*-2 position) of synthetic phosphatidylcholines almost exclusively.[41] Similarly, γ-benzyl-β-acyl-α-phosphoglyceride and a β-acyl-lysophosphoglyceride derivative were shown to be hydrolysed while the corresponding stereoisomers were not.[41] In addition, lecithinase A hydrolyzed *L*-α-phosphoglycerides but not *D*-α-phosphoglycerides, which also provided evidence in support of the stereospecificity of Lecithinase A for one stereoisomer of glycerol over its counterpart.[41]

1.2.4 Phospholipid Fatty Acyl Chain Stereochemistry

1.2.4.1 Development of the General Rule

The discovery of lecithinase in snake venom and the subsequent research into its specificity would have a significant impact on the structural analysis of phospholipids. By the 1950's, phospholipase A_2 was already being used in

conjunction with GC, liquid chromatography (LC) and thin layer chromatography (TLC) to examine the positional distribution of fatty acids in phospholipids of biological extracts, such as egg yolk.[39] In the 1960's, these same techniques were being applied to pork, spinach leaves, many bacterial species, human bile, human liver and chylomicrons, mink liver, cod flesh, mackerel, rat liver and more.[42-47] By the 1970's, the list of biological samples investigated in this way expanded to include spinach microsomes and chloroplast, cauliflower, mustard seed, cottonseed, sesame seed, groundnut, chicken embryo hepatocytes, mycoplasma and others.[48-51] Then in the 1980's, these types of analyses included taro, castor bean, tobacco, squash, tomato, pea, Japanese radish, dandelion, cabbage, oat, wheat and frog photoreceptor.[52-54] The list of phospholipids analyzed by phospholipase A_2 in combination with chromatography continued to grow at a rapid rate, however, the vast majority of these studies conducted prior to the 1990's, examined the pools of 1-acyl lysophospholipids alongside the pools of fatty acids released from the *sn*-2 position by phospholipase A_2. The majority of these studies found that the pools of fatty acids released from the *sn*-2 position were more highly unsaturated than the fatty acids still bound to the glycerol backbone at the *sn*-1 position as lysophospholipids. In many of these studies, this led to the assertion that the unsaturated fatty acid was usually found at the *sn*-2 position of phospholipids. Decades of these findings led to a tacit acceptance amongst lipid researchers that unsaturated fatty acids are found at the *sn*-2 position of a phospholipid. In fact, according to Lehninger's "Principles of Biochemistry", a popular undergraduate textbook, glycerophospholipids, in general, contain a C_{16} or C_{18} saturated fatty acid at *sn*-1 and a C_{18} or C_{20} unsaturated fatty acid at *sn*-2.[55] The significance of this trend however, is not widely understood. In one recent investigation, two phosphatidylcholine *sn*-positional isomers, 1-stearoyl-2-oleoyl-*sn*-glycero-3-phosphatidylcholine and 1-oleoyl-2-stearoyl-*sn*-glycero-3-phosphatidylcholine, were used to model the effect on membrane properties of placing the monounsaturated fatty acyl chain at the *sn*-1 and *sn*-2 positions, respectively.[56] Computation predicted that altering the position of the unsaturated fatty acyl chain from the *sn*-2 to the *sn*-1 position interfered with membrane cholesterol packing as well as phospholipid

bilayer membrane order.[56] This finding implies an importance to the location of the unsaturated acyl chain on the glycerol backbone to the structural integrity of the phospholipid bilayer.

1.2.4.2 Exceptions to the General Rule

It is important to recognize that the unsaturated fatty acyl chain is not always found at the *sn*-2 position of a phospholipid. For quite some time, researchers have been aware of the exceptions to the rule with discovery of numerous examples of glycerophospholipids with unsaturated fatty acids at the *sn*-1 position. By the mid 1960's, human lymph lecithins were shown to contain saturated fatty acids at the *sn*-2 position and unsaturated fatty acids at the *sn*-1 position.[44] Shortly thereafter, in 1967, Brockerhoff and Ackman stated that while saturated fatty acids always predominate at the *sn*-1 position and polyunsaturated at the *sn*-2 position of glycerophospholipids, the same rule does not hold for monounsaturates.[45] This was supported later in 1981 when a study of rat fetal lecithin revealed that the *trans*-polyunsaturated fatty acid, linoelaidic acid was found primarily at the *sn*-2 position while the *trans*-monounsaturated fatty acid, elaidic acid was found almost equally at *sn*-1 and *sn*-2.[52] However, this is not the only exception to the rule, as fatty acyl chain distribution can vary dramatically across different phospholipid classes. For instance, the polyunsaturated fatty acid, 18:3, was found predominantly at the *sn*-1 position in PG from plants such as taro, tomato, cabbage, spinach and oats while it was also found predominantly at the *sn*-2 position of PC from the same plants.[53] Several studies found that in some bacteria, the fatty acyl chain substitution order can be reversed as the saturated fatty acid, palmitic acid, was mainly located in the *sn*-2 position and unsaturated fatty acids, hexadecenoic acid and octadecenoic acid, at the *sn*-1 position.[46, 51, 57] In 1996, using PLA_2 enzymatic assays, soybean phospholipids were profiled and labelled such that phospholipids containing two saturated acyl chains were denoted "SS", two unsaturated acyl chains "UU", an unsaturated fatty acid at the *sn*-1 position with a saturated fatty acid at the *sn*-2 position "US" and a saturated fatty acid at the *sn*-1 position with an unsaturated fatty acid at the *sn*-2 position "SU".[58] The percentage composition of three phospholipid class reported, in

order of most to least abundant acyl chain composition, was as follows PC: UU>SU>>US>SS, PE: SU>UU>>SS>US, PI: SU>>SS>UU>US.[58] According to this study, the extent of the general rule claiming the unsaturated fatty acyl chain of a phospholipid usually present at the *sn*-2 position may depend on the phospholipid class and/or the type of biological sample analysed. This rule may not even hold true in all humans, as in 1997, the phospholipids of red blood cells from patients of sickle cell anaemia were found to contain fewer molecular species with polyunsaturated fatty acids at the *sn*-2 position.[59] More recently, the incorporation of four conjugated linoleic acid isomers into CHO and HepG2 cells was studied. This study found that while linoleic acid was preferentially incorporated into the *sn*-2 position over the *sn*-1 position approximately 80% of the time, for CLA isomers containing either two *cis* double bonds or one *cis* and one *trans* double bond, this preference was only 60%.[60] However, the CLA isomer, more closely resembling a saturated acyl chain with two double bonds in the *trans* configuration, was incorporated into the *sn*-2 position only 30% of the time.[60] This could be indicative of a biological preference for a specific fatty acyl chain configuration at the *sn*-2 position, rather than a preference for a higher degree of unsaturation at the *sn*-2 position. Research presented in Chapter 4 shows that glycerophosphatidylcholines are probably rarely present as a single *sn*-positional isomer and furthermore, the relative proportion of the two possible isomers can vary significantly between tissues and organisms.

1.2.5 Phospholipid Molecular Species using Chromatographic Approaches

A limitation of the phospholipase approach to assigning *sn*-positions for acyl chains in phospholipids is that, in general, they refer to trends across a crude extract or fraction and are thus blind to bonding arrangements in individual molecules. The first attempts towards a remedy to this problem were creative but somewhat laborious, as evidenced by the method developed in 1967 by Kuksis and Marai.[54, 61] Briefly, phospholipids extracted from egg yolk were separated into classes using silica gel TLC. Phosphatidylcholines were digested with phospholipase C to remove the head group, derivatized to form diglyceride acetates, separated by argentation TLC into groups according to degree of unsaturation and then analyzed by gas

chromatography. The molecular weights of the intact diglyceride acetates were obtained by GC analysis with tridecanoin as an internal standard. These diglyceride acetates were also hydrolyzed with pancreatic lipase, known to have phospholipase A_1 activity, thus releasing all fatty acyl chains present at the *sn*-1 position. This pool of free fatty acids from the *sn*-1 [and *sn*-3] position were analyzed [after derivatization] by GC along with the monoglycerides with a fatty acyl chain still attached at the *sn*-2 position. The underivatized phosphatidylcholines were also digested with phospholipase A_2. The resultant pool of free fatty acids released from the *sn*-2 position were derivatized [and analyzed by GC]. These datasets were then normalized and compared using algebraic manipulation so that phospholipid molecular species identities could be assigned based on a best-fit estimate. In the early 1980's, the major molecular species of PC and PE in frog photoreceptors was reported using this technique.[54] Later, the molecular species of human umbilical cord and vein endothelial cells were quantified using a similar approach.[62] Molecular species analysis of phospholipids in biological samples soon became the popular analytical method of phospholipids in biological samples in the 1990's. By the early 21st century, molecular species of phospholipids from human vein and umbilical artery cells, cow brain, cow liver, soybean and duck had been analyzed.[62-64] The term "molecular species" was used as a blanket term that described any phospholipids with known fatty acid compositions – even where the fatty acid substitution positions and/or the double bond positions within these fatty acids were not known.[65, 66] The study of phospholipids in complex biological samples had evolved in another way around this same time. Rather than phospholipid profiling alone, these phospholipid molecular species were being quantified and compared across biological samples with different treatment groups. The phospholipid molecular species profiles of multiple groups of related biological samples were analyzed including multiple strains of sunflower seeds.[67] The effect of modification of the diet on phospholipid composition was examined in dog retina in response to diets either poor or rich in ω-3 fatty acids, in humans in response to an antioxidant-enriched meal, as well as in chick tissues in response to dietary supplementation with conjugated fatty acids.[68-70] The effect of disease states (*i.e.*, sickle cell anaemia) on

phospholipid molecular species were also studied.[59] In 1996, the effect of stimulation by thrombin on the alterations in the molecular species of human platelet phospholipids was also studied.[71] By the early 2000's, the link between biosynthetic pathways and the composition of phospholipid molecular species was being researched.[72] For instance, in saccharomyces cerevisiae, saturated fatty acids were found predominantly at the *sn*-1 position, while for monounsaturated fatty acids, palmitoleate was found primarily at the *sn*-1 position but oleate was found mainly at the *sn*-2 position.[73] It was then proposed that, in yeast, PLA_2 mediated deacylation of phospholipids was followed by reacylation of the lysophospholipid to generate specific molecular species of phospholipids.[73] It is now known that 1-acyl *sn*-glycero-3-phosphocholine-*O*-acyltransferase, or lysolecithin acyltransferase, is responsible for transfer of a fatty acid to the *sn*-2 position of 1-acyl-glycero-3-phosphocholine while 2-acyl *sn*-glycero-phosphocholine-O-acyltransferase transfers a fatty acid to the *sn*-1 position of 2-acylglycero-3-phosphocholine; saturated fatty acids are preferentially transferred to 2-acylglycero-3-phosphocholine and unsaturated fatty acids are preferentially transferred to 1-acylglycero-3-phosphocholine.[74]

1.2.6 Technological Advancements for Structural Analysis of Phospholipids

By the late 1980's, technological advancements allowed for newer methods, electron spin resonance, nuclear magnetic resonance, infrared spectroscopy, X-ray scattering, differential scanning calorimetry and mass spectrometry, to be used to investigate phospholipid structural features including acyl chain conformation, acyl chain motion, acyl chain substitution position and the effect of acyl chain unsaturation and substitution position on physical properties of the phospholipid as well as higher-order structural properties like acyl chain order in phospholipid membranes and membrane dynamics and equilibrium.[75-78]

1.2.7 Liquid Chromatography and Mass Spectrometry of Phospholipids

1.2.7.1 LC-MS^n for Structural Analysis of Phospholipids

Although mass spectrometry (MS) had been used to study phospholipids prior to the 90's, it was during the early- to mid- 1990's that mass spectrometry became, and

remains today, the method of choice for structural analysis of phospholipids. This is evidenced by the shift in phospholipid analytical methods reported in the literature over time. This shift, occurred, in large part due to the development of electrospray ionization (ESI), which allowed LC to be used in conjunction with mass spectrometry. In doing so, ESI allowed the structure of intact phospholipids to be probed in interesting ways by mass spectrometry.[79, 80] This was a substantial step forward, as mass spectrometry offered improved sensitivity and specificity over other LC detection methods; for instance UV-absorbance and evaporative light scattering. In addition, it provided improved sample throughput, ease of sample preparation and a greater level of experimental flexibility, and as a result, a greater level of structural information. The natural propensity of these polar lipids to ionize, and exist stably as ions, makes these compounds well-suited for analysis by mass spectrometry. Multistage mass spectrometry (MS^n, where n indicates the number of stages) involves multiple stages of mass-to-charge-selection, usually staggered with multiple stages of fragmentation of the mass-selected precursor ion, to provide in-depth structural information about the initial analyte and its fragment ions. Multistage mass spectrometry has been used extensively for structural analysis of phospholipids. Though, on its own, mass spectrometry often proves insufficient for confident structural assignment when multiple phospholipid isomers or isobars are present in the same sample. To remedy this, mass spectrometry is often coupled with liquid chromatography (LC) for analysis of phospholipids in biological extracts. In this way, phospholipid isomers and isobars can be separated prior to identification using mass spectrometry. These LC, MS^n and combination LC-MS^n methods for the separation and/or identification of phospholipids have been comprehensively reviewed.[79, 81-98] In the simplest instance, Figure 1.5 illustrates how LC-MS^2 can be used to obtain structural information, but it is far from comprehensive. Shown in Figure 1.5 is the total ion chromatogram for a reversed-phase LC separation of an organic extract of sheep brain, the extracted ion chromatogram for *m/z* 760.5 (a) and the corresponding mass spectra for the peak at 64.4 min (b), 65.4 min (c) and 67.3 min (d). The $[M+H]^+$ and $[M+Na]^+$ precursor *m/z* values are labelled for PC 16:0_18:1 in panel (b) along with fragment ions corresponding to loss of the phosphocholine

headgroup, or portions thereof. Also labelled in panel (b) are fragment ions corresponding to the loss of acyl chains attached to the glycerol backbone. A comparison of the mass spectra shown in panels (b), (c) and (d) for the chromatographic peaks eluting at 64.4 min, 65.4 min and 67.3 min respectively, shows that there are no major differences in the MS^2 mass spectra to facilitate differentiation of these isomers. In addition, structural information is limited when using LC-MS^2 for identification of low abundance phospholipids. This observation is supported by the absence of *m/z* 478 and the low abundance of *m/z* 504 in the magnified region of the mass spectrum shown in panel (d) of Figure 1.5.

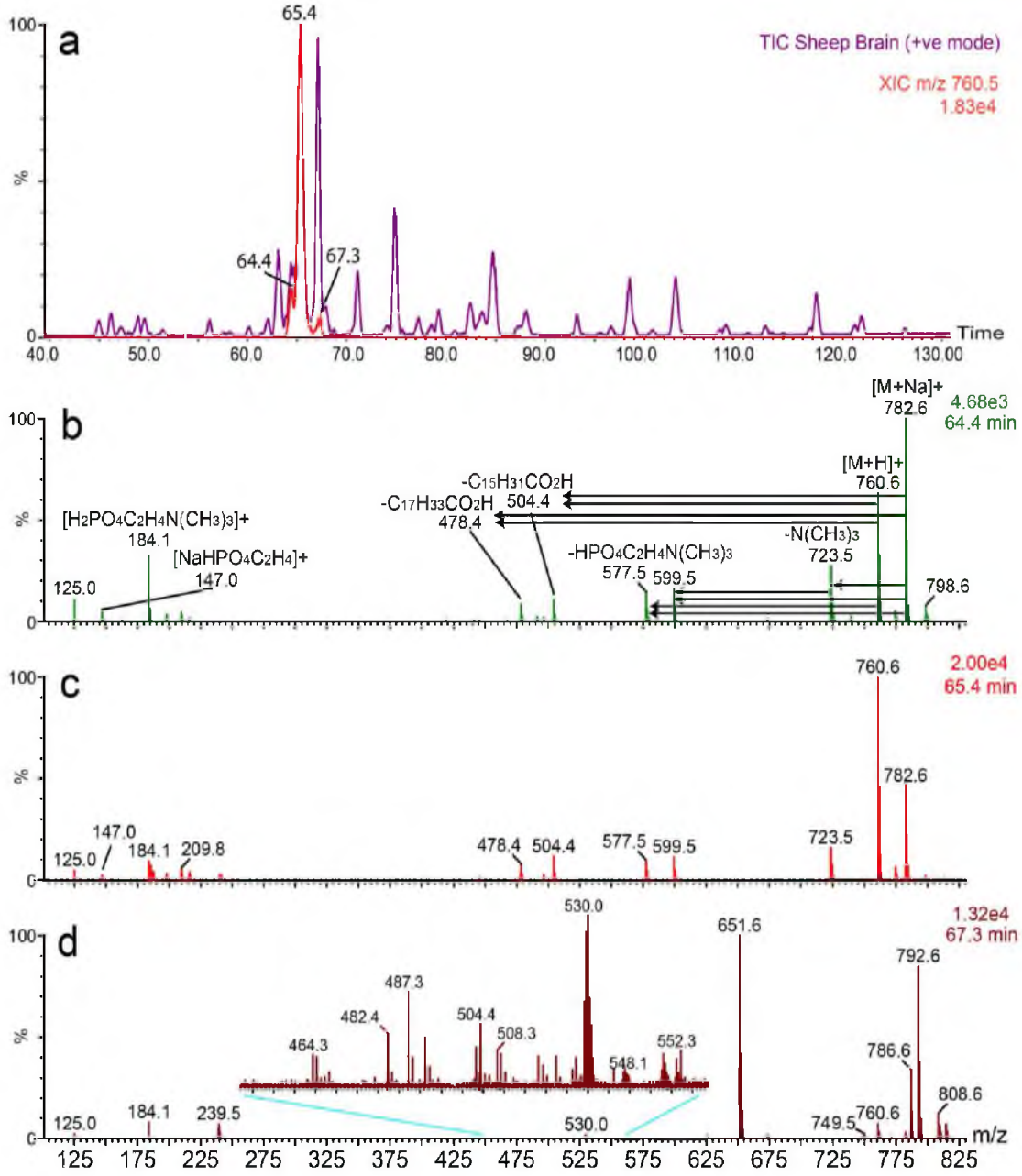

Figure 1.5 LC-MS^2 analysis of a sheep brain lipid extract.

The total ion chromatogram and extracted ion chromatogram for m/z 760.5 are overlaid for reversed phase chromatography of a sheep brain extract (a). The spectra corresponding to the chromatographic peaks at elution times of 64.4 min, 65.4 min and 67.3 min are shown in green (b) red (c) and maroon (d) respectively. Major structural ions of interest are labelled in panel (b). The maximum ion intensity is shown in the upper right hand corner of each panel.

Most pertinent to the research described herein, liquid chromatography can be used to separate the major phospholipid classes by head group polarity using either normal phase (NP) or hydrophilic interaction chromatography (HILIC), the latter being the more recently developed method.[82] However, the vast majority of chromatographic separations of phospholipids performed today are reversed phase or include a reversed phase separation step, as in two-dimensional LC separations of phospholipids. Reversed phase chromatography separates phospholipids primarily according to acyl chain hydrophobicity characteristics: acyl chain length, degree of unsaturation, double bond position, acyl chain conformation and/or acyl chain *sn*-position, for instance. A limited number of phospholipid double bond positional isomers and even fewer phospholipid *sn*-positional isomers have been separated using reversed phase chromatography (discussed in further detail in Chapters 2 and 3). As a result of decades of mass spectrometric analysis of phospholipids, the general fragmentation pathway of the main phospholipid classes, as well as many more minor classes, is well-understood for different adduct ions, in both positive and negative ion modes.[79, 90] The headgroup of a phospholipid and both fatty acid chains can be identified with relative ease using multistage mass spectrometry. However, there is not a single MS-based study in existence today that reports phospholipid abundances for individual, structurally distinct phospholipids and very few distinguish between phospholipid double bond positional isomers and/or phospholipid *sn*-positional isomers. This is due, in part, to the lack of methods specific, sensitive and simple enough for the confident structural identification of phospholipid isomers, especially in complex biological samples.

1.2.7.2 Mass Spectrometric Methods for Analysis of Double Bond Position in Phospholipids

Several mass spectrometric methods exist for the identification of double bond position in the acyl chain of a phospholipid (discussed in Chapter 2). While many of these methods are specific, many also generate complex spectra containing low abundance diagnostic ions and most are not very sensitive. The advantages and disadvantages of these pre-existing methods, contrasted with ozone-induced

dissociation (OzID) used here, are discussed in Chapter 2 and, again in the conclusions chapter. In general, these methods are not suitable for the identification of phospholipid double bond position in complex biological samples containing many phospholipid double bond positional isomers. OzID has been used to identify the double bond locations of phospholipid acyl chains by trapping phospholipids in the mass spectrometer with ozone. This approach is based on the gas-phase reaction of an ionised, unsaturated lipid with ozone in the ion-trapping region of a mass spectrometer.

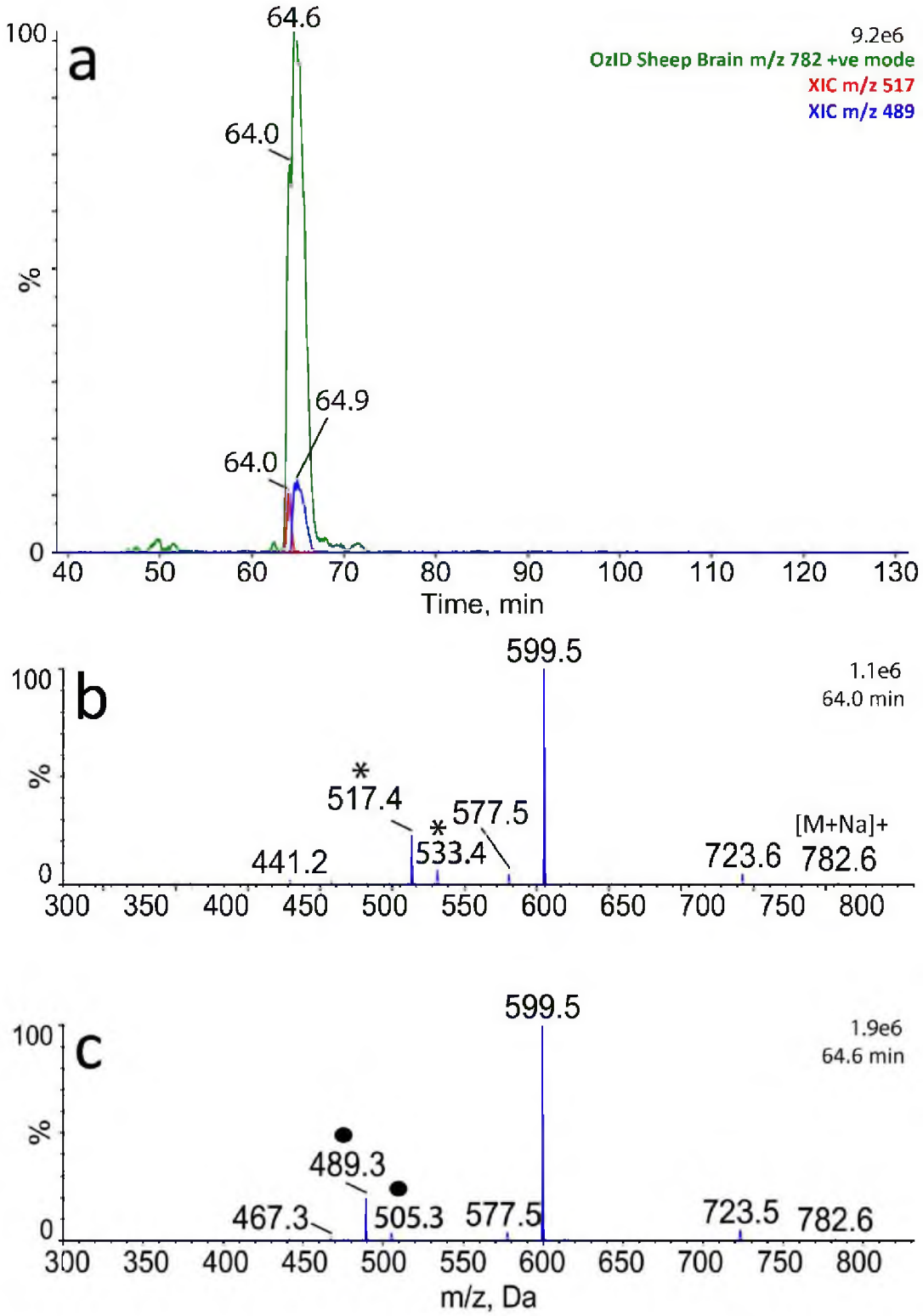

Figure 1.6 LC-OzID analysis of a sheep brain lipid extract.

The total ion chromatogram for the OzID scan for m/z 782 (green) and the extracted ion chromatograms for OzID ions m/z 517 (red) and 489 (blue) are overlaid for reversed phase chromatography of a sheep brain extract (a). The OzID spectra

corresponding to the chromatographic peaks at elution times of 64.0 min and 64.6 min are shown in the middle (b) and bottom (c) panels respectively. OzID ions indicative of a double bond at the n-7 position are labelled with an asterisk (b). OzID ions indicative of a double bond at the n-9 position are labelled with a circle (c). The maximum ion intensity is shown in the upper right hand corner of each panel.

Demonstrated in Figure 1.6 for LC-OzID analysis of a sheep brain extract, the reaction generates two diagnostic product ions from the ozonolysis of each carbon-carbon double bond. These are indicated with asterisks and circles in panels (b) and (c), and denote double bonds at positions *n*-7 and *n*-9, respectively. The extracted ion chromatograms for these diagnostic ions, *m/z* 517 and *m/z* 489, shown in panel (a) show that they are unique to each [partially] resolved chromatographic peak of the chromatogram. In comparison to Figure 1.5, showing LC-MS^2 of sheep brain extract, OzID generates abundant, diagnostic OzID ions indicative of double bond position, whereas this information is absent in the MS^2 spectra. This makes OzID more specific and sensitive with spectra that are easier to interpret for phospholipid mixtures. The presence of isobaric lipids in complex extracts means that when used in combination with direct infusion lipid mass spectrometry, OzID of an intact phospholipid ion alone does not permit confident assignment of double bond position. As a consequence, in this thesis the combination of LC and OzID is described for the first time (Chapter 2) and provides for the identification of double bond location of phospholipid acyl chains and differentiation of double bond positional isomers in complex biological samples.

1.2.7.3 Mass Spectrometric Methods for Analysis of Acyl Chain *sn*-position in Phospholipids

As previously demonstrated in Figure 1.5, conventional collision-induced dissociation (CID) mass spectra of ionised phospholipids often yield product ions characteristic of headgroup and acyl chain composition (*i.e.*, the number of carbons and degree of unsaturation of each chain). However, the *sn*-position of an acyl chain on the glycerol backbone of a phospholipid is more difficult to ascertain. Mass spectrometric approaches to determine the substitution position of an acyl chain on the glycerol backbone of a phospholipid are discussed in Chapters 3 and 4. Many of

these methods rely on calculating differences in ion abundance ratios – which can be affected by instrument parameters.[99, 100] Because each mass spectrometer may have different linear dynamic ranges, fragmentation methods, fragmentation energies and other parameters that can affect ion fragmentation, transfer and detection, using ion ratios or absolute ion intensities (or absolute peak areas) currently requires the use of a standard curve for each set of isomers analysed.[101] While some of these methods are more specific than others, even the best of these approaches becomes non-specific when highly unsaturated fatty acyl chains are found in the phospholipid, rendering these methods unsuitable for the identification and quantification of phospholipids in complex biological extracts. Thus, there is a need for improved methodology for the identification of *sn*-positional isomers in biological extracts. A recently-developed method that combines multistage mass spectrometry with ozonolysis (CID/OzID) is among the most specific and most sensitive of these methods.[102, 103] The combination of LC with CID/OzID for the separation and identification of phospholipid *sn*-positional isomers has been undertaken for the first time in this thesis and is discussed in Chapter 3. Also developed for the first time for simple, high-throughput analysis of phospholipid *sn*-positional isomeric composition in complex biological samples was DESI-CID/OzID, discussed in Chapter 4.

1.2.7.4 Mass Spectrometric Methods for Imaging of Phospholipid Isomers in Tissue

One of the drawbacks of using LC in combination with mass spectrometry is that, although a large number of phospholipids can be identified in a single chromatographic run, the overall analysis time is still relatively slow in comparison to direct infusion or desorption electrospray ionization (DESI). In addition, the optimization of LC parameters may also be time consuming. In order to meet the need for a high-throughput analytical method for relative quantification of phospholipid *sn*-positional isomers in complex biological extracts, DESI was combined with CID/OzID as described in Chapter 4 of this thesis. The instrumental setup used for DESI-CID/OzID of extracts is shown in Figure 8.1. However, the analysis of a biological sample as a liquid extract is not always ideal. This usually requires

homogenization and/or extraction of solid biological tissues prior to analysis. In doing so, spatial information about variation in relative abundance of phospholipid isomers across different regions of the tissue can be lost. As a result, in the last decade or so, phospholipid analysis has forayed into the field of mass spectrometry imaging (MSI). MSI of phospholipids, including three dimensional MSI, has generated much interest and has already been reviewed extensively.[104-113] Briefly, many of these methods identified phospholipids using mass spectrometers with accurate mass capabilities. However, this type of identification allows for the confident determination of elemental composition but not for the confident determination of molecular structure. Therefore, these methods could not distinguish between many types of phospholipid isomers, although phospholipid isomers are known to be present in many, if not all, biological tissues. In addition, these high mass accuracy imaging methods are often very slow requiring several seconds per scan. Even when faster, albeit less accurate, instrumentation was employed for MSI, these methods still could not distinguish between phospholipid isomers across different regions of an imaged tissue – including phospholipid double bond positional isomers and *sn*-positional isomers.[86] In fact, the vast majority of this phospholipid mass spectral imaging research did not employ tandem mass spectrometric techniques and thus, many lipid structural features cannot be confidently assigned. In order to work towards bridging this gap, DESI was successfully combined with CID/OzID for relative quantification of phospholipid *sn*-positional isomers across different regions of a brain tissue section, thus demonstrating the utility of CID/OzID for imaging applications. This is described in Chapter 4.

1.2.7.5 Summary of Technologies Developed and Discussed Herein for Phospholipid Analysis

A suitable method for the identification of double bond stereochemistry and chiral centre stereochemistry within intact phospholipids in complex biological samples currently does not exist. However, several methods for the analysis of double bond position and *sn*-position of acyl chains within intact phospholipids do exist. Nevertheless, these pre-existing methods are not well-suited for analysis of

phospholipids in complex biological samples, especially when phospholipids are present at low abundances in these samples and isomers are present. In order to work towards improving upon the lack of adequate methods available for complete structural elucidation of phospholipids in complex biological samples, LC-OzID has been developed to separate phospholipids and identify double bond position in complex biological samples (discussed in Chapter 2).[114] To the same end, LC-CID/OzID has been developed to separate phospholipids and identify phospholipid *sn*-position in complex biological samples (discussed in Chapter 3).[115]

Current methods used for structural identification of phospholipids do not match phospholipid isomeric variations with regions in tissue, involve time-consuming sample preparation procedures and/or lengthy analysis time making these methods unsuitable for high-throughput analysis of phospholipid isomers in complex biological samples and/or directly from biological tissues. In order to meet the need for a simple, fast way to analyze phospholipid structure, at the level of distinguishing between phospholipid *sn*-positional isomers, a simple, high-throughput DESI-CID/OzID method was developed for phospholipid isomeric analysis of complex biological extracts. Additionally, DESI-CID/OzID was used to monitor the changes in relative abundances of phospholipid *sn*-positional isomers across different regions of tissue, directly from tissue sections. Thus DESI-CID/OzID is very promising as an imaging technique for monitoring lipid isomeric compositions in different regions of tissues.[116] DESI-CID/OzID is discussed in Chapter 4.

2 COMBINING LIQUID CHROMATOGRAPHY WITH OZONE-INDUCED DISSOCIATION FOR THE SEPARATION AND IDENTIFICATION OF PHOSPHATIDYLCHOLINE DOUBLE BOND ISOMERS

2.1 Abstract

Revealing the inherent molecular diversity of lipid biology requires advanced analytical technologies. Distinguishing phospholipids that differ in the position(s) of carbon-carbon double bonds within their acyl chains presents a particular challenge because of their similar chromatographic and mass spectral behaviours. Here - for the first time - we combine reversed-phase liquid chromatography for separation of isomeric phospholipids with on-line mass spectral analysis by ozone-induced dissociation (OzID) for unambiguous double bond position assignment. The customised tandem linear ion-trap mass spectrometer used in our study is capable of acquiring OzID scans on a chromatographic timescale. Resolving the contributions of isomeric lipids, that are indistinguishable based on conventional mass spectral analysis, is achieved using the combination of liquid chromatography and OzID. Application of this method to the analysis of simple (egg yolk) and more complex (sheep brain) extracts reveals significant populations of the phosphatidylcholine PC 16:0_18:1(*n*-7) alongside the expected PC 16:0_18:1(*n*-9) isomer.

2.2 Introduction

At the cellular level, phospholipids are involved in numerous functions including; signalling, modulation of non-lipid biomolecules and maintaining the function and integrity of membranes, among other roles.[117-120] Phospholipids consist of a hydrophilic region (containing a phosphate-bound head group such as choline) connected to a hydrophobic region (containing a glycerol backbone to which two acyl chains are attached). Specific alterations in degree, and location(s) of unsaturation within the fatty acyl chains of phospholipids can alter their cellular functions.[121-123] The potential significance of variation in phospholipid double bond motifs necessitates the development of analytical tools capable of separating and identifying such variants in complex biological extracts.

Contemporary strategies for the separation and identification of phospholipids are focussed on the use of liquid chromatography (LC) generally coupled with mass spectrometry (MS). The use of hyphenated LC-MS techniques for phospholipid analysis has been reviewed and can be broadly classified by the application of either normal- or reversed-phase chromatography.[124, 125] Normal phase and hydrophilic interaction LC approaches exploit differences in polar regions of lipid structure and have thus been successfully deployed for the temporal segregation of phospholipids into different headgroup classes. This approach can aid in the quantification of lipids and can be useful in separating lipids of different classes that might share a common elemental composition (*e.g.*, phosphatidylcholines can be separated from isomeric phosphatidylethanolamines). Silver ion chromatography combines the affinity of silver ions for carbon-carbon double bonds with normal phase LC separation conditions. This approach can bring about separations based on differences in the degree, position and stereochemistry of unsaturation in lipids but is most generally successful for low-polarity lipids and has not been widely deployed in phospholipid analysis.[126-128] Reversed-phase LC uses non-polar stationary phases and can bring about separation of a wide variety of lipids, including phospholipids, based on structural differences in their hydrophobic acyl chains. Phospholipids possessing different acyl chain lengths and/or different numbers of double bonds, *e.g.*, phospholipid compositions of PC 36:1 and PC 36:2 can be routinely separated using reversed-phase techniques. Examples of separation of isomeric phospholipids that contain the same number of double bonds that are differentially distributed across the acyl chains, *e.g.*, PC 18:1_18:1 and PC 18:0_18:2, are also relatively common.[129-132] In contrast, analytical separations of phospholipid double bond positional isomers – where the acyl chains are themselves isomeric – by reversed-phase LC have proven more challenging. Prepared mixtures of two synthetic phosphatidylcholine double bond positional isomers, PC 18:1(*n*-9)/18:1(*n*-9) and PC 18:1(*n*-12)/18:1(*n*-12), have been successfully separated by reversed-phase LC using a C_8 column and, more recently, using charged surface hybrid C_{18} columns.[133, 134] While these analytical demonstrations are important, very few studies have differentiated between endogenous double bond positional isomers in

complex biological extracts. In one such example, Brouwers and co-workers extracted lipids from the parasitic worm, *S. Mansoni*, and subjected these extracts to two stages of chromatographic purification.[135] Initial lipid class fractionation using normal-phase LC was followed by interrogation of the phosphatidylcholine fraction on a C_{18} reversed-phase column with online detection by MS. These analyses revealed well-resolved chromatographic peaks corresponding to the phospholipid isomers PC 16:0_18:1(*n*-9) and PC 16:0_18:1(*n*-13) that differ only in the position of the double bond in the monounsaturated 18:1 acyl chain. The electrospray ionization (ESI) mass spectra of such isomeric lipids are identical, while tandem mass spectra obtained on most commercial instruments are also similar.[136] In order to identify the double bond positions within each isomer, Brouwers *et al.* collected fractions for each isomer and subjected them to further, offline interrogation including the use of high-energy collision-induced dissociation.[135] This study serves to highlight that chromatographic separation alone is insufficient for structure elucidation. Ideally, reliable methods for the identification of double bond location in phospholipids that can be achieved in real time with chromatographic separation of isomeric phospholipids should be developed.

Curtis and co-workers have implemented an ingenious approach to on-line lipid isomer analysis by using a gas-permeable membrane to allow ozone to interact with unsaturated lipids in the LC eluent prior to MS analysis.[137, 138] Ozone reacts with carbon-carbon double bonds to bring about oxidative cleavage and mass spectral analysis of the products enables the assignment of double bond position(s). Undertaking this same chemistry inside the mass spectrometer itself may have advantages in that the diagnostic products of ozonolysis can be attributed to a single, mass-selected population of ionized lipids. We have previously demonstrated that mass-selected ionized lipids react with ozone in the gas phase in a process referred to as ozone-induced dissociation (OzID).[139-141] The oxidative cleavage of carbon-carbon double bonds in the mass spectrometer gives rise to neutral losses that are characteristic of double bond position and can be used for structural assignment. OzID has previously been deployed in combination with direct infusion electrospray ionization protocols (*i.e.*, "shotgun lipidomics") to characterise lipids in

complex extracts derived from a range of sources including human ocular lens tissue, very-low density lipoprotein and insect pheromones.[142-144] The direct infusion approach – widely used in lipidomic workflows [90] – has the advantage of providing relatively long acquisition times for OzID but has the disadvantage, in some instances, of greater spectral complexity. It would be desirable therefore to be able to undertake OzID analysis within both direct infusion and LC-MS workflows with the later requiring significant re-optimisation of experimental protocols. Here, for the first time, we demonstrate the successful combination of OzID with reversed-phase LC for the separation and on-line identification of phospholipid double bond isomers. The method was optimized on simple binary mixtures of synthetic phospholipid isomers and then challenged by more complex biological extracts.

2.3 Materials and Methods

2.3.1 Materials

All solvents used, including water, were Optima LC-MS grade and purchased from Thermo Fisher Scientific (Scoresby, VIC, Australia). Formic acid (98% pure); sodium citrate (≥99% pure); and butylated hydroxytoluene (BHT) were purchased from Sigma-Aldrich (St. Louis, MO, USA). Ammonium acetate and sodium acetate (both analytical grade) were purchased from Ajax Chemicals (Auburn, NSW, Australia). Industrial-grade compressed oxygen was obtained from BOC (Cringila, NSW, Australia).

Synthetic phospholipid standards PC 18:1(*n*-12)/18:1(*n*-12) [1,2-di-(6*Z*-petroselinoyl)-*sn*-glycero-3-phosphocholine] and PC 18:1(*n*-9)/18:1(*n*-9) [1,2-di-(9*Z*-octadecenoyl)-*sn*-glycero-3-phosphocholine], were acquired from Avanti Polar Lipids (Alabaster, Alabama, USA). L-α-Phosphatidylcholine from chicken egg yolk was purchased from Sigma-Aldrich (St. Louis, MO, USA). Sheep brain was purchased frozen from Kieraville Butchery (Kieraville, NSW, Australia).

2.3.2 Sample Preparation

For direct infusion experiments used to optimize the mass spectrometer the lipid standard, PC 16:0/18:1(*n*-9), was dissolved to a final concentration of 30 µM in water/acetonitrile/2-propanol (50/25/25, v/v) with 1 mM sodium acetate. The working solution of egg yolk extract was prepared in the same manner with an estimated total PC concentration of 175 µM.

For chromatographic analyses, standards PC 18:1(*n*-9)/18:1(*n*-9) and PC 18:1(*n*-12)/18:1(*n*-12) were mixed at a 1:1 ratio and diluted to a final concentration of 40 µM each in water/acetonitrile/2-propanol (50/25/25, v/v). Egg yolk PC extract was prepared in the same way as for direct infusion experiments but without the addition of sodium acetate. The sheep brain was dissected to obtain one sample each of white matter and grey matter from the temporal lobe of the cerebrum. After dissection, 20-25 mg of each sample was processed using a bead homogenizer (FastPrep-24, MP Biomedical, Seven Hills, NSW, Australia) containing glass beads with

a 1 mm diameter. Total lipids were then extracted using methanol/chloroform according to a modified Folch extraction method.[142, 145] The lipid extracts from white and gray matter were pooled and the combined extract was washed 3 times with aqueous ammonium acetate (65 mM), dried under a stream of nitrogen and finally reconstituted with 750 µL of 2-propanol/acetonitrile (50/50, v/v). All prepared stock samples were stored at -80 °C until analysis.

2.3.3 Chromatography

All chromatography was performed using a Waters Acquity UPLC system (Waters, Milford MA, USA). For analysis of PC standards, mobile phase A was composed of water, formic acid (0.05%, v/v) with sodium citrate (50 µM) and mobile phase B was composed of acetonitrile/2-propanol (64/34, v/v), formic acid (0.05%, v/v) and sodium citrate (50 µM). For the analysis of egg yolk and sheep brain extracts, mobile phase A was composed of water with sodium acetate (100 µM) and mobile phase B was compsired of acetonitrile/2-propanol (75/25, v/v) with sodium acetate (100 µM).

Injections of the PC standard mixture (10 µL); PC egg yolk extract (7.5 µL); and sheep brain extract (7.5 µL) were loaded onto a reversed-phase Acquity C_{18} BEH column (1.7 µm, 150 mm x 1 mm I.D., Waters, Milford MA, USA). For the analysis of PC standards, the column was heated to 50 °C with a constant flow rate of 100 µL/min. A linear gradient was employed ramping mobile phase B from 40.0% to 99.9% over 60 min and then holding B at 99.9% B for 10 min before the column was re-equilibrated at 40% mobile phase B for 15 min. For the analysis of egg yolk PC extract and sheep brain extract, the flow rate was set to 125 µL/min. A linear gradient was employed ramping mobile phase B from 82.0% to 88.0% over 70 min and then holding mobile phase B at 99.9% for 5 min before the column was re-equilibrated for 15 min at 82% mobile phase B. All extracts were stored at 5 °C for the duration of the LC analyses and discarded after all LC analyses were complete.

2.3.4 Mass Spectrometry

Mass spectrometry was undertaken on a hybrid triple quadrupole linear ion-trap mass spectrometer (QTRAP 2000, AB SCIEX, Concord, ON, Canada) that has been modified for OzID experiments as previously described.[140] Minor adjustments were made to the online ozone delivery system and a schematic showing the configuration used in the present experiments is provided in the Supplementary Materials provided in Appendix A (see Figure 6.1). Ozone was generated from oxygen at *ca.* 170 g m^{-3} (normal) using an ozone generator (Titan 100 generator, Absolute Ozone, Edmonton Canada) at a constant flow of 0.2 L/min and was introduced via a variable leak valve (VSE Vacuum Technology, Lustenau, Austria).

All mass spectrometry was conducted in positive ion mode. For direct infusion electrospray ionization experiments, synthetic lipid standards dissolved in a solvent system comprised of water, acetonitrile and 2-propanol were infused at 8 µL/min with a declustering potential of 110 V and the source temperature was set to 70 °C. For on-line LC-MS protocols declustering potentials of 60 and 90 V and source temperatures of 200 and 350 °C were used for examining lipid standards and extracts, respectively (see LC methods above). Instrument parameters for OzID were controlled using a modified method file as previously described.[140] Typical conditons were: unit mass resolution on the first quadrupole (see Q1 in Supplementary Materials provided in Appendix A, Figure 6.1); pre-/post-reaction activation energies of 5/30 eV (except as noted); multi-channel acquisition was turned on; fill time for ions entering the collision cell (see q2 in Figure 6.1) was 50-200 ms with pre-/post-cell lenses (see lenses marked IQ2 and IQ3 in Figure 6.1) set to 25/100 V; and reaction time was 2000-4000 ms. For LC-MS analyses of biological samples, the alternating full scan (Q3 ion-trap scan) and OzID scans were undertaken thoughout the experiment.

2.3.5 Nomenclature

Lipid nomenclature used here is guided by the recommendations of the Lipid MAPS consortium and the recent suggestions of Liebisch *et al.* for mass spectrometry derived data.[13, 146] It is instructive for OzID analysis however, to annotate double bond position using the traditional nomenclature "*n*-x" where "n" refers to the number of

carbon atoms in the chain and subtracting "x" provides the location of the double bond relative to the methyl terminus.[15] For example, 18:1(9*Z*) becomes 18:1(*n*-9) and 18:1(11*Z*) becomes 18:1(*n*-7). Note that this nomenclature does not define the stereochemical configuration of the carbon-carbon double bond (*i.e.*, *cis* or *trans*): a structural feature not assigned by OzID without reference to standards.

2.4 Results and Discussion

2.4.1 Optimization of OzID Conditions

To optimize the mass spectrometry conditions for OzID, a solution containing a commercial egg yolk extract was infused directly into the ESI source operating in positive ion mode. Source and solution conditions were optimized for the production of, $[M+Na]^+$, sodium adduct ions of lipids as these have been shown previously to react more rapidly with ozone than protonated analogues.[147] Under these conditions, abundant ions at *m/z* 782 corresponding to the $[M+Na]^+$ ion of PC 34:1 were observed and subsequently mass-selected using the first quadrupole. The ions were transmitted to the collision cell where they were trapped in the presence of ozone for 2000 ms before being transferred to the linear ion trap for mass analysis. Representative OzID spectra obtained from the *m/z* 782 ion population are shown in Figure 2.1. Figure 2.1(a) was obtained using translational energies of 37 eV for ions entering the collision cell and the application of a post-reaction energy of 15 eV. Peaks corresponding to primary OzID ions are observed at *m/z* 672 and 688 (marked with a filled square, ■) corresonding to neutral losses of 110 and 94 Da, respectively, that are diagnostic for a carbon-carbon double bond at an *n*-9 position (see Supplementary Materials provided in Appendix A, Table 6.1).[136] In addition, a number of abundant ions arising from collision-induced dissociation (CID) are observed at *m/z* 723, 599 and 577 that are characteristic of the $[M+Na]^+$ ions of phosphatidylcholines.[148] Taken together, the combination of OzID and CID features in the spectrum allows the assignment of PC 16:0_18:1(*n*-9) as the major lipid at this mass-to-charge ratio.

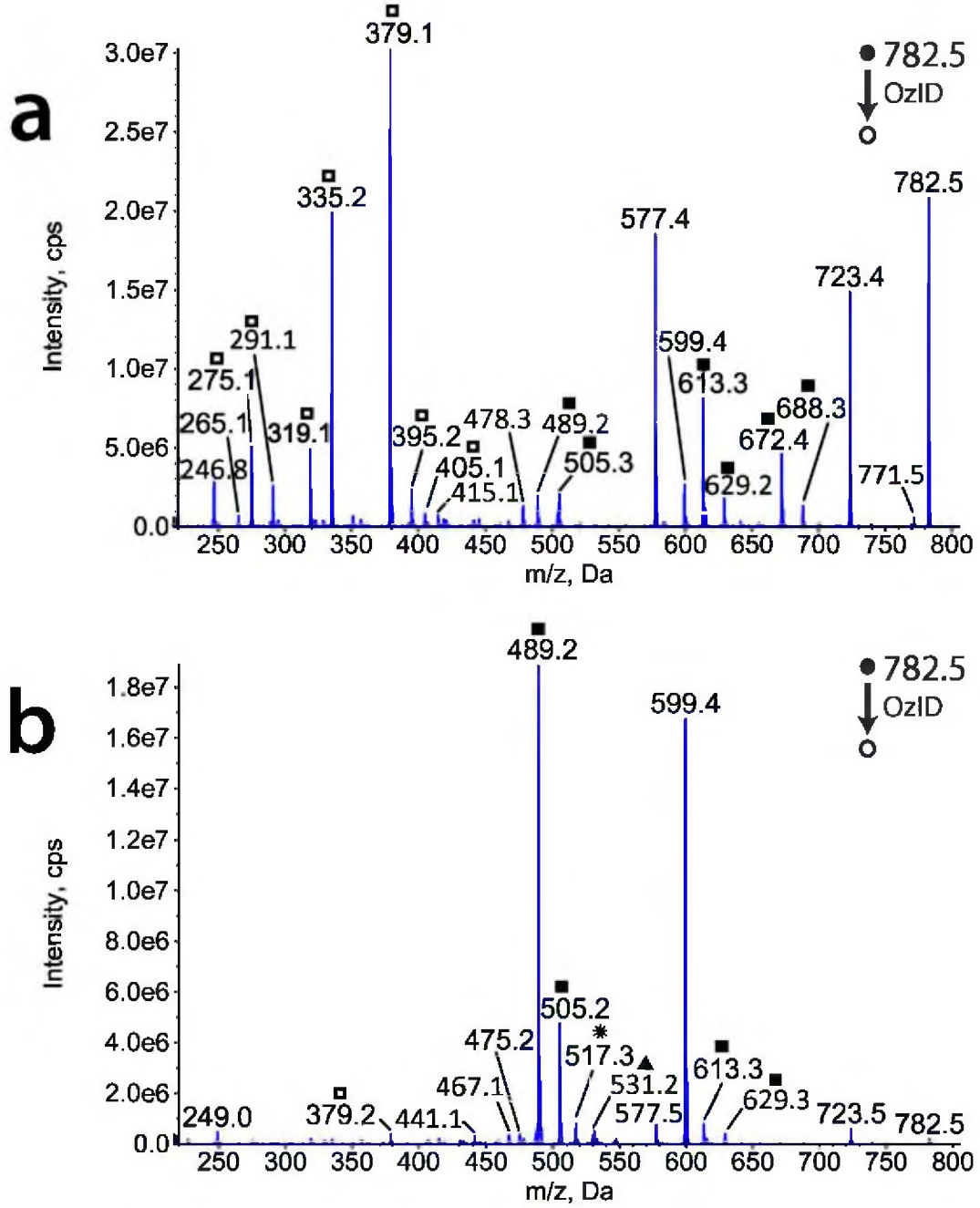

Figure 2.1 OzID spectra obtained from m/z 782.5 in egg yolk extract

OzID spectra obtained from isolation of *m/z* 782.5 (predominantly the $[M+Na]^+$ ions of PC 34:1) produced upon positive-ion electrospray ionization of a solution containing a commercial egg yolk extract. (a) The OzID spectrum obtained using pre- and post-reaction energies of 37 eV and 15 eV, respectively. (b) The OzID spectrum obtained using pre- and post-reaction energies of 5 eV and 30 eV, respectively. OzID product ions indicative of an *n*-9 (■), *n*-7 (✷) and *n*-6 (▲) are marked with different symbols while ions arising from the recently described CID/OzID processes are also marked (□).[102]

Interestingly, many of the CID ions in Figure 2.1(a) also have associated OzID peaks. For example, under these conditions the CID product ion at *m/z* 723 undergoes OzID to yield product ions at *m/z* 613 and 629 with the same characteristic neutral losses of 110 and 94 Da, respectively. in addition, very abundant ions such as the base peak at *m/z* 379 can be attributed to the recently described sequential CID/OzID processes (see also other ions marked by an open square (□) in Figure 2.1a).[102] This complex array of CID and OzID ions can be instructive of the structure of the lipids in question, including assigning the position of acyl chains on the glycerol backbone.[102, 103, 115, 116, 141, 149] However, in the present study where our aim was to combine LC with OzID, we focused on concentrating the signal in product ions carrying information on the carbon-carbon double bond position. To achieve this the translational energy of ions entering the collision cell was minimised to 5 eV (to decrease primary CID processes) while the energy of ions exiting the collision cell was raised to 30 eV to convert most OzID ions through to a single set of abundant products.[140] This approach is illustrated in Figure 2.1(b) where the base peak is *m/z* 489 which, along with the associated *m/z* 505 ion, can be assigned as OzID ions of the $[M+Na]^+$ precursor ion that have subsequently undergone CID with loss of the phosphocholine headgroup (see suggested mechanism in Scheme 2.1). The improvement in the abundance in the diagnostic ions is apparent by considering the *m/z* 489 in Figure 2.1(b) is more than 4-fold greater than *m/z* 672 in Figure 2.1(a). More importantly however, the signal-to-noise in these desired mass channels is enhanced with low abundant signals at *m/z* 517 and 531 in Figure 2.1(b) now discernible above the noise. These OzID ions are indicative of the presence of a small amount of an *n*-7 isomer, most likely PC 16:0_18:1(*n*-7) and a contribution from the [M+2] isotopologue of PC 16:0_18:2(*n*-6,*n*-9). The instrument conditions used to obtain the OzID spectrum in Figure 2.1(b) were also used in the online LC-OzID experiments described below. While it is beyond the scope of the current study, optimization of experimental conditions for other classes of glycerophospholipids (or indeed other lipid classes) could be readily undertaken using the same procedure as that documented here for phosphatidylcholines.

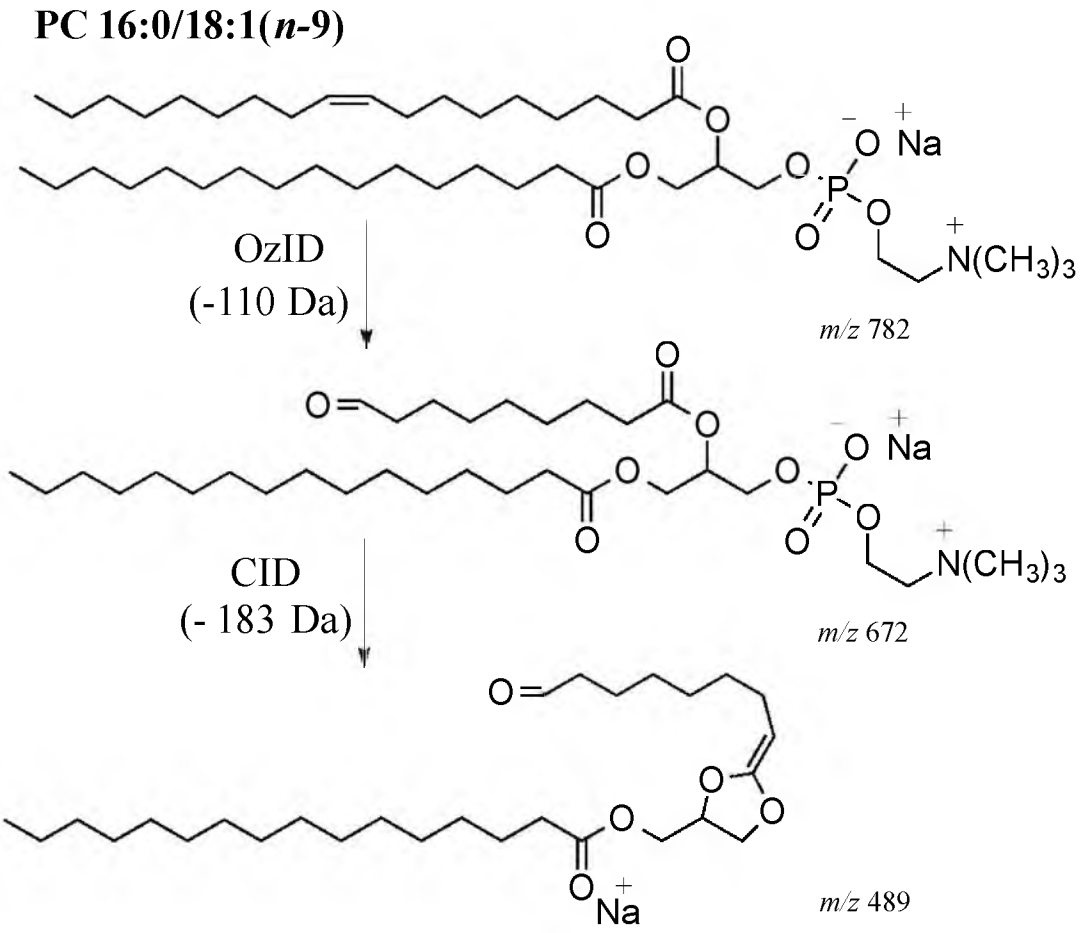

Scheme 2.1 Fragmentation of PC 16:0/18:1(*n*-9).

Fragmentation of the $[M+Na]^+$ precusor ion formed from PC 16:0/18:1(*n*-9) by sequential ozone- and collision-induced dissociation processes to yield abundant product ions diagnostic of carbon-carbon double bond position in the target lipid.

2.4.2 LC-MS of synthetic phospholipid isomers

Two synthetic phosphatidylcholines, PC 18:1(*n*-9)/18:1(*n*-9) and PC 18:1(*n*-12)/18:1(*n*-12), were combined as a 1:1 mixture and subjected to HPLC using a reversed-phase C_{18} column (see Methods section). Positive ion ESI of the eluent yielded abundant *m/z* 808 ions (*i.e.*, the $[M+Na]^+$ forms of the two isomeric lipids) that were analysed by OzID (Figure 2.2).

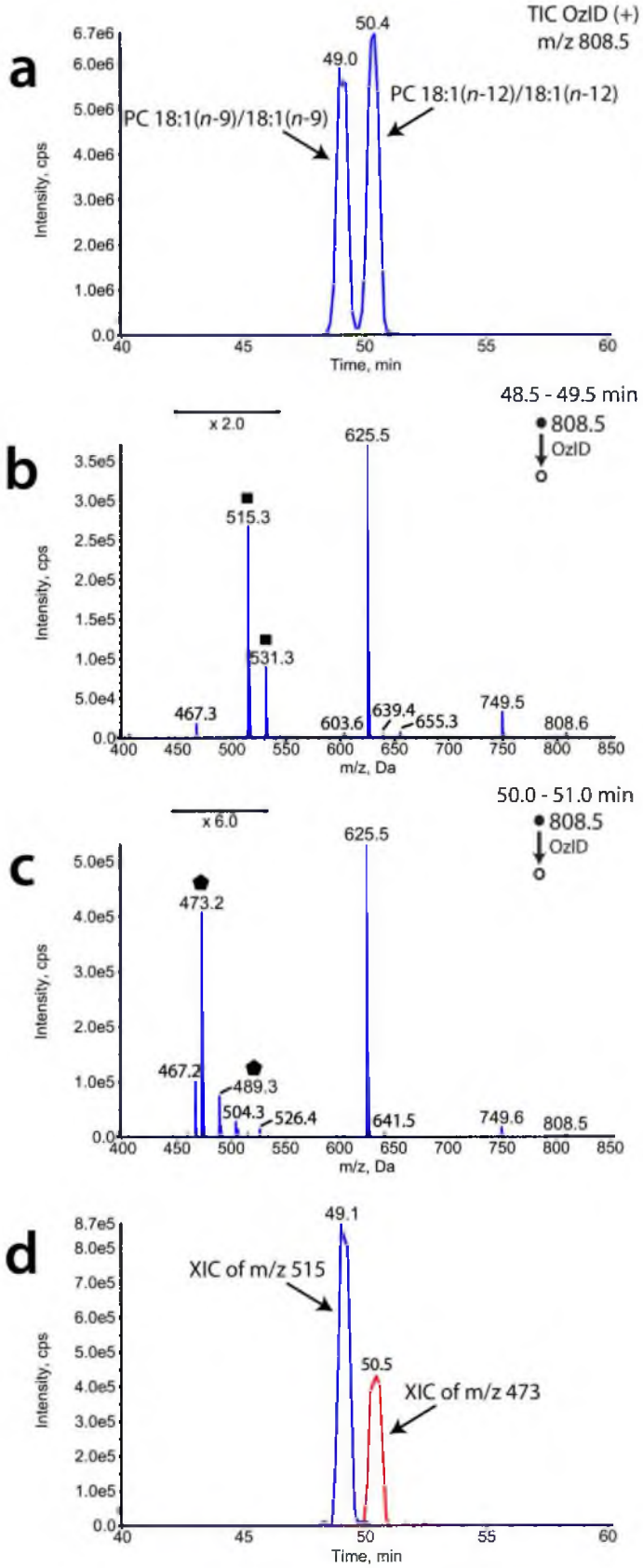

Figure 2.2 Results of LC-MS analysis of a 1:1 mixture of the synthetic phospholipid isomers, PC 18:1(n-9)/18:1(n-9) and PC 18:1(n-12)/18:1(n-12).

Shown above is (a) The region of interest of the chromatogram constructed from total abundance of ions detected in OzID scans of mass-selected *m/z* 808.5. The OzID mass spectra obtained by integrating all scans between (b) 48.5-49.5 min and (c) 50.0-51.0 min. (d) Extracted ion chromatograms (XICs) for OzID product ions at *m/z* 515 (blue trace) and m/z 473 (red trace). OzID product ions indicative of *n*-9 (■) and *n*-12 (⬟) double bond positions are marked with the symbols noted.

The total ion chromatogram (TIC) constructed from the abundance of all ions detected in OzID scans of *m/z* 808 is shown in Figure 2.2(a) and reveals two distinct chromatographic features of near equal abundance. Prior observation of the behaviour of unsaturated phosphatidylcholines on reversed phase columns suggests that the peaks eluting at 49.0 and 50.4 min correspond to the isomers PC 18:1(*n*-9)/18:1(*n*-9) and PC 18:1(*n*-12)/18:1(*n*-12), respectively.[133-135] Integration of OzID scans obtained across each of the chromatographic peaks gave the OzID mass spectra shown in Figures 2.2(b) and (c). The base peak in both mass spectra is at *m/z* 625, which corresponds to the neutral loss of 183 Da (*i.e.*, loss of the choline headgroup) from the precursor ion at *m/z* 808.[148] Distinctive product ion pairs at *m/z* 515, 531 (marked as ■ in Figure 2.2b) and *m/z* 473, 489 (marked as ⬟ in Figure 2.2c) are observed in the OzID spectra of the early-eluting and late-eluting chromatographic features, respectively. These can be assigned to OzID transitions of 110, 94 Da and 152, 136 Da from the base peak at *m/z* 625 that are characteristic of *n*-9 and *n*-12 double bond positions, respectively.[141] The bulk of these diagnostic ions are formed *via* sequential OzID then CID activations illustrated in Scheme 2.1 and enable unambiguous confirmation of the putative assignments of the chromatographic peaks to the *n*-9 (49.0 min) and *n*-12 (50.4 min) isomers. The uniqueness of the OzID product ions to each isomer is illustrated in Figure 2.2(d) where the extracted ion chromatograms (XICs) of *m/z* 515 (shown as blue trace) and the *m/z* 473 (shown as a red trace) are shown to be fully resolved. It is interesting to note that, despite the fact that the isomers were prepared as a 1:1 mixture and show similar peak areas in the total ion chromatograms in Figure 2.2(a), the peak area of the *m/z* 515 selected ion chromatogram is approximately double that of the *m/z* 473 peak. This phenomenon arises from the different rates of reaction of the two ionized lipid isomers with ozone in the gas phase. The general trend of faster ozonolysis reactions with double bonds

closer to the methyl terminus of lipid acyl chains has previously been noted.[140] This is consistent with the current observation where double bonds at the *n*-9 position react faster than those at the *n*-12 position. Importantly, this result suggests that while ion chromatograms generated from OzID transitions can provide an excellent means to identify and resolve overlapping double bond isomers, relative quantification using these data alone cannot be achieved without calibration of the relative ozonolysis reaction efficiencies of the isomers.

2.4.3 LC-MS of complex lipid extracts

Upon optimizing the LC-OzID workflow, this protocol was used to examine lipid extracts from chicken egg yolk and sheep brain. The phosphatidylcholine composition of such extracts is known to be rich in PC 16:0_18:1, although the position(s) of unsaturation have not been fully elucidated.[150, 151]

While the chicken egg yolk extract is a relatively simple lipid mixture (*i.e.*, a phosphatidylcholine fraction), it is substantially more complex than the standard mixtures described above. As a result of the increased complexity the chromatographic conditions were adjusted as described above (see Methods). Total ion chromatograms showing the elution of all components of the mixture detectable under the experimental conditions are provided as Supplementary Materials in Appendix A (see Figure 6.2) and also provide evidence for the reproducibility of the conditions across two injections. The chromatographic and mass spectral data obtained from OzID of *m/z* 782, corresponding to the $[M+Na]^+$ ion formed from PC 34:1, is shown in Figure 2.3. In the chromatographic region of interest in Figure 2.3(a) the early-eluting components at retention times of 21.3 and 22.4 min are assigned to [M+2] isotope contributions from PC 34:2. This assignment was confirmed by examining the full-scan mass spectra obtained at these elution times that were dominated by ions at *m/z* 780 (data not shown). The major peak in Figure 2.3(a) is centred at 31.3 min and features a discernible shoulder centred at approximately 30.4 min. The OzID spectrum of *m/z* 782, obtained from averaging the scans across the main chromatographic peak, is shown in Figure 2.3(c). This spectrum has a single major set of OzID product ions at *m/z* 489, 505 (marked with ■) corresponding to

transitions of 110, 94 Da from the *m/z* 599 base peak. The formation of these ions can be rationalized according to the sequence of OzID and CID events depicted in Scheme 2.1 and confirms the presence of an *n*-9 double bond in the eluting phosphatidylcholines. In contrast, the OzID spectrum obtained from the smaller chromatographic feature centred at 30.4 min is dominated by the product ion pair of *m/z* 517, 533 (marked with ✹ in Figure 2.3b) corresponding to transitions of 82, 66 Da from the *m/z* 599 base peak. These neutral losses have previously been reported to arise from oxidative cleavage of an *n*-7 double bond during OzID (see Supplementary Materials in Appendix A, Table 6.1 for a summary of characteristic OzID transitions).[136, 140, 141] The *n*-9 OzID product ion at *m/z* 489 is also observed, albeit at low abundance, in the spectrum shown in Figure 2.3(b) and arises from the incomplete chromatographic separation of two isomeric lipids that differ in the position of unsaturation. Support for this is provided by the overlay of ion chromatograms extracted from the diagnostic OzID ions at *m/z* 489 (*n*-9 marker ion, red trace) and *m/z* 517 (*n*-7 marker ion, blue trace) shown in Figure 2.3(d).

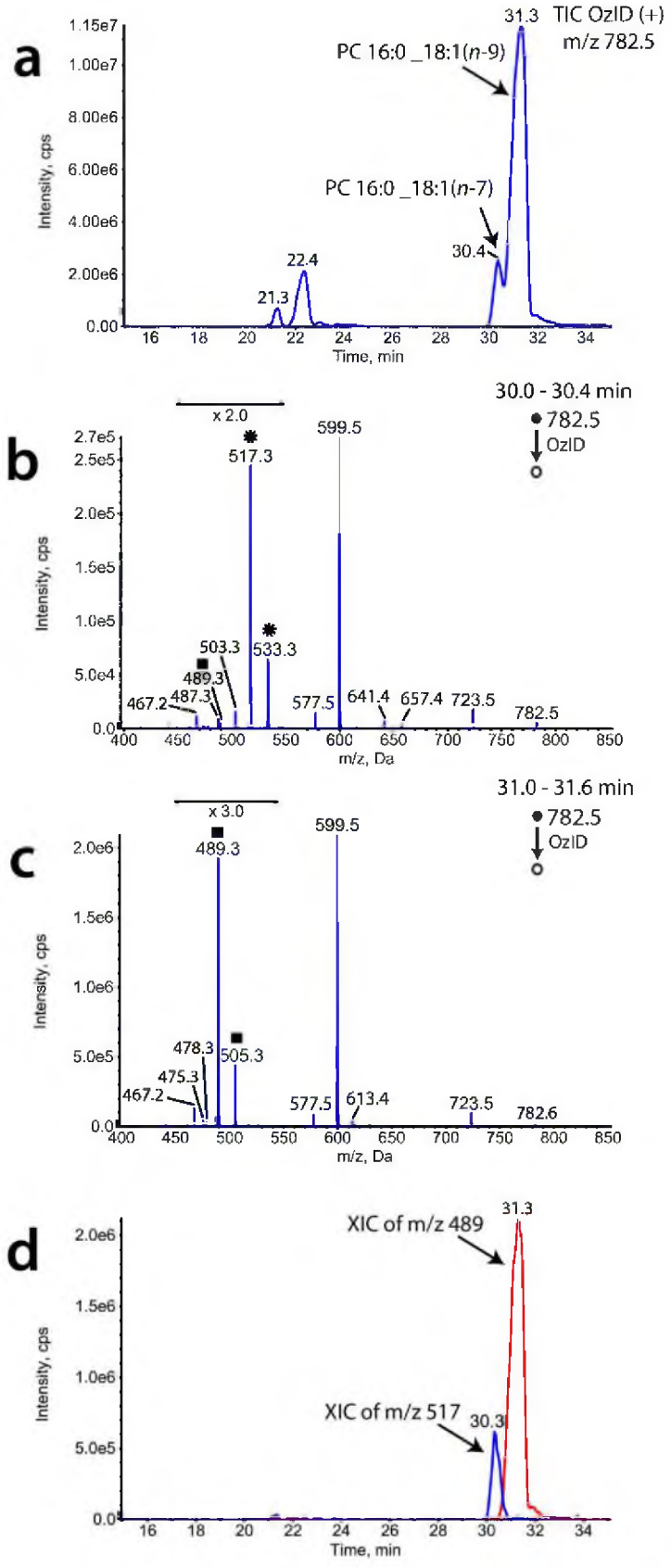

Figure 2.3 Results of LC-MS analysis of a purified phosphatidylcholine extract from egg yolk for m/z 782.5.

Shown above is (a) the region of interest of the chromatogram constructed from total abundance of ions detected in OzID scans of mass-selected *m/z* 782.5. The OzID mass spectra obtained by integrating all scans between (b) 30.0-30.4 min and (c) 31.0-31.6 min. (d) Extracted ion chromatograms (XICs) for OzID product ions at *m/z* 517 (blue trace) and m/z 489 (red trace). OzID product ions indicative of *n*-7 (✷) and *n*-9 (■) double bond positions are marked with the symbols noted.

While LC-MS^2 (LC-MS/MS) data has previously been used to assign the sum composition PC 34:1 in chicken egg yolk to the fatty acyl composition PC 16:0_18:1, those results provided no indication of the presence of double bond positional isomers.[150] Conversely, the LC-OzID data presented here demonstrate that the PC 34:1 lipid population in this extract is a mixture of the double bond positional isomers PC 16:0_18:1(*n*-9) and PC 16:0_18:1(*n*-7). While, the chromatographic resolution of these isomers is incomplete, we estimate that PC 16:0_18:1(*n*-9) is some 4-5 times more abundant that PC 16:0_18:1(*n*-7) (Figure 2.3a).

The incomplete chromatographic resolution of the PC 16:0_18:1 isomers in egg yolk extract stands in contrast to the complete separation of the binary mixture of synthetic double bond isomers of PC 18:1_18:1 (Figure 2.2a). The difference in chromatographic performance arises in part because of the greater complexity of the biological extract and the greater structural differences between each isomeric pair (*i.e.*, two double bonds versus one). This also suggests that separation of double bond positional isomers on reversed-phase columns becomes easier as the spacing between the sites of unsaturation increases and if double bonds are closer to the carboxylate moiety (*cf.* separation of *n*-9 and *n*-12 isomers in Figure 2.2a with separation of *n*-7 and *n*-9 isomers in Figure 2.3a).[135] it is also interesting to note that the relative peak areas in the extracted ion chromatograms in Figure 2.3(d) are actually representative of the total ion chromatograms shown in Figure 2.3(a). This suggests that the ozonolysis rates of the sodiated PC 16:0_18:1(*n*-9) and PC 16:0_18:1(*n*-7) isomers are similar. This is in contrast to the pattern observed for the PC 18:1(n-9)/18:1(*n*-9) and PC 18:1(*n*-12)/18:1(*n*-12) (Figure 2.2) where a clear bias was observed. This finding suggests that for the PC 16:0_18:1 isomers, extracted OzID traces could be used for approximating relative abundance where chromatographic resolution alone is insufficient (see below).

Lipid extracts from sheep brain tissue are substantially more complex mixture than phosphatidylcholine fractions from egg yolk. Previous investigations in our laboratory have shown phosphatidylcholines of composition PC 34:1 are abundant in this tissue and traditional tandem mass spectrometry has been used to assign the acyl chain composition to PC 16:0_18:1.[151] LC-MS analysis of sheep brain extract was undertaken using the methods described above and the results are summarised in Figure 2.4.

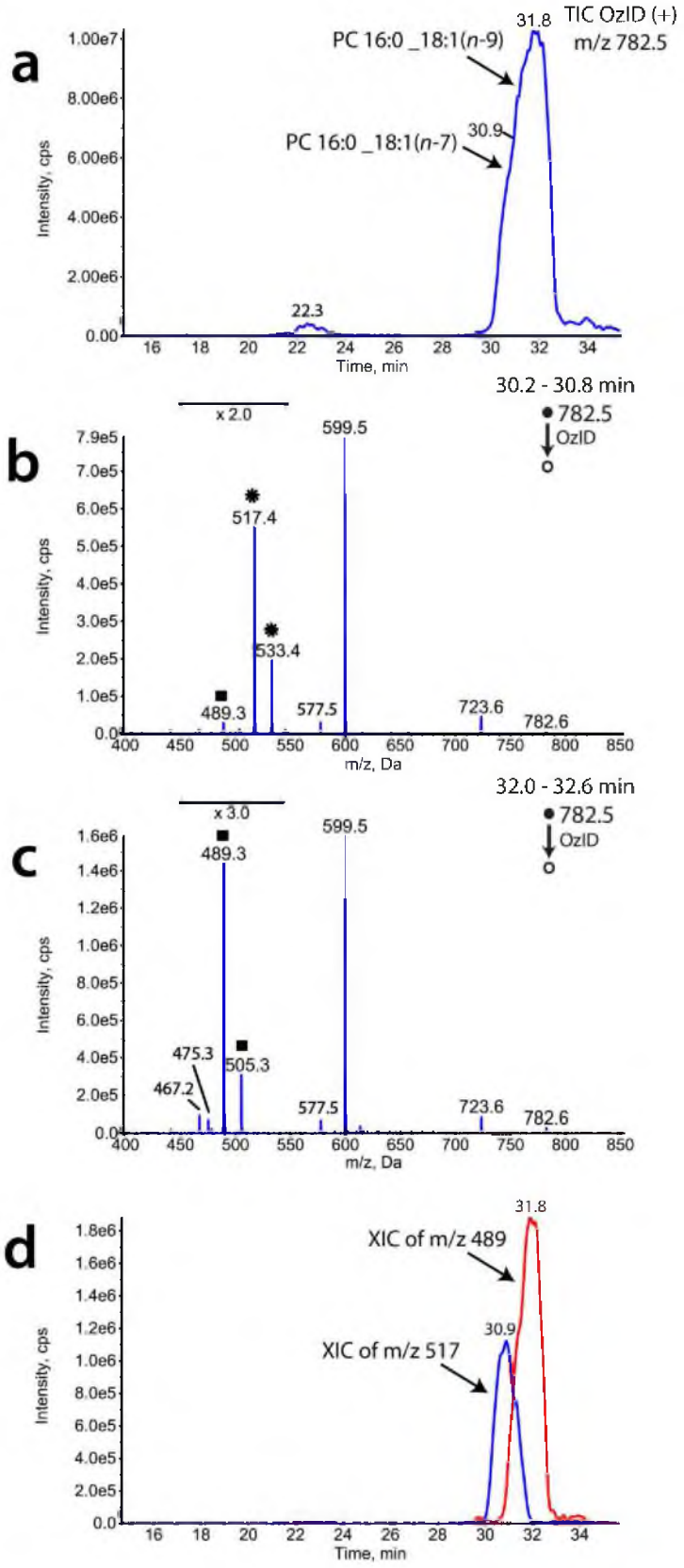

Figure 2.4 Results of LC-MS analysis of a lipid extract from dissected sheep brain tissue.

Shown above is (a) the region of interest of the chromatogram constructed from total abundance of ions detected in OzID scans of mass-selected *m/z* 782.5. The OzID mass spectra obtained by integrating all scans between (b) 30.2-30.8 min and (c) 32.0-32.6 min. (d) Extracted ion chromatograms (XICs) for OzID product ions at *m/z* 517 (blue trace) and m/z 489 (red trace). OzID product ions indicative of *n*-7 (✷) and *n*-9 (■) double bond positions are marked with the symbols noted.

The chromatogram extracted from the total abundance of ions detected from OzID scans of *m/z* 782 (Figure 2.4a) shows a low abundance feature centred at a retention time of *ca.* 22.3 min. This retention time is similar to that observed previously for the [M+2] isotope contributions from PC 34:2 (*cf.* Figure 2.3a) and this was confirmed by observation of the *m/z* 780 base-peak in the full scan mass spectra obtained at this retention time (data not shown). The chromatogram in Figure 2.4(a) is dominated by a large broad peak stretching from 30-33 min and, by analogy to the results obtained from egg yolk, this feature is assigned to isomers of PC 16:0_18:1. The absence of clear chromatographic resolution however, makes the assignment of this peak more challenging. Integration of the OzID scans obtained from the early (30.2-30.8 min) and late (32.0 – 32.6 min) eluting portions of the peak yielded the OzID mass spectra shown in Figures 2.4(b) and (c), respectively. These spectra are clearly distinct and reveal the characteristic OzID ion pairs of *m/z* 517, 533 (corresponding to an *n*-7 double bond) and *m/z* 489, 505 (diagnostic for an *n*-9 double bond, see Table 6.1). These data suggest that the chromatographic feature is a composite of the two double bond-positional isomers namely, PC 16:0_18:1(*n*-7) and PC 16:0_18:1(*n*-9). Extracted ion chromatograms of two of these characteristic transitions, *m/z* 517 (shown as a blue trace, Figure 2.4d) and *m/z* 498 (shown as a red trace, Figure 2.4d), reveal the different chromatographic behaviour of the two isomers. The *n*-7 isomer (30.9 min) elutes earlier than the *n*-9 isomer (31.8 min), which is analogous to the trend observed for the egg yolk extract (Figure 2.3a). Overall however, the isomer resolution for the sheep brain extract is lower than that achieved for egg yolk. The difference in chromatographic performance can be attributed to (i) the greater overall complexity of the sheep brain extract, which has significant contributions from all major classes of phospholipid,[151] but also (ii) the apparently greater contribution of the *n*-7 isomer in sheep brain. As noted above, for

the comparison of *n*-7 and *n*-9 isomers of PC 16:0_18:1 might be expected to give similar detection efficiencies in their respective OzID transitions. As such, the relative proportions can be estimated from Figure 2.4(d), suggesting that the ostensibly less common *n*-7 isomer might be present at up to 50% of the PC 16:0_18:1(*n*-9) species.

To assess the efficacy of this method for analyzing more complex lipids, the egg yolk extract was also interrogated for isomers of polyunsaturated phosphatidylcholines of sum composition PC 36:2. LC-MS results from this analysis are summarised in Figure 2.5. The total abundance of all ions observed in the OzID scans for *m/z* 808, corresponding to the $[M+Na]^+$ ion of PC 36:2, are plotted in Figure 2.5(a) and show three distinct features. The least abundant chromatographic peak, centred at 22.5 min, is assigned to the [M+2] isotope contribution of PC 34:3 (a lipid previously identified in egg yolk).[150] The contribution of these phosphatidylcholines was confirmed by the presence of abundant *m/z* 806 ions in the full mass spectra obtained at this retention time (data not shown). The two major chromatographic peaks in Figure 2.5(a) are baseline resolved and are centred at 31.4 and 32.8 min. OzID spectra obtained from averaging scans across these two peaks are shown in Figures 2.5(b) and (c), respectively. The OzID spectrum shown in Figure 2.5(b) is nearly identical to that obtained from the synthetic standard, PC 18:1(*n*-9)/18:1(*n*-9) (see Figure 2.2b). Indeed, even the relative abundance ratio of the diagnostic OzID ions at *m/z* 515 and 531 is identical (*ca.* 3:1), suggesting that not only are both double bonds at the *n*-9 position but they also carry *cis*-stereochemistry [140]. The OzID spectrum shown in Figure 2.5(c) reveals two sets of OzID ions at *m/z* 517, 533 (marked with ■) and *m/z* 557, 573 (marked with ▲), representing neutral losses from the *m/z* 625 base peak that are consistent with the *n*-9 and *n*-6 double bond positions in the unsaturated acyl chain of PC 18:0_18:2(*n*-6,*n*-9).[141] Both the PC 18:1_18:1 and PC 18:0_18:2 acyl chain compositions were previously assigned based on conventional tandem mass spectral analysis on egg yolk extract.[150] The LC-OzID results presented here enable the separation of these isomeric forms with unambiguous assignment of double bond positions in each case (*e.g.*, see XICs in Figure 2.5d).

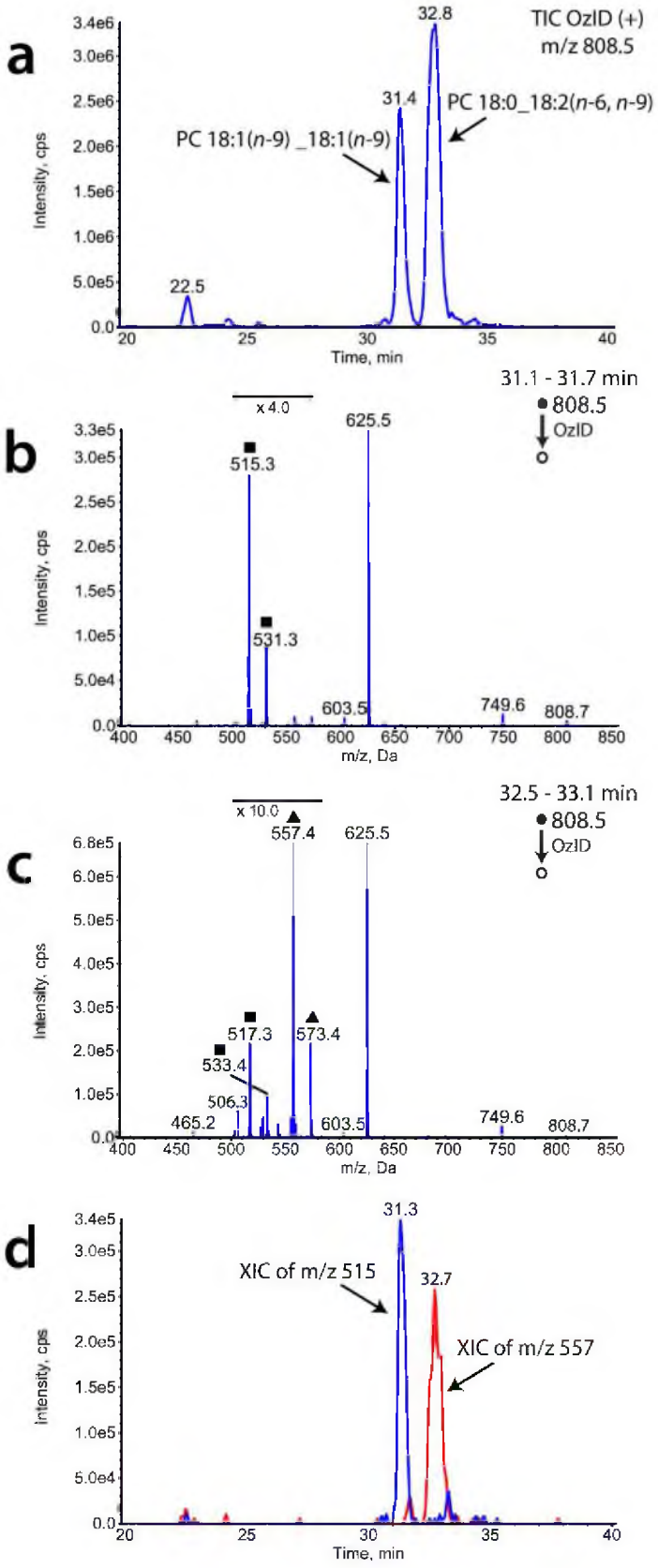

Figure 2.5 Results of LC-MS analysis of a purified phosphatidylcholine extract from egg yolk for m/z 808.5.

Shown above is (a) the region of interest of the chromatogram constructed from total abundance of ions detected in OzID scans of mass-selected *m/z* 808.5. The OzID mass spectra obtained by intergrating all scans between (b) 31.1-31.7 min and (c) 32.5-33.1 min. (d) Extracted ion chromatograms for OzID product ions at *m/z* 515 (blue trace) and m/z 557 (red trace). OzID product ions indicative of *n*-6 (▲) and *n*-9 (■) double bond positions are marked with the symbols noted.

2.5 Conclusions

The results presented here demonstrate that it is possible to obtain high quality OzID mass spectra on a timescale that is compatible with conventional LC. While OzID scans remain intrinsically slow compared to CID experiments, we have shown here that it is possible to obtain up to 20 OzID scans, interleaved with other scan functions, during the elution of a chromatographic peak (*ca.* 1 min). When combined with other mass spectral and chromatographic information, this hybrid workflow enables the structural elucidation of complex lipids and, importantly, the identification of distinct isomeric forms of lipids differing only in the position(s) of carbon-carbon double bonds. In complex extracts where chromatographic separation of such isomers is poor, OzID enables the LC profiles of each isomer to be deconvoluted and, in some instances, the relative proportions of each isomer can be approximated. This hyphenated LC-OzID approach has some advantages over infusion in simplifying OzID spectra through minimizing isomer overlap and removing contributions of [M+2] isotopes. While the methods used here targeted specific phosphatidylcholines of interest, examples provided as Supplementary Materials, in Appendix A (Figures 6.3 and 6.4) demonstrate that (i) the method can be applied to lower abundance, polyunsaturated lipids and (ii) LC-OzID spectra with good signal-to-noise can be achieved on even shorter timescales should future applications require faster chromatography or the interrogation of more molecular species. OzID has previously been shown to work effectively on a wide variety of lipid structures in infusion ESI experiments[139] so the application of LC-OzID to the examination of other classes (*e.g.*, other glycerophospholipids, sphingolipids, triacylglycerols) represents a ready extension of the workflows described herein. Future workflows for LC-OzID, will take advantage of information dependent approaches where OzID scans are triggered based on precursor ion detection in a

preceding full scan analysis. The ability to conduct the ozonolysis event using data-dependent selection criteria (*e.g.*, inclusion lists, exclusion lists, tandem mass spectral criteria such as neutral losses, *etc.*) will ensure that the majority of unsaturated lipids are detected and the position(s) of unsaturation within their acyl chains are established.

Under the conventional reversed-phase chromatographic conditions used here, the closer the double bond of the acyl chain to the carboxylate group, the more strongly it was retained on the column (*cf. n*-9 elutes before *n*-12, Figure 2.2a). This observation is consistent with previous reports of separation of double bond positional isomers and evidence from new column technologies suggests further improvements in isomer separation can be achieved.[133-135] Full structure elucidation of complex lipids however, also requires separation and/or mass spectral differentiation of isomers that differ in (i) the position of acyl chains on the glycerol backbone (*i.e.*, *sn*-positional isomers) and the stereochemistry about the double bond(s) (*i.e.*, *cis* and *trans*). Some preliminary reports have suggested that separation of such isomers is possible in selected circumstances but it is by no means routine.[152, 153] Perhaps the addition of complementary mechanisms of separation, such as ion-mobility spectrometry with LC and mass spectrometry may provide a means to achieve full structure assignments for lipids in complex biological extracts.[149, 154, 155]

Although OzID and other technologies reveal the presence of multiple isomeric forms of phospholipids within biological samples, very little is currently understood about the biological role and/or evolutionary reason for these isomers.[136, 141] Future application of LC-OzID to extracts from different biological sources will aid in the identification of the presence of isomeric lipids and may assist in revealing changes in isomer populations that will provide essential clues as to the different role(s) of these isomers *in vivo*.

3 SEPARATION AND IDENTIFICATION OF PHOSPHATIDYLCHOLINE REGIOISOMERS BY COMBINING LIQUID CHROMATOGRAPHY WITH A FUSION OF COLLISION- AND OZONE-INDUCED DISSOCIATION

3.1 Abstract

The differentiation of closely related lipid isomers is increasingly important to our evolving understanding of lipid biochemistry but is equally challenging to contemporary chromatographic and mass spectral analyses. Recently we have described a novel ion activation approach based on combining collision- with ozone-induced dissociation (CID/OzID) for identification of the relative acyl chain substitution positions in glycerophospholipids. Here we demonstrate, for the first time, that CID/OzID can be effectively combined with reversed-phase chromatography to enable separation and unambiguous identification of regioisomeric pairs of phosphatidylcholines differing only in the arrangement of acyl chains on the glycerol backbone.

3.2 Introduction

The composition of the lipidome (*i.e.*, the structure and abundance of different lipids within a biological system) can vary significantly between different organisms, different organs or even within different regions of the same tissue.[17] While enzymatic regulation, lipid synthesis, recycling pathways and transport all play an important role in dictating the molecular structure and abundance of the lipids present, factors such as diet, exercise, infection or other insult can also have a profound influence.[156] In order to unravel these complex biochemical mechanisms and to understand the role(s) of lipids in health and disease it is essential to have access to sensitive and highly specific methods for the identification and quantification of individual lipid molecular species.

Glycerophospholipids are among the most abundant classes of lipids in nature and significant attention has been focused on developing analytical methods to elucidate the molecular structure of these species and to quantify them within complex lipid extracts.[80] Contemporary tandem mass spectrometry is an essential and powerful tool for such analyses and can provide rapid identification of the class

of the lipid (*e.g.*, phosphatidylcholine (PC)) and the number of carbons and degree of unsaturation in each of the acyl chains (*e.g.*, PC 16:0_20:4 where the presence of a saturated 16-carbon chain (16:0) and 20-carbon polyunsaturated chain (20:4) are indicated).[157] A significant limitation of commonly deployed mass spectrometric assays however, is the inability to differentiate closely related isomeric lipids. For example, the collision-induced dissociation mass spectrum of PC 16:0/20:4 (where the 20:4 chain is esterified to the *sn*-2 position on the glycerol backbone) is very similar to that obtained from the positional isomer PC 20:4/16:0 (where the 20:4 is at the *sn*-1 position). This challenge is further compounded by the fact that both isomers are likely present in many complex extracts.[99, 149] While these structures may appear quite similar, the biochemistry of the isomers can be profoundly different indicating that in order to answer certain biological questions the isomeric pairs need to be resolved and separately characterized.

Liquid chromatography (LC) has been extensively used in conjunction with mass spectrometry for dramatically reducing the complexity of lipid extracts prior to mass spectral analysis.[150, 158-164] There are however, only a limited number of examples where LC has successfully been combined with mass spectrometry for the separation and identification of phospholipid isomers.[124, 135, 152, 153, 165] Of these, only one previous study has demonstrated successful separation of pairs of phosphatidylcholine *sn*-positional isomers using reversed-phase ultra-high performance liquid chromatography.[153] In the same study, tandem mass spectrometry – specifically MS^3 fragmentation – was used to assign the molecular structure to each of the separately eluting isomers. As noted above however, such product ions are usually not unique to a particular isomer and rather the relative abundance of the spectral peaks is used to infer the acyl chain substitution positions.[99, 166] Uncertainty in such structural assignments is further compounded by the often-low abundance of the mass spectral peaks. Recently our group has developed a novel ion activation method that combines collision- and ozone-induced dissociation in sequence (CID/OzID) to yield abundant product ions that are diagnostic of *sn*-position and can thus be deployed to identify and differentiate regioisomeric lipids.[102] Here we describe, for the first

time, the combination of LC and CID/OzID into a single workflow to enable the separation and identification of phosphatidylcholine *sn*-positional isomers.

3.3 Materials and Methods

3.3.1 Materials

All solvents used, including water, were Optima LC-MS grade and purchased from Thermo Fisher Scientific (Scoresby, VIC, Australia). Analytical-grade butylated hydroxytoluene (BHT) was purchased from Sigma-Aldrich (St. Louis, MO, USA). Analytical-grade sodium acetate was purchased from Ajax Chemicals (Auburn, NSW, Australia). Industrial-grade compressed oxygen was obtained from BOC (Cringila, NSW, Australia). The following synthetic phospholipid standards were purchased from Avanti Polar Lipids, Inc. (Alabaster, Alabama, USA): PC 18:1/16:0 (1-(9*Z*-octadecenoyl)-2-hexadecanoyl-*sn*-glycero-3-phosphocholine); PC 16:0/18:1 (1-hexadecanoyl-2-(9*Z*-octadecenoyl)-*sn*-glycero-3-phosphocholine); PC 16:0/20:4 (1-hexadecanoyl-2-(5*Z*,8*Z*,11*Z*,14*Z*-eicosatetraenoyl)-*sn*-glycero-3-phosphocholine); and PC 16:0/22:6 (1-hexadecanoyl-2-(4Z,7Z,10Z,13Z,16Z,19Z-docosahexaenoyl)-*sn*-glycero-3-phosphocholine).

3.3.2 Methods

Stock solutions of all phosphatidylcholine standards were prepared in acetonitrile/2-propanol (50/50, v/v) to a final lipid concentration *ca.* 300-400 µM with 1% BHT (w/w) and stored at -80 °C until analysis. Using the corresponding stock solution, phosphatidylcholine standards, PC 16:0/20:4 and PC 16:0/22:6 were each separately diluted using water/acetonitrile/2-propanol (50:25:25, v/v) to a final concentration of 40 µM. The phospholipid standards, PC 16:0/18:1 and PC 18:1/16:0 were mixed at a 1:1 molar rato in water/acetonitrile/2-propanol (50:25:25, v/v) to a final total lipid concentration of 80 µM each (*i.e.*, total lipid concentration of 160 µM).

Chromatography was performed using a Surveyor high-performance liquid chromatograph system coupled to an LTQ linear ion trap mass spectrometer (Thermo Fisher Scientific, San Jose, CA). Injections of 2.5-10 µL of each PC standard sample were loaded onto an Acquity C_{18} BEH column (1.7 µm, 150 mm x 1 mm I.D.,

Waters, Milford MA, USA). For all analyses, the column was maintained at 60-65 °C and samples held at 5 °C. For analysis of PC standards, PC 16:0/20:4 and PC 16:0/22:6, mobile phases were prepared as follows: A: water, sodium acetate (50 μM) and B: acetonitrile/2-propanol (75/25, v/v), sodium acetate (50 μM). The gradient elution was run at a flow rate of 60 μL/min as follows: 0-10 min: 70% B, 10-90 min: 75% B, 90-95: 99% B, 95-110 min: 70% B. For the 1:1 mixture of PC 16:0/18:1(9Z) and PC 18:1(9Z)/16:0, the mobile phases were prepared as follows: A: water, sodium acetate (70 μM) and B: acetonitrile/2-propanol (66:34, v/v), sodium acetate (70 μM). The gradient elution was run at a flow rate of 60 μL/min as follows: 0-60 min: 50-100%B, 60-63 min: 100% B, 63-75 min: 50% B.

The mass spectrometer has been modified to enable the introduction of ozone into the ion trap as previously described.[139, 140, 167] All analyses were undertaken in positive ion mode and respresentative source conditions included: capillary voltage 45 V; ionization spray voltage 4 kV; capillary temperature 200 °C; tube lens voltage 180 V. Nitrogen gas served as the sheath gas, auxiliary gas and sweep gas and helium as the bath gas with the addition of a small bleed from a continuous flow of externally generated ozone (produced at 170 g/Nm^3 by a Titan 100 generator, Absolute Ozone, Edmonton Canada). These conditions provide a constant level of ozone within the ion trap throughout the experiments. The Xcalibur instrument control software (Thermo Fisher Scientific, San Jose, CA) was used to trigger an alternating full scan MS and a targetted CID/OzID scan with all data acquired in centroid mode except for analysis of PC 16:0_18:1 isomers, acquired in profile mode. The CID/OzID sequence is formally an MS^3 experiment where intact $[PC+Na]^+$ ions are mass selected (using an isolation width of 5 Th) and subjected to CID (using a normalised collision energy of 40). The [PC+Na-183] CID product ion is then re-isolated (using an isolation width of 3 Th) and trapped for 200-1000 ms, with no collision energy, in the presence of ozone. The ion injection time was 100 ms for all CID/OzID scans.

3.4 Results and Discussion

3.4.1 Separation and identification of isomeric phosphatidylcholines

The results of LC-MS analysis of a commercially available, synthetic standard provided as 1-palmitoyl-2-arachidonoyl-*sn*-glycero-3-phosphocholine (annotated here as PC 16:0/20:4) are shown in Figure 3.1. The total ion chromatogram for ions at *m/z* 804 (Figure 3.1a), corresponding to the sodium cation of PC 36:4, reveals two peaks with maxima at 44.8 and 46.4 min. The presence of two chromatographic features with a common *m/z* suggests the presence of isomeric phospholipids within the sample. Previous chromatographic investigations using an extremely similar reversed-phase column showed isomer separation could be observed for synthetic phosphatidylcholines with PC 36:4 sum composition. In that study, relative peak abundances in tandem mass spectra suggested that the major and minor chromatographic peaks corresponded to the *sn*-positional isomers PC 16:0/20:4 and PC 20:4/16:0, respectively.[153] With these putative peak assignments in mind, CID/OzID mass spectra were obtained across the chromatographic peaks at 44.8 and 46.4 min and the results are shown in Figure 3.1(b) and (c), respectively. These spectra are obtained by first mass selecting the $[M+Na]^+$ precursor ion and subjecting it to CID. Ozone is present in the ion trap throughout the experiment but at sufficiently low concentrations that it does not impact on the conventional functions of the instrument. For example, the CID spectra obtained under these conditions are not significantly affected by the presence of the reagent gas in the helium. In a formal MS^3 experiment, the product ion at $[M+Na-183]^+$ was then mass-selected and stored in the ion trap for 1000 ms in the presence of ozone. The carbon-carbon double bond linking the *sn*-2 acyl chain to the glycerol backbone in the $[M+Na-183]^+$ ion is chemically cleaved by the ozone resulting in neutral loss characteristic of the acyl chain at this position. The origins of these ions have previously been described and the process is briefly summarized in Scheme 3.1.[102] The CID/OzID spectrum of the first eluting peak (Figure 3.1b) shows abundant product ions at *m/z* 427 and 443, corresponding to neutral losses of 194 and 178, respectively. Importantly however, the observed neutral losses in the CID/OzID spectrum are consistent with predictions

for a 16:0 acyl chain occupying the *sn*-2 position of the glycerol backbone (Table 3.1) and thus support the assignment of the chromatographic peak to the PC 20:4/16:0 isomer. The CID/OzID spectrum of the late-eluting peak is shown in Figure 3.1(c) and is dominated by the product ion at *m/z* 379 corresponding to a neutral loss of 242 Da with a minor product ion also observed at *m/z* 395 (-226 Da). Such transitions are indicative of the 20:4 acyl chain occupying the *sn*-2 position and supports the assignment of the major chromatographic feature to the expected PC 16:0/20:4. Integration of the chromatographic peaks in Figure 3.1(a) suggests that the synthetic phosphatidylcholine, is composed of approximately 88% PC (16:0/20:4) and 12% of the alternate PC (20:4/16:0) isomer; with the latter eluting first upon reversed-phase chromatography. The presence of low-abundance *sn*-positional isomers in synthetic glycerophospholipids has been noted before.[99, 149, 166] This likely arises from transacylation of the intermediate lysophosphatidylcholine during the preparation.[168] Importantly however, the LC protocol employed here provides effective separation of the isomers and the CID/OzID affords rapid identification of the isomeric structure of each chromatographic peak. Indeed, visualization of the extracted ion chromatograms for the diagnostic product ions at *m/z* 427 and 379 (see Figure 3.1d) provides a selective means to interrogate the chromatographic data for the presence of each isomer.

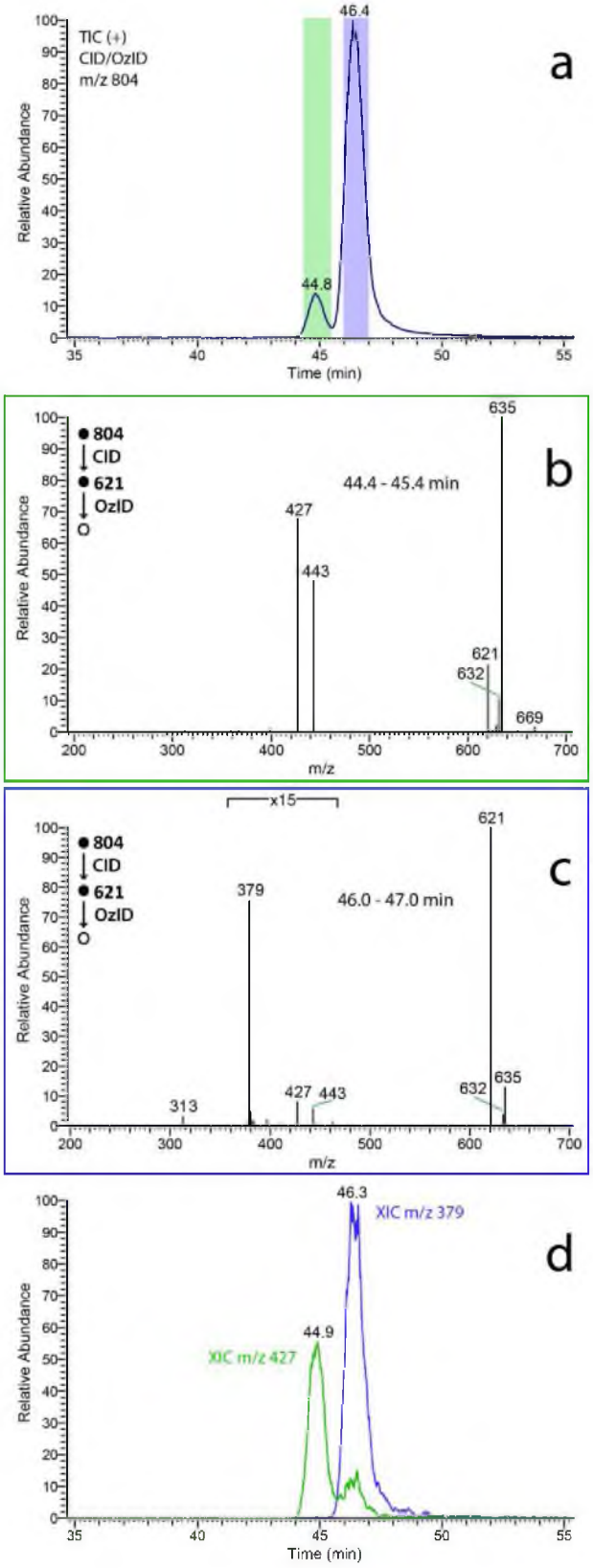

Figure 3.1 MS analysis of synthetic standard provided as PC 16:0/20:4.

Shown above is (a) the total ion chromatogram for LC-CID/OzID of *m/z* 804. (b) The CID/OzID spectrum obtained from integrating across the chromatographic peak between 44.4-45.4 min. (c) The CID/OzID spectrum obtained from integrating across the chromatographic peak between 46.0-47.0 min. (d) The extracted ion chromatogram for CID/OzID product ions at *m/z* 427 (indicative of PC 20:4/16:0) is shown in green, while the extracted ion chromatogram for *m/z* 379 (indicative of PC 16:0/20:4) is shown in blue.

Table 3.1 List of CID/OzID transitions for common fatty acyl chains.

Displayed below are CID/OzID transitions for common fatty acyl chains when substituted at the *sn*-2 position on the glycerol backbone. Predicted neutral losses for fatty acyl chains commonly found in eukaryotes upon OzID of the fragment [PC+Na-183]+ resulting from CID of the [PC+Na]+ precursor ion.

Fatty acid (no. carbon: no. db)	CID/OzID Apparent Neutral loss (from $[PC+Na-183]^+$ trapped w/ O_3)	
	Aldehyde	Criegee
16:0	194	178
16:1	192	176
18:0	222	206
18:1	220	204
18:2	218	202
18:3	216	200
20:0	250	234
20:1	248	232
20:2	246	230
20:3	244	228
20:4	242	226
20:5	240	224
22:0	278	262
22:1	276	260
22:2	274	258
22:3	272	256
22:4	270	254
22:5	268	252
22:6	266	250

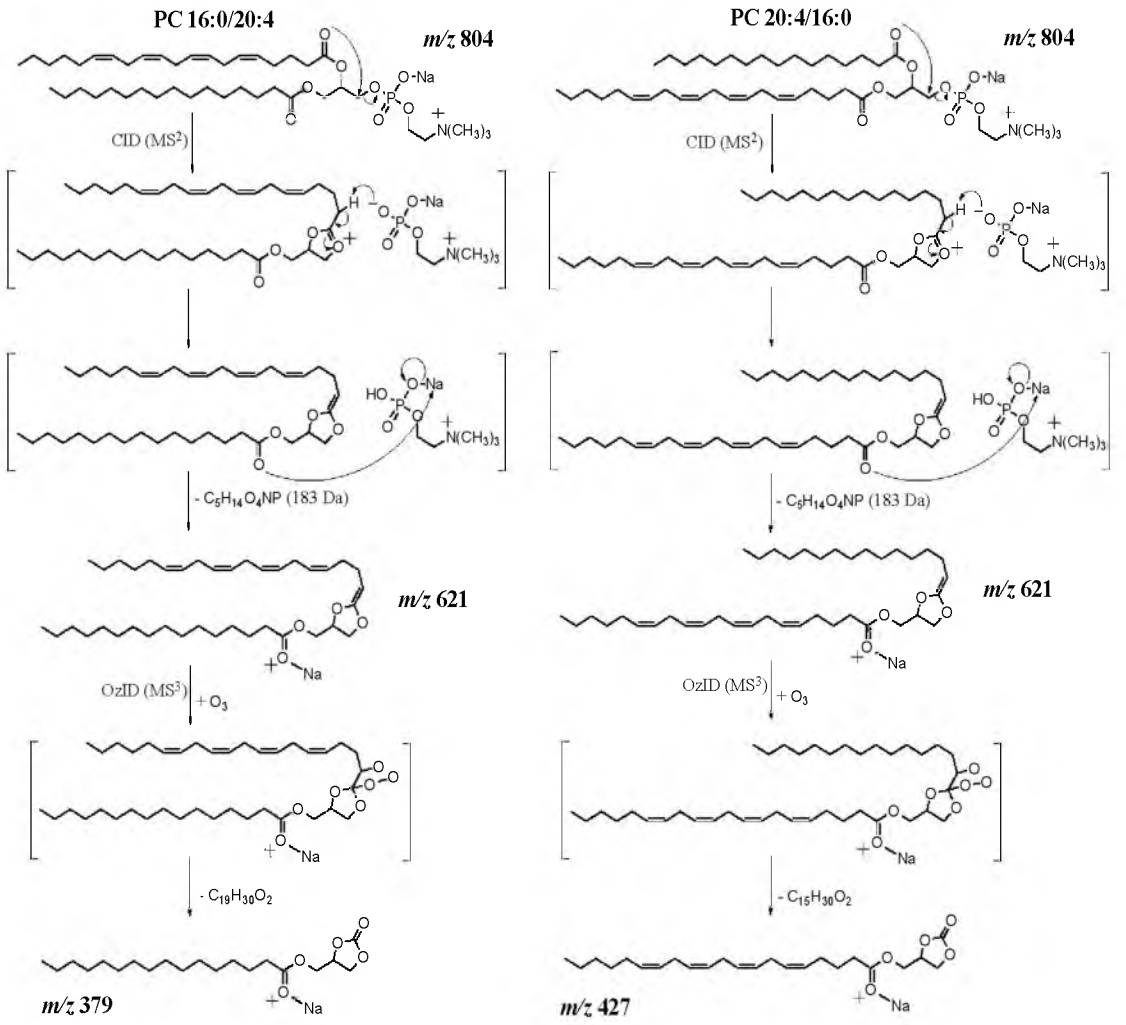

Scheme 3.1 CID/OzID dissociation of *sn*-positional isomers PC 16:0/20:4 and PC 20:4/16:0.

Aldehyde product ions are shown. Criegee ions are not shown but are 16 Da heavier than the aldehydes (*cf.* Table 3.1) and arise from incorporation of an additional oxygen atom upon ozonolysis.

Using a similar LC-MS protocol to that described above, a synthetic standard provided as 1-palmitoyl-2-docosahexaenoyl-*sn*-glycero-3-phosphocholine (annotated here as PC 16:0/22:6) was examined. The resulting LC and mass spectral data are summarized in Figure 3.2. The total ion chromatogram for ions of *m/z* 828 is illustrated in Figure 3.2(a) and shows two features with maxima at 41.4 and 42.8 min, respectively. These features correspond to the $[M+Na]^+$ cation of phosphatidylcholines with a sum composition of PC 38:6. By analogy with the

previous example, the early eluting feature would be expected to arise from the less abundant PC 22:6/16:0 isomer while the more abundant, late-eluting feature can be tentatively assigned to PC 16:0/22:6. CID/OzID mass spectra acquired over each chromatographic peak are shown in Figures 3.2(b) and (c) and among other features, show product ions consistent with neutral losses of 194 and 266 Da, respectively. These signature transitions indicate that the *sn*-2 acyl chain is 16:0 for the first, earlier-eluting peak and 22:6 for the second (*cf.* Table 3.1) thus confirming the assignment based on relative retention time. Integration of the chromatographic peaks in Figure 3.2(a) indicates that this phosphatidylcholine sample, is composed of approximately 79% PC (16:0/22:6) and 21% of the alternate PC (22:6/16:0) isomer.

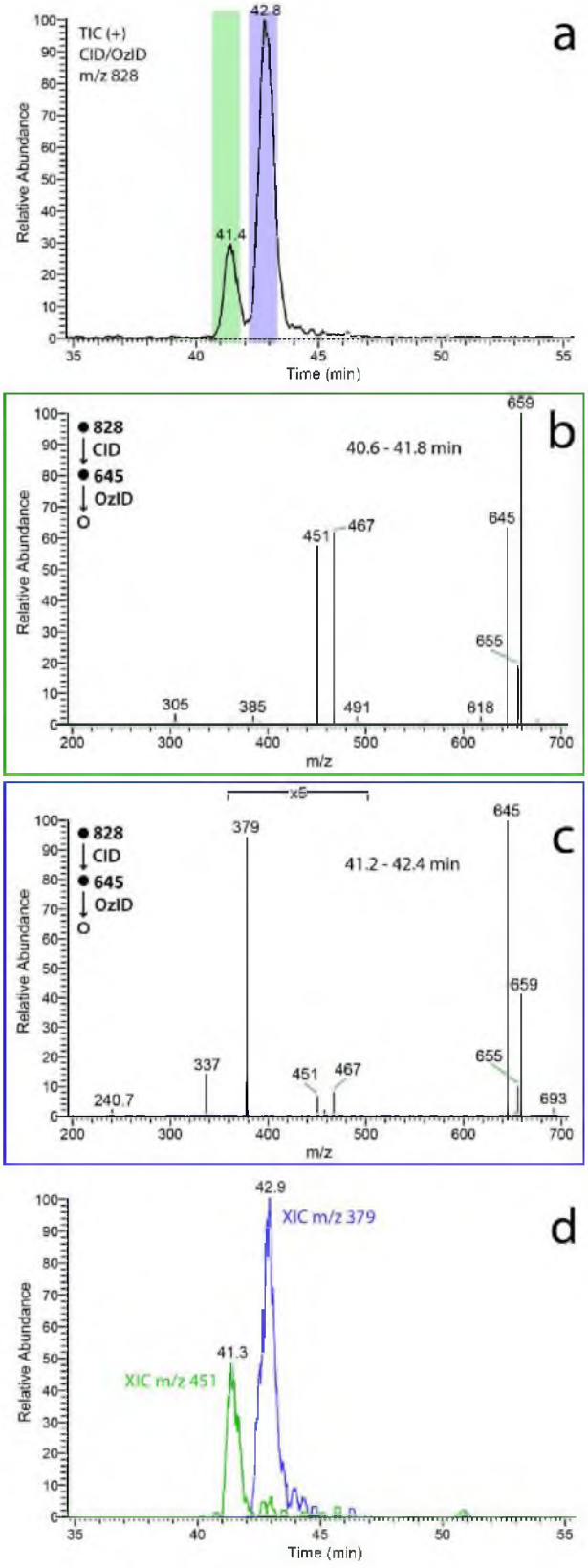

Figure 3.2 LC-MS analysis of synthetic standard provided as PC 16:0/22:6.

Shown above is (a) the total ion chromatogram for LC-CID/OzID of *m/z* 828. (b) The CID/OzID spectrum obtained from integrating across the chromatographic peak between 40.6-41.8 min. (c) The CID/OzID spectrum obtained from integrating across the chromatographic peak between 41.2-42.4 min. (d) The extracted ion chromatogram for CID/OzID product ions at *m/z* 451 (indicative of PC 22:6/16:0) is shown in green, while the extracted ion chromatogram for *m/z* 379 (indicative of PC 16:0/22:6) is shown in blue.

Chromatographic separation of *sn*-positional isomers has previously been shown to become more challenging as the level of unsaturation in the acyl chains is reduced and the difference in the relative lengths of the acyl chains is reduced.[153] Therefore, to challenge the LC-CID/OzID protocol developed here a sample was prepared consisting of an approximately 1:1 mixture of synthetic phosphatidylcholines supplied as 1-palmitoyl-2-oleoyl-*sn*-glycero-3-phosphocholine (annotated here as PC 16:0/18:1) and 1-oleoyl-2-palmitoyl-*sn*-glycero-3-phosphocholine (annotated here as PC 18:1/16:0). The chromatographic and mass spectral results from analysis of this mixture are summarized in Figure 3.3. The total ion chromatogram for all signals deriving from *m/z* 782, corresponding to the $[M+Na]^+$ of lipids with the sum composition of PC 34:1, is shown in Figure 3.3(a) and provides only a single broad feature with no resolution between the two components of the mixture. CID/OzID mass spectra averaged across data points from the early-eluting and late-eluting portions of the chromatographic peak (indicated by the green and blue boxes in Figure 3.3a) are shown in Figures 3.3(b) and (c), respectively. These mass spectra share the same product ions, with peaks at *m/z* 405 and 421 indicative of a 16:0 chain at the *sn*-2 position (*i.e.*, PC 18:1/16:0) and peaks at *m/z* 379 and 395 that are consistent with the 18:1 chain occupying the *sn*-2 position (*i.e.*, PC 16:0/18:1). Importantly, the relative abundance of these characteristic product ion pairs changes across the chromatographic peak. Spectra obtained during the early-eluting part of the peak show *m/z* 405 and 421 at higher abundance than the *m/z* 379 and 395 ion pair (Figure 3.3b), while in contrast the latter ions are more abundant in spectra obtained from the peak tail (Figure 3.3c). The mass spectral data thus indicate that two isomer populations are being partially separated on the reversed-phase column with PC 18:1/16:0 being more concentrated at shorter

retention times while PC 16:0/18:1 dominates at longer retention times; consistent with relative retention time trends for other phosphatidylcholines as described above (*cf.* Figures 3.1 and 3.2). While the total ion chromatogram shows no clear resolution of the isomer populations these can be easily visualized in the extracted ion chromatograms for the ions at *m/z* 405 and 379 shown in Figure 3.3(d). This example serves to highlight the unique capabilities of combining reversed phase chromatography with the characteristic and abundant mass spectral signatures obtained from CID/OzID analysis.

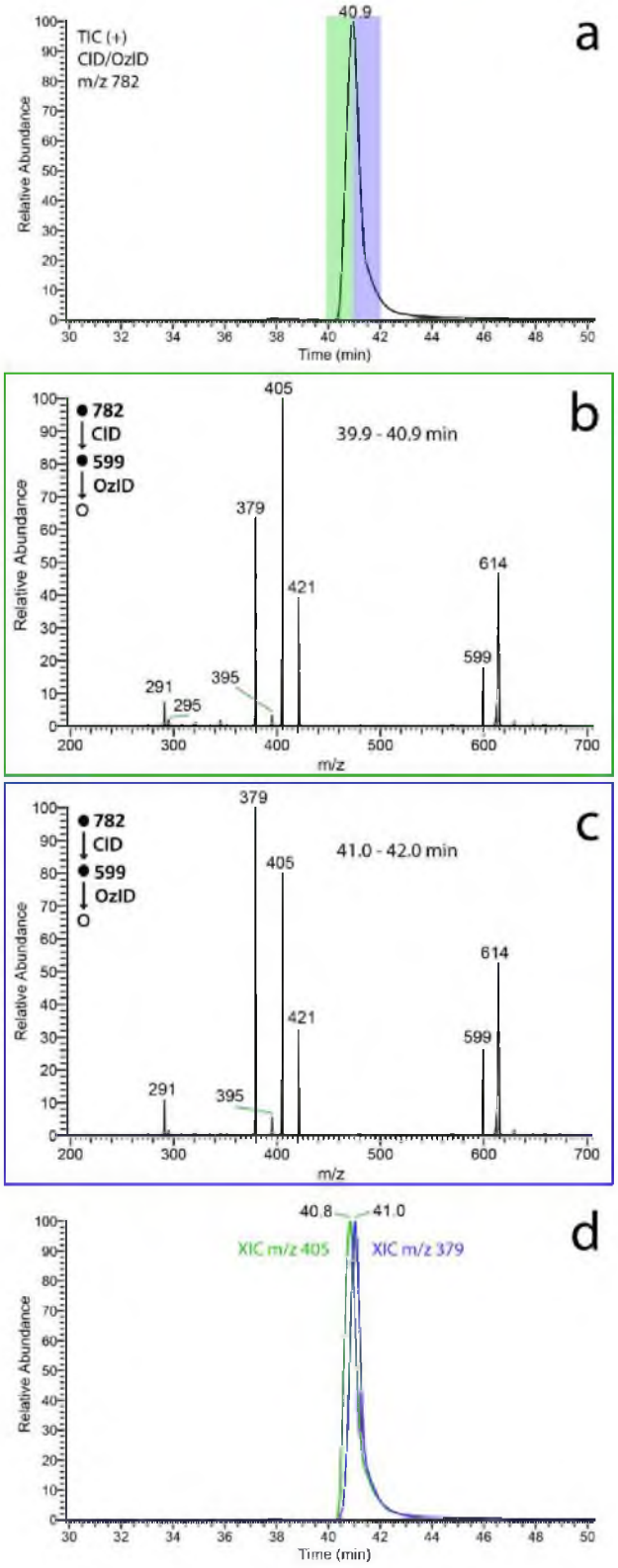

Figure 3.3 LC-MS analysis of a 1:1 mixture of two synthetic standards provided as PC 16:0/18:1 and PC 18:1/16:0.

Shown above is (a) the total ion chromatogram for LC-CID/OzID of *m/z* 782. (b) The CID/OzID spectrum obtained from integrating across the chromatographic peak between 39.9-40.9 min. (c) The CID/OzID spectrum obtained from integrating across the chromatographic peak between 41.0-42.0 min. (d) The extracted ion chromatogram for CID/OzID product ions at *m/z* 405 (indicative of PC 18:1/16:0) is shown in green, while the extracted ion chromatogram for *m/z* 379 (indicative of PC 16:0/22:6) is shown in blue.

3.4.2 Implications for dissociation and oxidation mechanisms

Efforts to understand the unimolecular mechanisms for the dissociation of ionized glycerophospholipids in the past, have been hampered by the presence of lipid isomers. As illustrated here, the synthetic glycerophospholipids routinely used in such studies, typically represent a mixture of both *sn*-positional isomers. The chromatographic separation achieved here however, enables the tandem mass spectra of each phosphatidylcholine isomer to be separately acquired and the mechanisms of the underlying CID/OzID ion activation processes investigated. Comparing the spectra in Figure 3.1(b) and (c) reveals several interesting differences. Outside of the characteristic ions already discussed, the product ion apparent at *m/z* 635 is the base peak in Figure 3.1(b) while it is only a minor contributor to the spectrum in Figure 3.1(c). This signal has previously been assigned to the addition of oxygen to the mass-selected $[M+Na-183]^+$.[102] The fragile nature of this ion leads to peak tailing and the assignment of an apparent *m/z* 635 in centroid mode rather than the true *m/z* 637.[169] The greater abundance of this feature correlates with the presence of the polyunsaturated chain at the *sn*-1 position and is consistent with other polyunsaturated phosphatidylcholines (*cf. m/z* 659 in Figure 3.2b). Also of note is that the *m/z* 427 and 443 ions that dominate in Figure 3.1(b) are also present, albeit at low abundance, in Figure 3.1(c). The converse does not apply; with no significant *m/z* 379 contributions to the spectrum in Figure 3.1(b). This is best illustrated in the extracted ion chromatograms for the diagnostic ions at *m/z* 427 and *m/z* 379 shown in green and blue, respectively in Figure 3.1(d). While the *m/z* 379 trace follows exactly the chromatographic profile of the peak at 46.4 min, the *m/z* 427 trace shows features arising from both isomers. A similar - although less pronounced - phenomenon is observed for the extracted ion chromatograms shown in Figure 3.2(d) where the *m/z* 379 signal is exclusive to the peak at 42.9 min, while the *m/z* 451

signal is dominant for the peak at 41.3 min but also has some abundance for the feature at 42.9 min. This is better illustrated in the chromatograms provided as Supplementary Materials in Appendix B (Figure 7.1) where a higher concentration of the lipid was loaded onto the column. Taken together, these observations provide new insight into the possible mechanisms of ion dissociation for the different *sn*-positional isomers. That is, upon collision-induced dissociation the [(PC 16:0/20:4)+Na]$^+$ and [(PC 16:0/22:6)+Na]$^+$ cations undergo loss of the headgroup exclusively driven by the ester of the *sn*-2 acyl chain (*cf.* Scheme 3.1). In contrast, the isomeric [(PC 20:4/16:0)+Na]$^+$ and [(PC 22:6/16:0)+Na]$^+$ cations may exhibit competition between nucleophilic attack from the *sn*-2 and *sn*-1 acyl chains resulting in isomeric 5- and 6-membered dioxalane structures (Scheme 3.2, pathways a and b, respectively). Alternatively, a small proportion of energetic [M+Na-183]$^+$ ions may isomerise *via* a transacylation pathway such as that shown in Scheme 3.3. Differentiating the mechanistic possibilities in Schemes 2 and 3 is not possible based on available data, however these results suggest that the mechanism of dissociation can be influenced by the relative *position* and *identity* of the acyl chains. These experimental observations are consistent with recent computational studies of the unimolecular dissociation of triacylglycerols where both the relative energetics and entropy were found to play a role.[170]

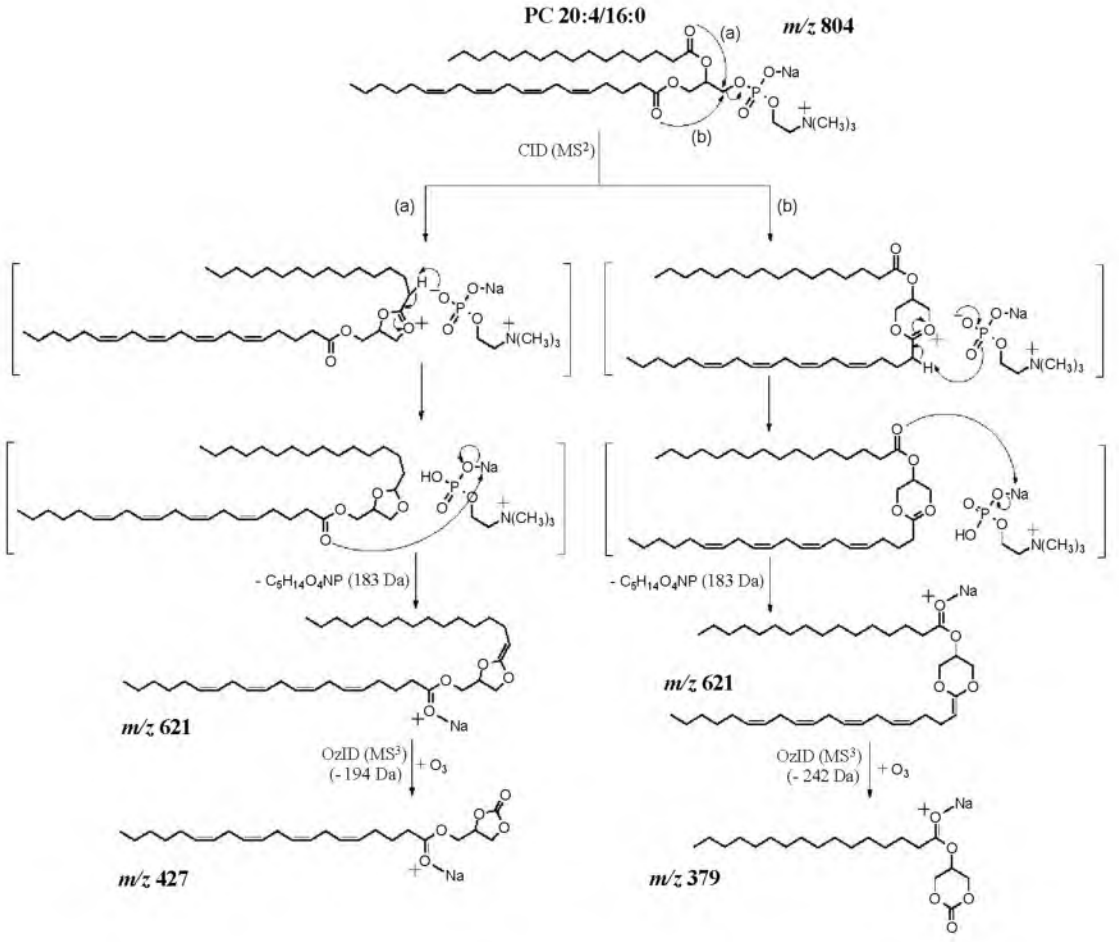

Scheme 3.2 Competition between 5- and 6-membered ring formation in the CID of the [M+Na]+ ions of PC 20:4/16:0.

This competition could account for the low abundant *m/z* 379 product ions observed in the CID/OzID spectrum of this isomer.

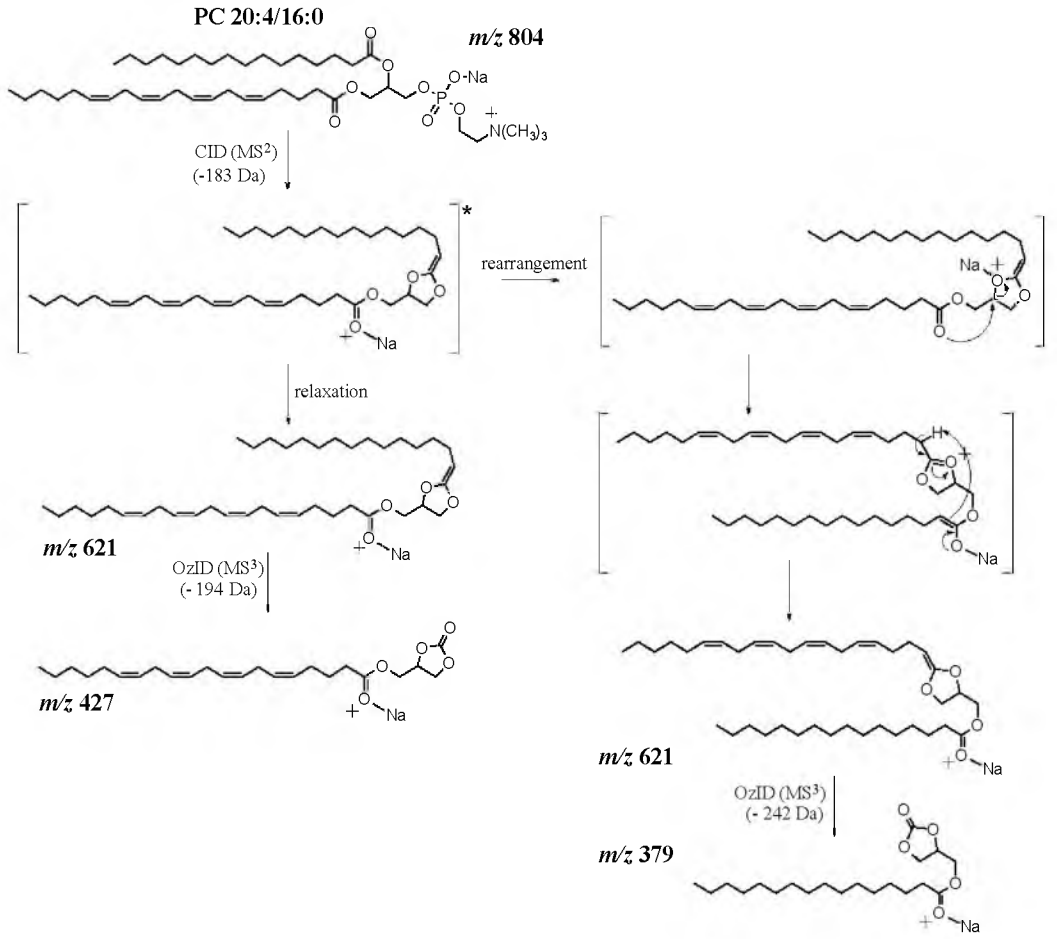

Scheme 3.3 Possible isomerisation of energetic [M+Na-183]+ ions via a unimolecular trans-acylation pathway following CID of [PC 20:4/16:0+Na]+.

This isomerization may account for the low abundant *m/z* 379 product ions observed in the CID/OzID spectrum of this isomer.

3.5 Conclusions

Consistent with prior work, the separation of *sn*-positional isomers of phosphatidylcholines can be achieved using reversed-phase HPLC, provided that the acyl chains are of sufficiently different lengths and degrees of unsaturation. In general, the isomer with the unsaturated chain occupying the *sn*-1 (*e.g.*, PC 20:4/16:0) position elutes first while the isomer with the unsaturated chain at the *sn*-2 position is more strongly retained on the reversed phase column (*e.g.*, PC 16:0/20:4). The novel CID/OzID ion activation approach yields tandem mass spectra with abundant product ions diagnostic of the relative position of the acyl chains on

the glycerol backbone. The data presented indicate that CID/OzID spectra can be readily obtained on the chromatographic timescale and enable simple identification of the isomers and thus unequivocal assignment of chromatographic features. In the future, these protocols could be programmed into data-dependent workflows with consecutive CID and CID/OzID events triggered on abundant lipid ions as they exit the column and enter the mass spectrometer.

The product ions obtained in the LC-CID/OzID mass spectra are generally of higher abundance and more selective (although not exclusive) than conventional CID mass spectral signatures used for this purpose.[99] This is illustrated by the fact that extracted ion chromatograms can be obtained from these diagnostic ions, which can assist in resolving isomers that are not completely separated on LC (*cf.* Figure 3.3d). While it is tempting to suggest that these extracted ion chromatograms could provide a convenient means to quantify the relative proportions of *sn*-positional isomers, we note that the reaction efficiencies of the different isomeric forms can be substantially different; compare, for example, the peak abundances in Figure 3.1(a) with the extracted ion chromatograms in Figure 3.1(d). Future work will endeavour to better understand and calibrate these response factors to enable relative quantification in complex mixtures.

Finally, undertaking CID/OzID analysis of chromatographically resolved *sn*-positional isomers has provided new insight into the differences in dissociation behaviour of ionized phospholipids. Our prior work had implied that the CID of $[PC+Na]^+$ were largely independent of acyl chain identity.[102] These new data however, suggest that the nature of the acyl chains, as well as their position on the glycerol backbone, can affect the mechanisms of dissociation and thus potentially the structure and branching ratio of product ions.

4 A RAPID AMBIENT IONIZATION-MASS SPECTROMETRY APPROACH TO MONITORING THE RELATIVE ABUNDANCE OF ISOMERIC GLYCEROPHOSPHOLIPIDS

4.1 Abstract

Glycerophospholipids with two, non-equivalent fatty acyl chains can adopt one of two isomeric forms depending on the relative position of substitutions on the glycerol backbone. These so-called *sn*-positional isomers can have distinct biophysical and biochemical behaviours making it desirable to uniquely assign their regiochemistries. Unambiguous assignment of such similar molecular structures in complex biological extracts is a significant challenge to current analytical technologies. We have recently reported a novel mass spectrometric method that combines collision- and ozone-induced dissociation in series (CID/OzID) to yield product ions characteristic of acyl chain substitution patterns in glycerophospholipids. Here phosphatidylcholines are examined using the CID/OzID protocol combined with desorption electrospray ionization (DESI) to facilitate the rapid exploration of sample arrays comprised of a wide variety of synthetic and biological sources. Comparison of the spectra acquired from different extracts reveals that the *sn*-positional isomers PC 16:0/18:1 and PC 18:1/16:0 (where the 18:1 chain is present at the *sn*-2 and *sn*-1 position of the glycerol backbone, respectively) are most often found together in lipids of either natural or synthetic origin. Moreover, the proportions of the two isomers vary significantly between extracts from different organisms or even between adjacent tissues from the same organism.

4.2 Introduction

Glycerophospholipids are amphiphilic molecules comprised of a hydrophilic headgroup anchored by a phosphate ester to one of the terminal positions of the glycerol backbone with one or two hydrophobic fatty acids esterified at the remaining hydroxyl positions.[171] This substitution of the glycerol results in chirality about the central carbon with the relative positions of headgroup and acyl chain attachment defined by a *stereospecific numbering* (*sn*) convention.[15] For

glycerophospholipids found in eukaryotes, the headgroup is typically esterified at the *sn*-3 position of the glycerol backbone with the fatty acyl chains attached at the *sn*-1 and *sn*-2 positions. While the chirality of glycerophospholipids is thought to be largely conserved across different organisms, for lipids with non-equivalent fatty acyl chains, two regioisomers are possible with alternate substitutions at the *sn*-1 and *sn*-2 positions. Selective enzymatic digests have been used to examine lipid extracts (*vide infra*) and suggest a general trend for unsaturated fatty acyl chains to be preferentially esterified at the *sn*-2 position.[50] There is a growing body of evidence however, that suggests both *sn*-positional isomers are often present and that their proportions may vary in lipid pools of different origin. For example, Figure 4.1 shows the structures of two *sn*-positional isomers of a phosphatidylcholine substituted with oleic (18:1(9*Z*)) and palmitic (16:0) acids; both of which have been observed in biological extracts.[99, 149, 166] Given the potential for distinct biological function(s) for each *sn*-positional isomer, there is a need for analytical methods that can rapidly distinguish these closely related structures and can monitor their relative proportions within complex matrices.

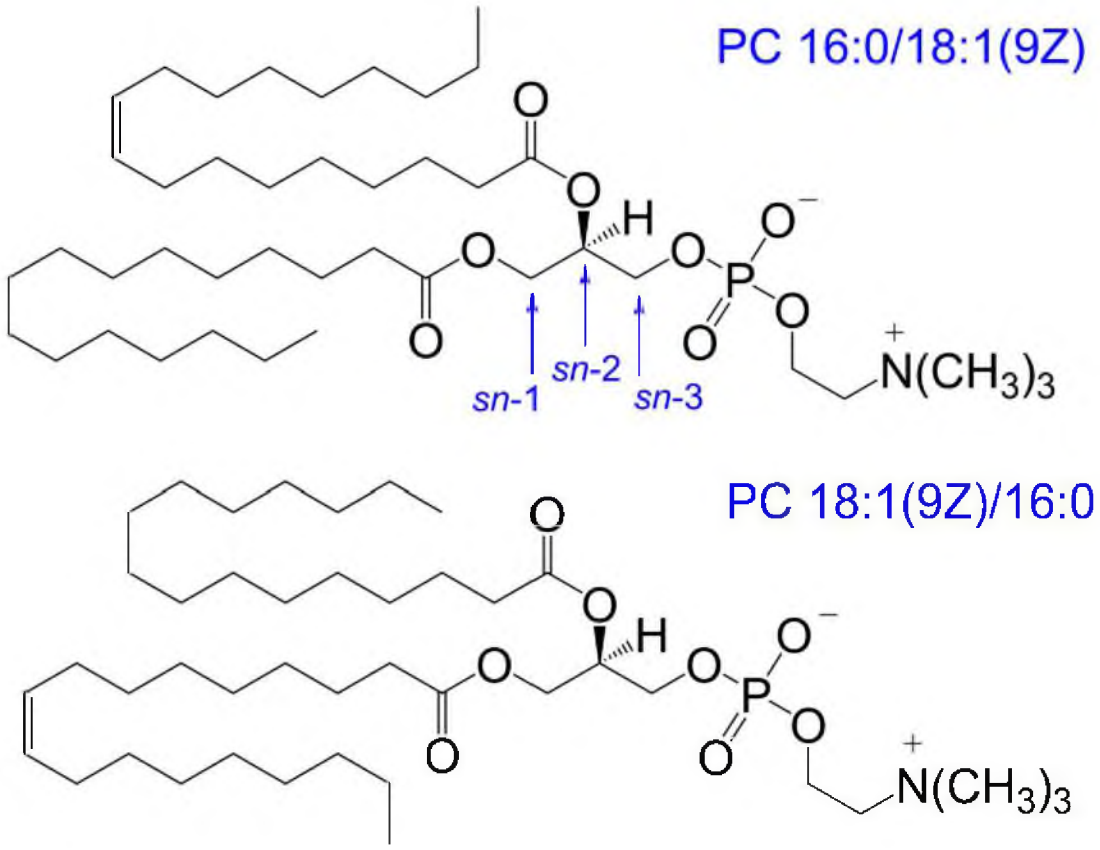

Figure 4.1 Structures of *sn*-positional isomers, PC 16:0/18:1(9Z) and PC 18:1(9Z)/16:0.

Structures of the phosphatidylcholine *sn*-positional isomers, PC 16:0/18:1(9Z) and PC 18:1(9Z)/16:0 that differ only in the relative position of the acyl chains on the glycerol backbone. The stereospecific numbering (*sn*) of carbons of the glycerol backbone is indicated.

Existing research suggests different biophysical and biochemical properties of glycerophospholipid regioisomers that may confer distinct functions on these isomers in nature. For example, differential scanning calorimetry measurements found significantly different melting temperatures for hydrated bilayers composed of the regioisomers, PC 18:0/16:0 or PC 16:0/18:0, where the longer 18:0 acyl chain is substituted at the *sn*-1 or *sn*-2 position, respectively.[172, 173] Indeed, this trend was observed between *sn*-positional isomers of many different acyl chain combinations and headgroup classes (including phosphatidylcholines, phosphatidylethanolamines and phosphatidylglycerols) and results from different self-packing efficiencies of the isomers within the bilayer. Recent molecular dynamics simulations of model membrane bilayers incorporating glycerophospholipids and cholesterol reveal

important interactions between the off-plane methyl groups of the cholesterol and carbon-carbon double bonds in the acyl chains of the phospholipids. The availability of the double bonds for these preferred interactions is affected by the position of substitution of unsaturated acyl chains on the glycerol backbone such that membrane disorder was found to be greater for PC 16:0/18:1, where the unsaturated acyl chain is located at the *sn*-2 position compared with membranes comprised of the PC 18:1/16:0 isomer.[56] The different susceptibilities of isomeric glycerophospholipids to peroxidation have also been demonstrated. When present in liposomes, 1-palmitoyl-2-linoleoyl-3-*sn*-PC (PC 16:0/18:2) was found to be more sensitive to oxidation by aqueous radicals while 1-linoleoyl-2-palmitoyl-3-*sn*-PC (PC 18:2/16:0) was more susceptible to attack by lipid-soluble radicals.[174]

Different biochemical behaviours of glycerophospholipid *sn*-positional isomers have also been shown *in vivo*. For example, enzymes involved in the modification of glycerophospholipids usually have some degree of specificity for certain acyl chains and/or the site of acyl chain attachment on the glycerol backbone. Human lecithin-cholesterol acyltransferase (LCAT), at first believed to exclusively remove the acyl chain at the *sn*-2 position, has now been shown to have substantial activity for removal of specific acyl chains when present at the *sn*-1 position. Interestingly, while human LCAT utilizes 16:0 acyl chains present at the *sn*-2 position of PC, rat LCAT prefers PC with the 16:0 chain at *sn*-1.[175] Many types of secreted phospholipase A_2 (PLA_2) enzymes also have very high specificities for glycerophospholipids containing arachidonic acid (20:4) at the *sn*-2 position.[176] Thus, if both PC 20:4/16:0 and PC 16:0/20:4 are present *in vivo*, PLA_2 will release arachidonic acid almost exclusively from the latter isomer.

Despite growing evidence of the distinct biochemical and biophysical behaviours of glycerophospholipid *sn*-positional isomers, very little is known about the contribution of lipid isomers to the lipidomes of cells and tissues. This paucity of information arises, in part, from the lack of analytical techniques that are capable of (i) the confident assignment of the positions of acyl chain substitution in glycerophospholipids; and (ii) the rapid assessment of the relative proportions of *sn*-positional isomers within a complex biological sample. Historically, PLA_2 assays of

lipid extracts (or simplified fractions thereof) have used gas chromatography to identify the fatty acids released from the *sn*-2 positions of all glycerophospholipids present.[42, 46, 50, 52] Such approaches provide a global picture of how fatty acyl chains are distributed throughout the lipidome or within a headgroup-class fraction but do not directly identify the substitution pattern(s) at the molecular level.

Modern tandem mass spectrometry approaches enable the rapid identification of the acyl chain composition of a mass-selected lipid ion. This is made possible due to product ions indicative of acyl chain length and degree of unsaturation that are present in the collision-induced dissociation (CID) mass spectra of ionized glycerophospholipids. It has been demonstrated that the relative abundance of these diagnostic ions is often affected by the relative position of substitution on the glycerol backbone and, with care, it can be used to assign the structure of the more abundant *sn*-positional isomer present in an extract. Perhaps the most specific example involves tandem mass spectrometry in negative ion mode where many glycerophospholipids dissociate to yield lysophospholipid product ions from the loss of the acyl chain at the *sn*-2 position.[99, 166, 177] Extracting the relative proportions of the *sn*-positional isomers using such methods relies on comparing the abundances of these product ions. Such signals, however, are often of low intensity and their relative abundance can also be affected by differences in lipid structure (*e.g.*, the identity of lipid headgroup and/or fatty acyl chains); the instrument geometry (*e.g.*, ion-trap versus beam-type mass spectrometers); and experimental configuration (*e.g.*, the collision energy applied).[99, 149] Such ambiguity in CID data often results in incorrect or over-interpreted reporting of *sn*-position in glycerophospholipids. The identification of this problem has led to new nomenclature for the annotation of lipids based on tandem mass spectra that avoids the assignment of *sn*-position unless it has been explicitly determined (see also Methods - Lipid Nomenclature).[13]

We have recently introduced an alternative ion activation method that combines collision- with ozone-induced dissociation (OzID).[102, 144, 178] In this strategy, $[M+Na]^+$ ions formed from glycerophospholipids during electrospray ionization (ESI) are mass-selected and subjected to CID to remove the headgroup; the resulting

product ion is then mass-selected and allowed to react with ozone in an ion trapping region of the mass spectrometer. In contrast to conventional CID approaches, CID/OzID mass spectra show highly abundant product ions that can identify the acyl chain at the *sn*-2 position. Indeed, where both *sn*-positional isomers are present, the relative abundance of the diagnostic CID/OzID ions correlates strongly with the relative proportions of the two lipids.[149] CID/OzID mass spectra can be rapidly acquired and thus the approach can be exploited to survey large numbers of biological samples and to explore isomeric variations between lipid extracts. Conducting such studies using conventional infusion ESI approaches however, runs the risk of contamination by carryover and would thus be rate limited by the time required to purge the system between samples. To circumvent these limitations, we have exploited desorption electrospray ionization (DESI) to enable rapid screening of lipid extract arrays and also examination of lipids directly from tissue sections.[106] Combining DESI with the novel CID/OzID ion activation protocol for the first time, has yielded new insight into the isomeric composition of glycerophospholipids within a diverse range of extracts and also demonstrates how the relative populations of *sn*-positional isomers can vary appreciably, even between adjacent tissues.

4.3 Materials and Methods

4.3.1 Materials

All solvents used, including water, were Optima LCMS grade (Thermo Fisher Scientific, Scoresby, VIC, Australia). Butylated hydroxytoluene (BHT) was purchased from Sigma-Aldrich (St. Louis, MO, USA). Ammonium chloride and sodium acetate were analytical grade and purchased from Ajax Chemicals (Auburn, NSW, Australia). Industrial-grade compressed oxygen was purchased from BOC (Cringila, NSW, Australia). Synthetic glycerophospholipid standards PC 18:1(9*Z*)/18:1(9*Z*) (1,2-di-(9*Z*-octadecenoyl)-*sn*-glycero-3-phosphocholine); PC 16:0/18:1(9*Z*) (1-hexadecanoyl-2-(9*Z*-octadecenoyl)-*sn*-glycero-3-phosphocholine); PC 18:1(9*Z*)/16:0 (1-(9*Z*-octadecenoyl)-2-hexadecanoyl-*sn*-glycero-3-phosphocholine); PC 18:0/18:1(9*Z*) (1-octadecanoyl-2-(9*Z*-octadecenoyl)-*sn*-glycero-3-phosphocholine); and PC 18:1(9*Z*)/

18:0 (1-(9Z-octadecenoyl)-2-octadecanoyl-*sn*-glycero-3-phosphocholine) were purchased from Avanti Polar Lipids, Inc. (Alabaster, AL, USA). *L*-α-Phosphatidylcholine from egg yolk was purchased from Sigma-Aldrich (St. Louis, MO, USA) and all biological tissues used for extractions and tissue sections were purchased from Kieraville Butchery (Kieraville, NSW, Australia). Where available, biological replicates were obtained and these details are provided as Supplementary Materials in Appendix C (see footnote to Table 8.1).

4.3.2 Lipid Nomenclature

Lipid nomenclature used here is guided by the recommendations of the Lipid MAPS consortium and the recent suggestions of Liebisch *et al.* for mass spectrometry derived data.[13, 146] Briefly, the number of carbon atoms present in an acyl chain is written before the colon and the number of double bonds after the colon, such that "18:1" represents an acyl chain containing 18 carbon atoms and 1 double bond. If the double bond positions are known, these are noted in brackets after the acyl chain double bond number, as counted from the carboxyl carbon of the fatty acid, *e.g.*, 18:1(9). If the *E*/*Z* configurations of the double bonds are known, they are noted within brackets immediately after each corresponding double bond position, *e.g.*, 18:1(9*Z*). For glycerophospholipids, the headgroup class is indicated by the two letter abbreviation, *e.g.*, phosphatidylcholine is presented as PC and the acyl chains at the (*stereospecifically numbered*) *sn*-1 and *sn*-2 positions are presented before and after the forward slash, respectively (*e.g.*, PC 16:0/18:1 indicates 16:0 at the *sn*-1 position and 18:1 at the *sn*-2 position). Where the acyl chain composition is known but the relative positions of the chains on the glycerol backbone are uncertain, or a mixture of isomers may be present, the acyl chains are separated by an underscore, *e.g.*, PC 16:0_18:1.

4.3.3 Sample Preparation

The synthetic glycerophospholipid standards, PC 16:0/18:1(9*Z*), PC 18:1(9*Z*)/16:0, PC 18:1(9*Z*)/18:1(9*Z*), PC 18:0/18:1(9*Z*) and PC 18:1(9*Z*)/18:0, were each separately dissolved to a final concentration of 200 μM in acetonitrile/2-propanol

(50/50, v/v). Egg yolk extract was weighed then dissolved in acetonitrile/2-propanol (50/50, v/v) to an approximate final concentration of 175 μM total lipid. For biological tissues 15-150 mg of tissue was dissected and extracted using a modified Folch extraction method.[142, 145] Briefly, dissected tissues were homogenized using a bead homogenizer (glass beads, 1 mm diameter) and extracted using methanol/chloroform (33/67 v/v). The organic extract was washed three times with water, and once with aqueous ammonium chloride (50 mM) before being dried under a stream of nitrogen and redissolved with 750 μL of acetonitrile/2-propanol (50/50, v/v). Aliquots (3 μL) of the lipid solutions were deposited onto PTFE sample spots on dedicated glass slides (Prosolia, Indianapolis, IN, USA) for DESI analysis. Technical replicates of each standard or extract were prepared, with each solution applied to a minimum of four PTFE spots that were rapidly air dried (*ca.* 5 mins) and immediately stored. Sample arrays were stored in an airtight box at -80 °C to avoid unwanted oxidation by ambient ozone (see also Supplementary Materials, Appendix C, Figure 8.3).[179, 180]

For direct tissue analysis, one hemisphere of sheep brain cerebrum was flash frozen at -80 °C and coronal slices were sectioned to a thickness of 30 μm using a Leica cryostat CM1950 (Leica, St Louis, MO, USA) maintained at -17 °C. The sheep brain section was then mounted onto a glass slide and stored at -20 °C until analysis.

4.3.4 Mass Spectrometry

Mass spectra were acquired using an linear ion-trap mass spectrometer operating Xcalibur 2.0 control software (LTQ Thermo Fisher Scientific, San Jose, CA, USA). The instrument has been previously modified to undertake ion-molecule reactions.[181] Ions were generated using a desorption electrospray ionization source fitted with a motorised DESI 2D Source (Prosolia, Indianapolis IN, USA). The LTQ heated capilary inlet was replaced with a modified inlet capillary (Prosolia, Indianapolis IN, USA). The source was configured with the spray emitter tip angled at 55° with respect to the plate, while the height of the emitter tip and the sample stage were both optimized with respect to the inlet to maximize signal intensity. The stage holding the slide was set at 9 mm in the z-axis while the emitter tip was set at 11 mm

in the x-axis, 6 mm in the y-axis and 17 mm in z-axis as determined by the markings on the DESI source. A mixture of acetonitrile and isopropoanol (50/50 v/v) containing sodium acetate (100 μM) was used as the spray solvent at a flow rate of 7 μL/min for analyses of biological extracts and lipid standards and 2 μL/min when sampling directly from tissue. For long acquisitions, a liquid chromatography pump was used to provide a constant flow rate for DESI experiments (Surveyor HPLC system, Thermo Fisher Scientific, San Jose, CA). The DESI sample stage was traversed at rates of 50 - 100 μm/s for analyses of biological extracts and lipid standards and 25 μm/s for tissue sections. Mass spectrometer parameters used were as follows: ionspray voltage 5.00 kV; capillary temperature 275 °C; the capillary voltage -35.0 V; and tube lens 125.0 V. Automatic gain control was turned on (as is the default) but ion counts were typically low and thus the instrument always operated with the maximum ion injection time of 500 ms. Under these conditions limits of detection for a single phosphtaidylcholine on a PTFE spot were estimated at 40 fmol. CID/OzID spectra were obtained by operating the mass spectrometer in MS^3 mode with ozone present in the ion trapping region. CID of the mass-selected $[M+Na]^+$ precursor ion (isolation width 5 Th) was performed with a normalized collision energy of 38 (arbitrary units) and an activation time of 30 ms. The targeted $[M+Na-183]^+$ product ion was then isolated (isolation width 3 Th) and trapped for 200 ms in the presence of ozone before mass-selective ejection of all ions from the trap. Experimental parameters for ozone-induced dissociation on this platform have been previously described and involve the introduction of ozone generated off-line and collected in a plastic syringe.[139, 167] Recent modifications to this procedure enable online generation and supply of ozone (see Supplementary Materials, Appendix C, Figure 8.1 for a schematic of the instrument configuration), providing a stable concentration of ozone over extended periods.[140, 147] Both methods have been used to obtain the CID/OzID spectra reported herein and these are indicated throughout as "offline" and "online", respectively (see also Supplementary Materials, Appendix C, Figure 8.2 and associated discussion). Spectra used in this study represented an average of *ca.* 30-70 individual scans.

4.4 Results and Discussion

4.4.1 Results

The ability of the DESI-CID/OzID method to distinguish *sn*-positional isomers of glycerophospholipids was examined using a pair of synthetic phosphatidylcholine standards namely, PC 16:0/18:1(9*Z*) and PC 18:1(9*Z*)/16:0. Each compound was prepared in acetonitrile/2-propanol and the solutions were loaded onto arrays of PTFE spots on glass sample slides before being dried and subjected to DESI analysis. Abundant $[M+Na]^+$ ions were observed from the lipids deposited on each spot and these ions were then subjected to CID in the ion-trap mass spectrometer to yield the abundant $[M+Na-183]^+$ product ion resulting from neutral loss of the phosphocholine headgroup.[88, 148] This product ion was then re-isolated and retained in the ion trap in the presence of ozone for 200 ms before the fragment ions were mass analyzed giving the mass spectra shown in Figure 4.2.

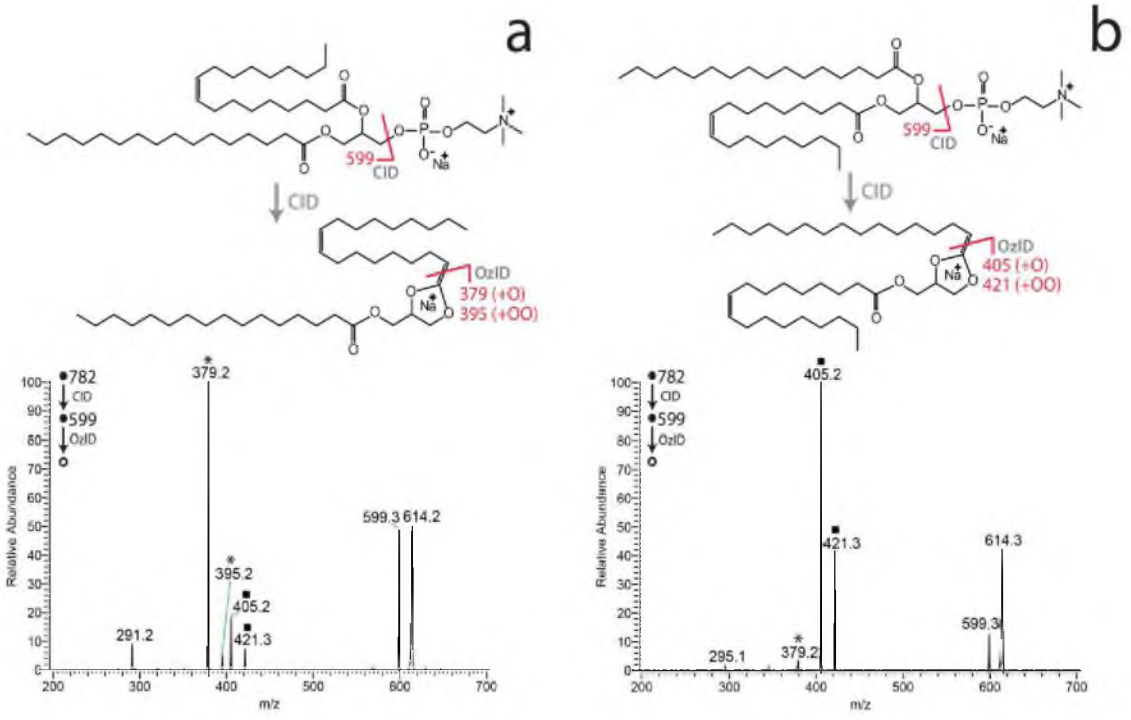

Figure 4.2 DESI-CID/OzID mass spectra of synthetic glycerophospholipids.

DESI-CID/OzID mass spectra obtained from $[M+Na]^+$ ions of synthetic glycerophospholipids (a) PC 16:0/18:1(9*Z*) and (b) PC 18:1(9*Z*)/16:0. The CID/OzID peaks indicative of the presence of the 18:1 chain at the *sn*-2 position (*) and 16:0 at the *sn*-2 position (▪) are marked. The dissociation pathways for the two ionized glycerophospholipid *sn*-positional isomers are indicated above the corresponding mass spectra. Putative dissociation pathways are based on the study of Pham *et al.*[102] and full reaction mechanisms for CID and OzID steps are provided as Supplementary Materials in Appendix C (Scheme 8.1). Spectra acquired using offline ozone generation (see Methods).

The DESI-CID/OzID mass spectra obtained for PC 16:0/18:1(9*Z*) and PC 18:1(9*Z*)/16:0 are significantly different with the former dominated by a base peak of *m/z* 379 with a low abundant product ion at *m/z* 405 (Figure 4.2a), while the latter has a base peak at *m/z* 405 with the signal at *m/z* 379 barely visible above the noise (Figure 4.2b). Previous studies identify the ion at *m/z* 379, and its companion peak at *m/z* 395, as resulting from oxidative cleavage of the 18:1 acyl chain from the *sn*-2 position of the glycerol backbone. Conversely, *m/z* 405 and its companion peak at m/z 421 are markers for the presence of the 16:0 acyl chain at the *sn*-2 position. The CID/OzID reaction pathways giving rise to these diagnostic ions have previously been proposed[102] and are summarized above the relevant spectra in Figure 4.2. Full

reaction schemes, based on current understanding of the reaction mechanism, are provided as Supplementary Materials in Appendix C (see Scheme 8.1). Importantly, these CID/OzID product ions can thus be used to identify the isomeric composition of the lipids present on the surface. The presence of the *m/z* 405, 421 ion pair in the spectrum obtained from PC 16:0/18:1(9*Z*) (Figure 4.2a) and conversely the presence of *m/z* 379 in the spectrum obtained from PC 18:1/16:0(9*Z*) (Figure 4.2b) suggest that neither sample is isomerically pure. This observation is consistent with previous mass spectrometric and enzymatic analyses of synthetic glycerophospholipids, which find some abundance of the alternative regioisomer is nearly always present.[99, 149] This is likely a result of acyl chain migration during synthesis procedures.[168]

DESI-CID/OzID mass spectra obtained from both synthetic PC isomers show a broad peak centered on *m/z* 614 (Figure 4.2). This feature has previously been suggested to be a fragile epoxide of *m/z* 615 that dissociates upon mass analysis in the ion trap resulting in an unusual broad peak shape and a lower apparent *m/z* ratio.[102] Putative structures for these ions, based on prior investigations, are provided as Supplementary Materials in Appendix C (see Scheme 8.1) and their appearance as broad, tailing peaks of apparently lower mass is consistent with the well-documented behaviour of fragile ions in ion-trap mass spectrometers.[169, 182] Another interesting observation from the data presented in Figure 4.2 is that the overall conversion of the mass-selected *m/z* 599 into product ions is lower for PC 16:0/18:1(9*Z*) (Figure 4.2a) than for PC 18:1(9*Z*)/16:0 (Figure 4.2b). Given that the time permitted for reaction of the ions at *m/z* 599 with ozone (200 ms) is the same for each isomer, this observation suggests slightly different rates of reaction for the isomeric ions undergoing ozonolysis in each case. As a consequence, for the concentration of ozone and the reaction time employed in this study, a slight detection bias exists in favour of PC 18:1(9*Z*)/16:0 over PC 16:0/18:1(9*Z*). This small bias could be removed by extending reaction times such that *m/z* 599 was completely quenched but this would consequently increase the overall analysis time. Comparison to prior measurements of these standards using alternative methods (see later) suggested that small bias was acceptable given that the aim of this investigation was to develop a method to rapidly probe changes in relative *sn*-

positional isomer populations for comparison between extracts rather than to obtain absolute concentrations for each lipid.

Once optimized for synthetic glycerophospholipids, DESI-CID/OzID analysis was undertaken for lipid extracts obtained from a range of biological sources. Representative mass spectra obtained from *m/z* 782 produced upon DESI of deposited extracts from egg yolk, cow kidney and cow eye lens are shown in Figure 4.3. In all cases the spectra are consistent with the $[M+Na]^+$ ions formed from the abundant monounsaturated phosphatidylcholine, PC 34:1 and show product ions identical to those observed for the PC 16:0_18:1 isomers shown in Figure 4.2. Notably, the relative abundance of product ions compared to *m/z* 599 in the spectra in Figure 4.3 is lower than that shown in Figure 4.2. This reflects the different ozone concentration present in the ion trap when each data set was acquired. Significantly however, the ozone concentration was constant during the acquisition of all spectra in Figure 4.3. As such, the changes in relative abundance of the diagnostic product ions pairs at *m/z* 379, 395 and *m/z* 405, 421 are evidence of different proportions of the *sn*-positional isomers PC 16:0/18:1 and PC 18:1/16:0 in each of the lipid extracts. Even a qualitative comparison of the differences between the spectra shown in Figure 4.3 suggests significant variation in isomeric composition between samples. For example, in the CID/OzID spectrum from egg yolk (Figure 4.3a) the ion pair at *m/z* 379, 395 is dominant with the very little signal for *m/z* 405, 421 detectable above the noise. This suggests that phosphatidylcholines of the form PC 34:1 present in egg yolk comprise almost entirely PC 16:0/18:1. Indeed, the very low abundance of product ions at *m/z* 405, 421 suggests that there is very little of the regioisomer PC 18:1/16:0 present in egg yolk - even less than the isomeric impurity observed for the PC 16:0/18:1 synthetic standard (*cf.* Figure 4.2a). Comparison of the analogous spectra obtained from extracts of cow perinephric adipose tissue and kidney medulla (Figures 4.3b and c) shows the ion pair at *m/z* 379, 395 again dominating the product ion signals but with *m/z* 405, 421 readily observable. These data suggest that PC 16:0/18:1 is still the major isomer in these tissues but - unlike egg yolk - significant amounts of PC 18:1/16:0 are also present. Intriguingly, variation in the relative abundance of the diagnostic product ions is also apparent when comparing spectra

obtained from different regions of the same tissue (*cf.* Figures 4.3b and c). Finally, the CID/OzID spectrum obtained from a cow ocular lens extract shows product ion pairs at *m/z* 379, 395 and *m/z* 405, 421 to be of comparable abundance. This suggests that the isomers PC 16:0/18:1 and PC 18:1/16:0 are likely to be present in near equal abundance in this tissue.

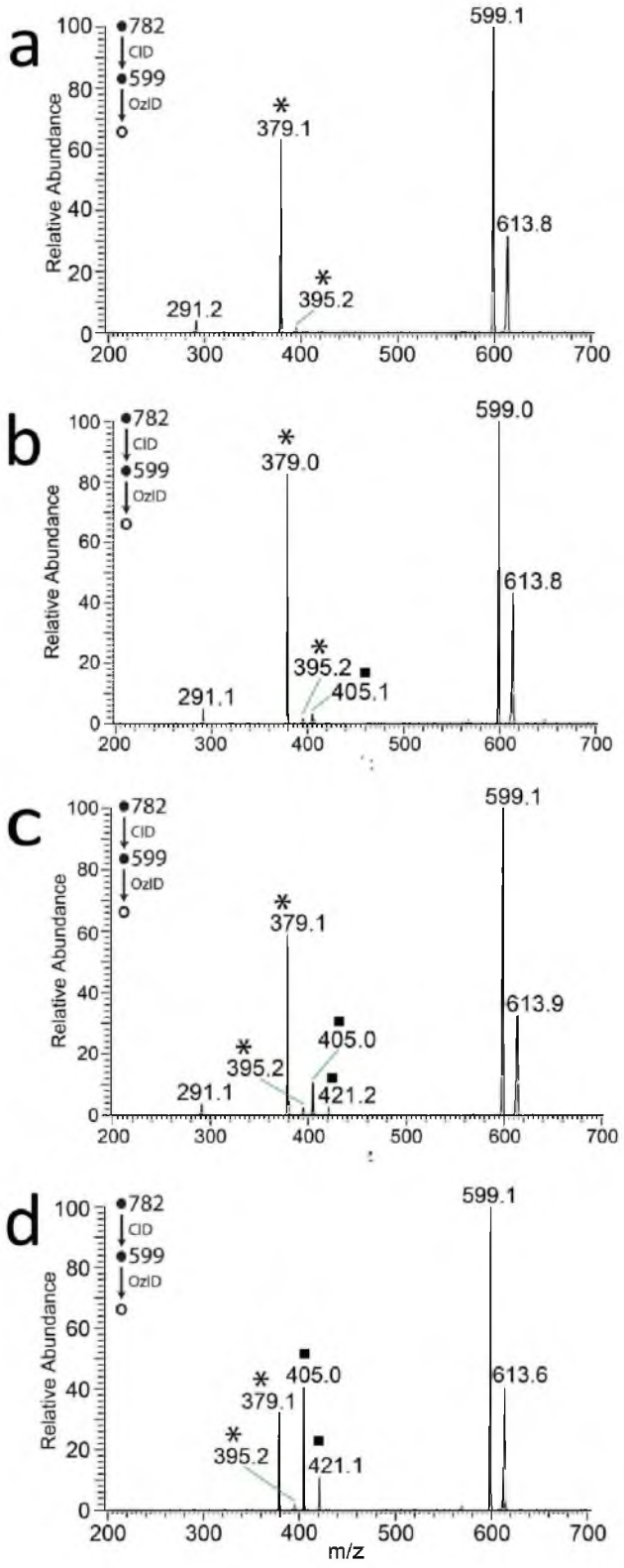

Figure 4.3 DESI-CID/OzID mass spectra obtained from m/z 782 corresponding to PC 34:1 isomers from different biological sources.

DESI-CID/OzID mass spectra obtained from the [M+Na]+ ions at m/z 782 corresponding to PC 34:1 isomers from (a) egg yolk, (b) cow perinephric adipose, (c) cow kidney medulla and (d) cow ocular lens. Peaks indicative of the *sn*-positional isomers PC 16:0/18:1 (*) and PC 18:1/16:0 (▪) are marked as indicated. Spectra acquired using online ozone generation (see Methods).

The DESI interface enabled the rapid acquisition of CID/OzID mass spectra from an array of lipid extracts spotted onto sample slides (see Methods). All DESI-CID/OzID mass spectra of *m/z* 782 ions were dominated by the product ion pairs at *m/z* 379, 395 and *m/z* 405, 421 indicative of the *sn*-positional isomers PC 16:0/18:1 and PC 18:1/16:0, respectively. In some instances, low abundant product ion pairs were also observed at *m/z* 377, 393 and *m/z* 407, 423 which, by analogy to the analysis above, were assigned to the *sn*-positional isomers PC 16:1/18:0 and PC 18:0/16:1, respectively. From the spectra acquired at each spot on the array, the relative contribution of a single isomer to the PC 34:1 lipid population could be estimated by normalizing the abundance (A_i) of the characteristic ion pair for the nominated isomer (*e.g.*, the combined ion abundance [A_{379}+A_{395}] of *m/z* 379 and 395 formed from PC 16:0/18:1 as indicated in Equation 1) to the sum of product ion signals from all four contributors. Combining these data across replicate measurements enabled a more rigorous comparison of changes in isomer profiles between lipid extracts of different biological origins and the results are summarized in Figure 4.4. Estimates of the relative contribution of the PC 16:1/18:0 and PC 18:0/16:1 to the composition PC 34:1 were found to be typically less than 2% (see Supplementary Materials in Appendix C, Table 8.1) and are thus not presented in Figure 4.4.

$$\%\text{PC 16:0/18:1 in PC 34:1} = \frac{[A_{379}+A_{395}]}{[(A_{379}+A_{395})+(A_{405}+A_{421})+(A_{377}+A_{394})+(A_{407}+A_{423})]} \times 100 \quad (1)$$

The estimates of relative contribution shown in Figure 4.4 indicate that the synthetic samples supplied as PC 16:0/18:1(9*Z*) and PC 18:1(9*Z*)/16:0 include levels of the alternate isomer at *ca.* 20% and 2%, respectively. These results are consistent

with recent investigations of synthetic standards using CID/OzID with infusion electrospray, ion-mobility separations and enzymatic assays (see Supplementary Materials in Appendix C, Table 8.2 for comparison).[102, 149] In contrast to the synthetic standard, PC 34:1 in egg yolk was found to be almost exclusively comprised of a single *sn*-positional isomer. With an estimated abundance of 97% PC 16:0/18:1 this extract was found to be the most isomerically pure of any biological sample investigated in this study. Cow kidney tissue (medulla) was found to have both isomers present with PC 16:0/18:1 and PC 18:1/16:0 estimated to comprise 82% and 17%, respectively, of the PC 34:1 population. Interestingly, the analogous tissue in sheep showed a relative amount of the PC 18:1/16:0 isomer of only 6%, while sheep brain tissue had the same isomer present at 15% in white matter and 39% in grey matter. Finally, the estimates in Figure 4.4 confirm the preliminary finding that the PC 18:1/16:0 isomer is likely more abundant than PC 16:0/18:1 in lipid extracts of cow eye lens. While these data do not provide absolute quantification of the isomers present in these extracts, they provide a unique insight into the substantial variation in the relative abundance of these two distinct lipid molecules in samples of different biological origin (Figure 4.4).

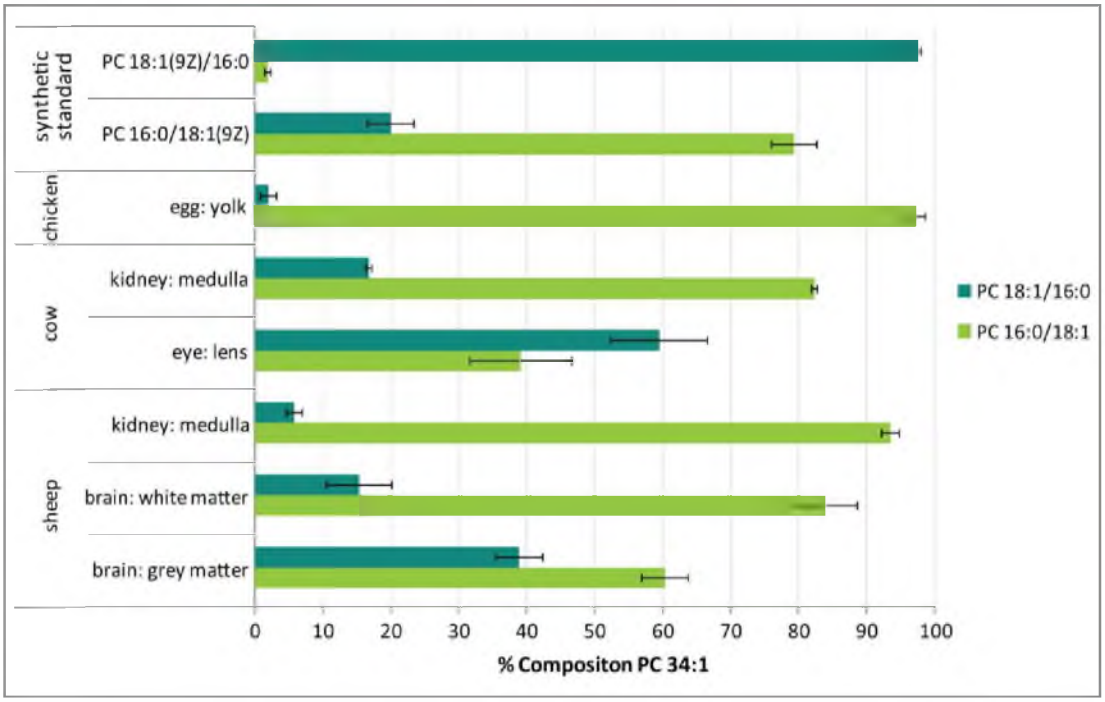

Figure 4.4 Estimated abundance of *sn*-positional isomers of PC 34:1 in biological extracts and synthetic standards.

The estimated abundance of *sn*-positional isomers PC 18:1/16:0 and PC 16:0/18:1 as a percentage of phosphatidylcholines of composition PC 34:1 in different biological extracts and commercially available synthetic standards. Isomer contributions are estimated from the normalized product ion abundances in DESI-CID/OzID mass spectra as described in the text. Product ions assigned to isomers of PC 16:1_18:0 were included in all computations but represented < 2% of the composition and are thus not shown here. All data points represent an average of at least four technical and, where available, biological replicates (see Supplementary Materials in Appendix C, Table 8.1). Uncertainties shown represent standard deviation. This graph was generated using spectra acquired using offline and online ozone generation methods (see Methods).

The data summarized in Figure 4.4 suggest wide variation in isomer contributions to the PC 34:1 lipid population. In an effort to establish if this was unique to phosphatidylcholines of this composition, the isomeric contributions to PC 36:1 were also investigated. The same sample arrays were examined by using sequential CID of mass-selected $[M+Na]^+$ precursor ion at *m/z* 810 and subjecting the abundant product ion $[M+Na-183]^+$ at *m/z* 627 to OzID. Thus obtained, the CID/OzID spectra yielded a series of product ion pairs that could be assigned to the isomers indicated: *m/z* 379, 395 corresponding to PC 16:0/20:1; *m/z* 433, 499 corresponding

to PC 20:1/16:0; *m/z* 407, 423 corresponding to PC 18:0/18:1 and; *m/z* 405, 421 corresponding to PC 18:1/18:0. Comparing the relative peak areas of these diagnostic ions according to an analogous version of Equation 1 enabled an estimate of the relative contribution of these isomers to the total PC 36:1 pool. These data are provided as Supplementary Materials in Appendix C (Table 8.1) and are summarized in Figure 4.5.

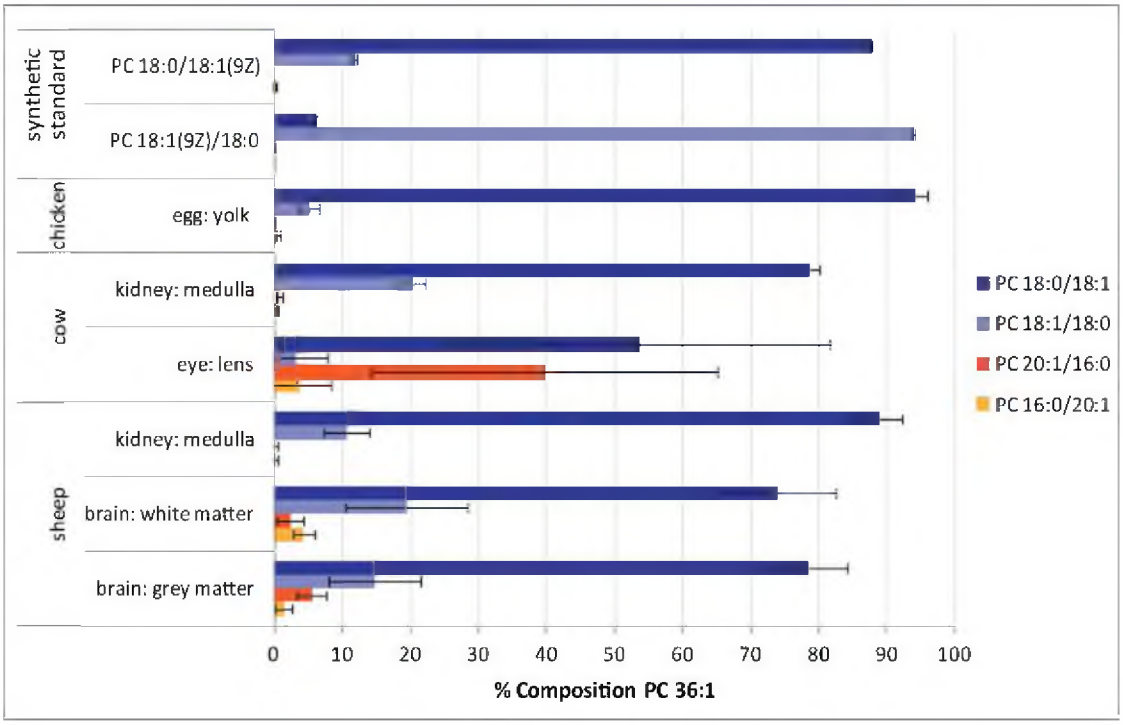

Figure 4.5 Estimated abundance of *sn*-positional isomers of PC 34:1 in biological extracts and synthetic standards.

The estimated abundance of *sn*-positional isomers PC 18:0/18:1; PC 18:1/18:0; PC 20:1/16:0; and PC 16:0/20:1 as a percentage of phosphatidylcholines of composition PC 34:1 in different biological extracts and commercially available synthetic standards. Isomer contributions are estimated from the normalized product ion abundances in DESI-CID/OzID mass spectra as described in the text. All data points represent an average of at least four technical and, where available, biological replicates (see Supplementary Materials in Appendix C, Table 8.1). Uncertainties shown represent standard deviation. This graph was generated using spectra acquired using offline and online ozone generation methods (see Methods).

The data presented in Figure 4.5 suggest that commercially available synthetic standards PC 18:0/18:1(9*Z*) and PC 18:1(9*Z*)/18:0 contain detectable contributions from the alternate *sn*-positional isomer at *ca.* 12% and 6%, respectively.

This is comparable to the data obtained from synthetic lipid PC 16:0/18:1(9Z) and PC 18:1(9Z)/16:0 (see Figure 4.4). Interestingly however, the PC 36:1 pool of lipids in egg yolk shows the presence of both PC 18:0/18:1 at ~94% and PC 18:1/18:0 at ~5% whereas the PC 34:1 lipids in the same extract are comprised almost exclusively of PC 16:0/18:1. For the remaining biological extracts the lower abundance of PC 36:1 compared to PC 34:1 led to lower signal-to-noise in the DESI-CID/OzID spectra obtained from the former. As a result, technical variation was larger in these data; as evidenced by the more substantial standard deviations shown in Figure 4.5. Notwithstanding this variation, the overall trend is of similar abundance ratios of PC 18:0/18:1 to PC 18:1/18:0, with the former being substantially more abundant in every case. These findings contrast with the widely varying ratios of PC 16:0/18:1 to PC 18:1/16:0 reported in Figure 4.4. In a similar way, DESI-CID/OzID analysis was undertaken for lipids of composition PC 34:2 and PC 36:2. The lower abundance of these lipids meant that reliable data could not be obtained across the full sample set and these results are summarized as Supplementary Materials in Appendix C (see Table 8.1).

The observation that adjacent tissue extracts had variation in the relative abundance of *sn*-positional isomers PC 16:0/18:1 and PC 18:1/16:0 (*cf.* grey and white matter extracts in Figure 4.4) suggested that it may be possible to visualise the changing isomer populations from direct analysis of the tissue itself. To examine this, a thin section of sheep brain tissue was prepared, mounted on a glass slide and subjected to DESI-CID/OzID. The data acquired from direct analysis of sheep brain tissue are summarised in Figure 4.6 and show ion chronograms obtained from the single transect of the tissue under the DESI emitter. The extracted ion chronograms of the diagnostic *m/z* 379 and *m/z* 405 product ions plotted in Figure 4.6 can be considered to represent the abundance of PC 16:0/18:1 and PC 18:1/16:0, respectively. These data show that the abundance of the m/z 379 ion remains relatively constant across the tissue boundaries. In contrast, a substantial drop in the relative abundance of the *m/z* 405 ion is observed in white matter compared to grey (see shaded areas in Figure 4.6). This finding suggests that while PC 16:0/18:1 is somewhat evenly distributed throughout the brain, PC 18:1/16:0 is differentially

distributed between grey and white matter. These data represent an important proof-of-principle that this approach can be used to visualise changes in lipid isomer populations in direct tissue analysis. Similar transects were repeated across the entire tissue and the abundance data were reconstructed as mass spectral images. These images are provided as Supplementary Materials in Appendix C (Figure 8.4) but the low signal-to-noise in these data made resolving the different brain regions challenging. Nevertheless, there is some delineation between white and grey matter in the image corresponding to the distribution of PC 18:1/16:0 (Figure 8.4b).

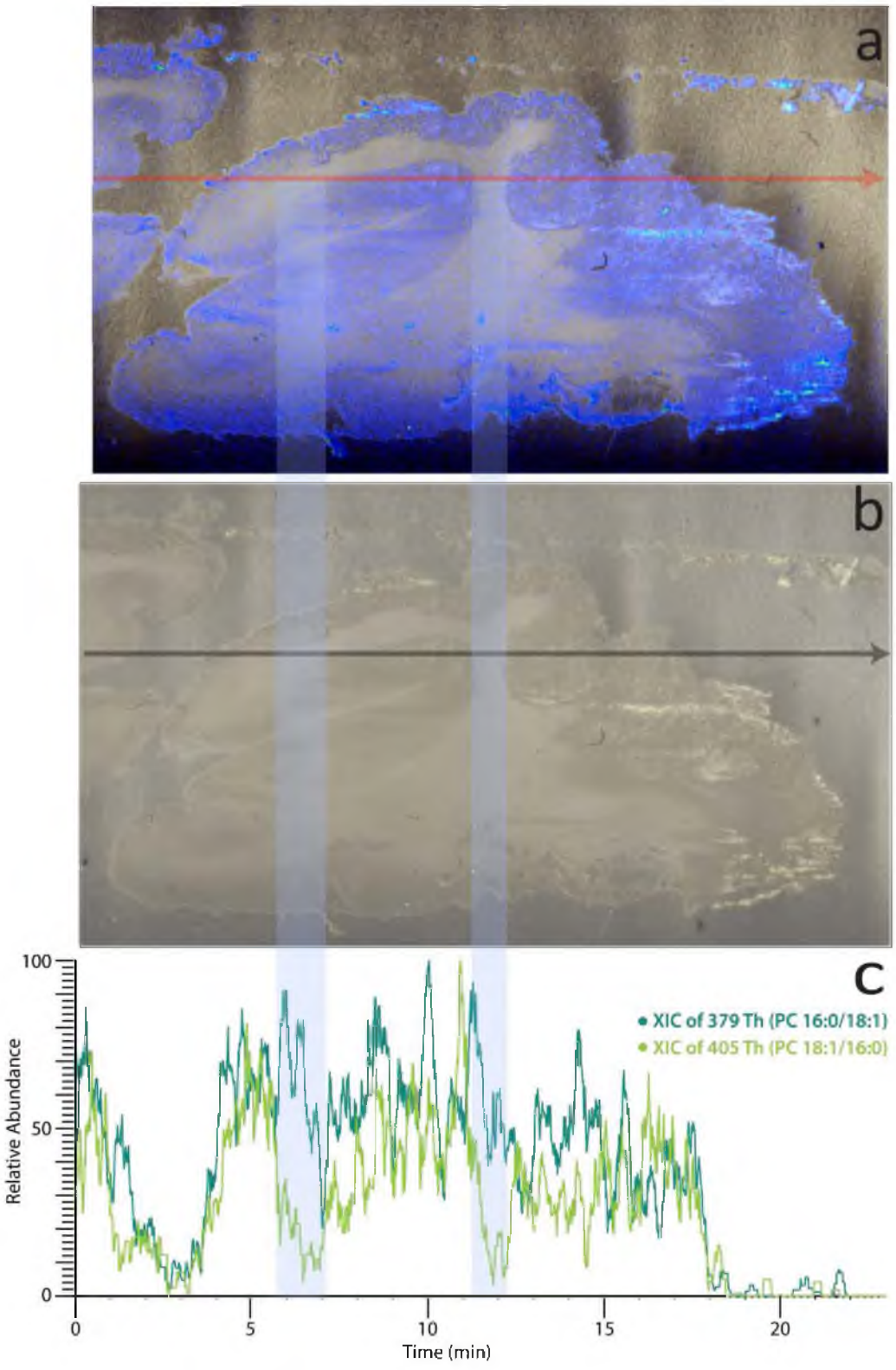

Figure 4.6 DESI-CID/OzID analysis of isomers of PC 34:1 desorbed directly from a sheep brain tissue section.

DESI-CID/OzID analysis of isomers of PC 34:1 desorbed directly from a sheep brain tissue section. Panels (a) and (b) show a photograph of the sheep brain tissue section analyzed with panel (a) digitally coloured to highlight the regions of grey matter (blue) and white matter (white). (c) The overlaid extracted ion chronograms acquired from a single transect, indicated by the grey arrow in panel (b), for diagnostic ions at *m/z* 379 (dark green) corresponding to PC 16:0/18:1, and *m/z* 405 (light green) corresponding to PC 18:1/16:0. The light blue shading indicates where the transect crosses regions of white matter.

4.4.2 Discussion

In this study, we have demonstrated the utlility of DESI-MS in analyzing arrays of lipid extracts. No cross-contamination between adjacent samples was noted as evidenced by the data obtained from egg yolk showing a near pure sample of the PC 16:0/18:1 isomer. DESI-MS has proven to be an extremely useful means to rapidly survey the phosphatidylcholines present in a diverse range of lipid extracts. Combining DESI with ion activation by CID/OzID, for the first time, has enabled the acquisition of spectra that uniquely identify the presence of each of the possible *sn*-positional isomers of asymmetric diacylphosphatidylcholines. Such clear differentiation of isomeric lipids would not be possible using conventional tandem mass spectral approaches. By comparing the relative abundance of diagnostic marker ions it has been shown that the relative contribution of each isomer to the lipid population can be determined. While only providing an approximation, this approach has enabled the comparison of the relative isomer populations in biological extracts and has revealed remarkable variation in the proportions of *sn*-positional isomers in nature. Data obtained for the isomeric pair, PC 16:0/18:1 and PC 18:1/16:0, suggest that while common assumptions that the unsaturated acyl chain is found at the *sn*-2 position are borne out in some biological extracts (*e.g.*, egg yolk), such assumptions would lead to the wrong conclusions in others (*e.g.*, the near equal proportions of the two possible isomers found in cow ocular lens). Although phosphatidylcholines were the only lipid class investigated here, in previous infusion ESI studies CID/OzID has been proven effective for examining *sn*-positional isomers of all major glycerophospholipid classes and even some triacylglycerols.[102, 144] This suggests that the methods described here could be deployed in the future to examine the similarlities and differences in acyl chain substitution patterns across the

glycerolipidome. Such data could help in understanding the biosynthetic connections between different lipid structures.

Direct analysis of sheep brain tissue by DESI-CID/OzID has revealed that while PC 34:1 is homogeneously distributed throughout, the relative concentration of the constituent isomers has local variation (*cf.* Figure 4.6 and Supplementary Materials, Appendix C, Figure 8.4). These data highlight current limitations in imaging mass spectrometry for lipid applications where monitoring quasi-molecular ions (enabling assignment at the sum composition level, *e.g.*, PC 34:1) or even CID product ions (enabling assignment of the acyl chain composition level, *e.g.*, PC 16:0_18:1) may not be sufficient to reveal regional differences in lipid abundances. As such, further development of targeted ion activation strategies is required, to be used in combination with desorption/ionization mass spectrometry to enable more precise assignment of lipid molecular structure and distribution. These protocols must yield abundant and diagnostic product ions for closely related lipid isomers and must be obtained on short timescales and on relatively low abundant ions. The data presented here suggest that, with further optimization, CID/OzID may serve as one such method for future applications.

4.5 Conclusions

The results of the current study serve to reinforce the importance of careful annotation of lipid mass spectral data to ensure lipid structures are not incorrectly assigned to a single *sn*-positional isomer based only on CID data. Based on our findings it seems reasonable to project that in most living systems both isomers are present albeit in different proportions. The underlying reasons for these subtle, molecular-level differences between lipidomes remains to be determined. It is clear however, that understanding the biological roles of different lipid isomers requires analytical tools such as those described here.

5 CONCLUSIONS AND FUTURE WORK

5.1 New Findings

5.1.1 Methodology

5.1.1.1 LC-OzID advantages

LC-OzID has been used successfully for online separation and identification of phospholipid double bond positional isomers in mixtures of phospholipid standards, simple biological extracts and complex biological extracts (see Chapter 2). LC-OzID methods optimized herein show that it is possible to chromatographically resolve some phospholipid double bond positional isomers with online OzID providing the location of the double bond present in the acyl chain of each eluting phospholipid. The reversed phase LC method used here for LC-OzID analyses can accomplish more challenging separations than those accomplished by previously-published LC methods. This is evidenced by the separation of PC 16:0_18:1 (*n*-7) from PC 16:0_18:1 (*n*-9) using LC OzID whereas previous methods, discussed in Chapter 2, were only able to separate PC 16:0_18:1 (*n*-9) from PC 16:0_18:1 (*n*-12) or PC 16:0_18:1(*n*-13), which are more easily separated. By modifying the parameters of the OzID scan slightly, it is possible to simultaneously identify the double bond location and the location of each acyl chain on the glycerol backbone (*sn*-position) or identify solely double bond position at a 2-3 fold increase in sensitivity in addition to a proportional decrease in mass spectral complexity. The chromatographic protocol proposed in this thesis for use with OzID has been used to successfully separate phospholipid double bond positional isomers in complex biological samples. The LC-OzID method discussed here is thus a useful analytical tool for partial separation of isomers with unambiguous identification of double bond position(s); even within in complex biological samples. In addition, by using the LC-OzID approach described in Chapter 2, the LC-MS TIC can be used for quantification while the LC-OzID TIC is used for identification of phospholipid double bond positional isomers. In cases where the chromatographic resolution is inadequate, extracted ion chromatograms for OzID ions can reveal the presence of isomers and provide a guide to changing populations of isomers between samples even where these isomers cannot be clearly

distinguished from visually inspecting the TIC for the OzID scans or the MS scans (Figure 2.4).

LC-OzID has several advantages over pre-existing methods for the identification of double bond position. High energy CID and multistage mass spectrometry of alkali metal-adducted lipids are the most common approaches to isomer discrimination presented in the literature.[136] In comparison, LC-OzID offers improved signal-to-noise of diagnostic ions and greatly reduced mass spectral complexity. Another recently published approach also uses liquid chromatography in conjunction with ozonolysis for the identification of double bond position in phospholipids.[138] These authors use hydrophilic interaction liquid chromatography (HILIC) in combination with reversed-phase chromatography for 2-D chromatographic analysis prior to ozonolysis. In addition, the ozonolysis is conducted after lipids elute from the column and before they enter the mass spectrometer so that all phospholipids eluted travel through the semi-permeable Teflon tubing to react with ozone. LC-OzID offers several advantages over this approach, in that ions of a selected *m/z* can be isolated and trapped with ozone for a desired period of time (with trapping times as short as 500 ms), with the ability to continuously switch between full MS scans and LC-OzID. This ability to obtain both full scan and OzID scans in the same chromatographic run aids in the identification of phospholipids from ozonolysis product ions and can improve the apparent chromatographic resolution, and thus quantification and identification, by implementing data dependent acquisition protocols. In addition, because phospholipid isomers are reacted with ozone inside the mass spectrometer, and not within the post column tubing, the post column tubing length and internal diameter, and thus the extra-column volume, can be minimized for maximal chromatographic resolution. LC-OzID also makes use of sodiated phospholipid ions that react approximately 5x faster than their protonated counterparts in the gas phase, offering improved apparent chromatographic resolution and/or sensitivity.[139] However, it is also possible that this may not translate to ozonolysis in solution. Finally, the chromatographic method used here for LC-OzID was able to resolve phospholipid double bond positional isomers (*i.e.*, PC 16:0_18:1 (n-9) and PC 16:0_18:1 (n-7)) in

multiple types of complex biological extracts whereas evidence was not presented to support the capability of the aforementioned method combining 2D-LC with ozonolysis to separate and identify these same types of phospholipid double bond positional isomers in complex biological samples.

5.1.1.2 LC-OzID limitations

Like any method, LC-OzID also has limitations. While the chromatographic method used could separate phospholipid isomers with double bonds differing by only two positions (*e.g.*, *n*-9 and *n*-7), not all phospholipid double bond positional isomeric pairs could be baseline separated using this LC-OzID method.[153] However, this decreased chromatographic resolution did not affect the ability of LC-OzID to identify each phospholipid double bond position. Also, as mentioned in Chapters 2 and 3, because the reactivity of double bonds within a phospholipid is dependent on the structural environment of the double bond (including double bond position, stereochemical configuration and any adjacent double bonds) extracted ion chromatograms for ozonolysis products generated from LC-OzID chromatograms cannot currently be used for absolute quantification of phospholipid isomeric pairs without the use of an identical set of phospholipid standards.[140] LC-OzID can however, still be used for relative quantification of phospholipid double bond positional isomers across multiple extracts. The instrumental setup for LC-OzID, described in Chapter 2, can either be used to identify double bond location alone or it can be used to simultaneously obtain information about both the acyl chain *sn*-position and double bond location but it cannot currently be used to determine acyl chain *sn*-position alone. Another consideration is instrument modification. Although OzID provides several advantages over other ozone-free methods, it involves additional laboratory equipment including an ozone generator, modification of a mass spectrometer and associated health and safety considerations.[167]

5.1.1.3 LC-CID/OzID Advantages

Using the experimental setup described in Chapter 3, LC-CID/OzID has been used to separate and identify phospholipid *sn*-positional isomers. In this way, it is possible to generate easily-interpretable mass spectra for high-sensitivity

identification of phospholipid acyl chain *sn*-position. The chromatographic method described for LC-CID/OzID does not require the purchase or use of newer, more expensive chromatographs and can still successfully separate some phospholipid *sn*-positional isomers with near-baseline resolution. The separation of phospholipid *sn*-positional isomers has not previously been demonstrated using conventional HPLC (although UPLC separations have been reported). This HPLC method is powerful enough to elucidate the contributions of phospholipid *sn*-positional isomers that could not be visualized using traditional LC-MS methods (*e.g.*, the isomeric pair PC 16:0/18:1 (9Z) and PC 18:1 (9Z)/16:0). Also, when LC is combined with alternating CID/OzID and MS scans in a single chromatographic run, the LC-MS scans can be used to calculate peak area for quantification of phospholipid *sn*-positional isomers while the LC-CID/OzID scans can be correlated with the LC-MS scans and used for identification of phospholipid double bond positional isomers. For the identification of acyl chain location within a phospholipid, CID/OzID is more specific than other pre-existing methods. This is because other approaches typically rely on ion abundance ratios to determine relative amounts of isomeric phospholipids. For example, a method that uses chemical ionization in conjunction with HPLC can be used to determine the acyl chains belonging to a phospholipid.[161] As an example of a more recently-developed method, phospholipids can be analyzed in positive ion mode and the neutral loss of a fatty acid resulting from CID of either protonated or lithiated adduct ions are used to assign acyl chain location.[79] Reliable quantification using these methods is difficult as diagnostic ion populations can be affected by instrument parameters such as collision energy and instrument geometry. Given such limitations these methods, at most, confirm the presence of the most abundant phospholipid isomer. Quantitative data can only be acquired with careful use of a standard curve obtained from phospholipid standards.[99] In contrast however, a comparison of CID/OzID to conventional PLA_2 enzymatic digests showed greater agreement than CID alone.[149] Another advantage over most existing approaches is the improved signal-to-noise of CID/OzID diagnostic product ions over those of the aforementioned methods. This makes use of competing methods with LC challenging, especially for the identification of low-abundance phospholipids and/or

samples containing mixtures of phospholipids that cannot be separated. The most recent method used to separate and identify phospholipid *sn*-positional isomers using combination LC and MS^n (neutral loss of fatty acid as ketene in negative ion mode), successfully separated several phosphatidylcholine *sn*-positional isomers.[153] Next to LC-CID/OzID, this method is debatably the most useful method for the separation and identification of highly unsaturated phospholipid *sn*-positional isomers. This method was not however, able to separate pairs of phospholipid *sn*-positional isomers containing two sites of unsaturation, whereas LC-CID/OzID was able to partially resolve a phospholipid *sn*-positional isomeric pair containing only a single site of unsaturation. Recently, DESI-CID/OzID was developed to provide a fast alternative to LC separation, while still identifying phospholipid *sn*-positional isomers in complex biological samples – this is discussed in Chapter 4 and summarized later in this chapter.

5.1.1.4 LC-CID/OzID Limitations

There are several limitations to the use of LC-CID/OzID for the analysis of phospholipid *sn*-positional isomers. Although this LC method is a powerful chromatographic method developed for the separation of intact phospholipid *sn*-positional isomers, some phospholipid *sn*-positional isomers could not be separated with baseline resolution, such as PC 16:0/18:1 (9Z) and PC 18:1 (9Z)/16:0. This decreased chromatographic resolution did not affect the ability of CID/OzID to identify phospholipid acyl chain *sn*-position. As discussed in Chapter 4, it is also important to remember that the CID/OzID reaction rate can vary slightly depending on the acyl chain composition. Therefore, not only does the sensitivity of this method decrease for some highly-unsaturated phospholipid isomers, LC-CID/OzID alone can only currently be used for relative quantification of phospholipid *sn*-positional isomers. Extracted ion chromatograms generated for CID/OzID product ions are not currently recommended for quantification outside of elucidating changing populations within an isomeric pair across multiple samples.

While the specificity of LC-CID/OzID can decrease with certain phospholipids, the same can be said of the aforementioned competing method combining LC with

neutral loss of phospholipid fatty acids as ketenes.[153] In the latter case, this non-specificity seems to preferentially affect highly unsaturated pairs of phospholipid *sn*-positional isomers, which also appears to be the case with LC-CID/OzID, however, to a lesser extent.

5.1.1.5 DESI-CID/OzID Advantages

The combination of DESI with CID/OzID can be used for high-throughput comparison of relative quantities of phospholipid *sn*-positional isomeric pairs in mixtures of phospholipid standards, simple biological extracts and complex biological extracts. Information about the spatial distribution of phospholipid *sn*-positional isomers can be obtained using DESI-CID/OzID (see Chapter 4). The abundant diagnostic ions generated by CID/OzID facilitate relatively short scan times enabling acquisition of data from DESI-generated ions. This strategy facilitates high-throughput analysis of phospholipid isomers from sample spots and directly from tissue sections. Indeed, DESI-CID/OzID has successfully been used to image relative quantities of phospholipid *sn*-positional isomers in different regions of a sheep brain tissue section at a spatial resolution of *ca.* 300 μm (see Figure 8.4).

5.1.1.6 DESI-CID/OzID Limitations

One limitation of DESI-CID/OzID is that the ozone concentration, gas flow rate and ion trapping time must be consistent in order to compare DESI-CID/OzID results across multiple days. A control sample must be analyzed across multiple days along with the samples of interest in order to allow for accurate normalization of the variation in phospholipid *sn*-positional isomer abundance due to variations in ozonolysis conditions. This is not a large concern with the online ozone generation setup, but should be considered when using the offline ozone generation setup (see Figure 8.1). Another limitation of this method is that even with a commercially available DESI source, small changes in DESI source parameters may correspond to large differences in precursor ion signal, thus optimization of the DESI source parameters can be time consuming. Even under optimal conditions, the signal can be nearly 100-fold lower than that achieved with ESI of the same sample. Therefore, this method is not recommended for the *sn*-positional isomeric analysis of low-

abundance phospholipids. Also, many software suites developed for mass spectral imaging are biased towards matrix-assisted laser desorption ionization (MALDI) over DESI; sometimes only including data processing methods for MALDI-based images. This can make data interpretation more difficult for DESI-based imaging applications. In addition, many imaging software suites are not flexible or customizable and do not allow for much user-intervention during image processing. This leaves little room for accurate image processing for more creative or novel imaging methods like DESI-CID/OzID, which makes use of an MS^3 scan, where several selected fragment ions should ideally be added together or averaged for a more accurate depiction of phospholipid *sn*-positional isomeric distribution. However, as the number of multistage mass spectrometric imaging experiments increases, so too will the need for improved software to manage multistage mass spectrometric imaging datasets. These types of imaging experiments are already providing useful information that cannot be obtained by imaging using solely full MS scans only, and so, make use of MS^n – this is demonstrated in Chapter 4 and discussed in recent publications.[183] As this realization becomes more widespread, an opportunity exists for increased numbers of multistage mass spectral imaging datasets to drive the creation of powerful yet simple software to manage these datasets.

5.1.2 Biological findings

Using LC-OzID, the analysis of *m/z* 782 and *m/z* 808 showed the presence of phospholipid isomers for both mass-to-charge ratios. For *m/z* 782, PC 16:0_18:1 (11) and PC 16:0_18:1 (9) were identified while for *m/z* 808, both PC 18:1 (9)_18:1 (9) and PC 18:0_18:2 (9,12) were identified (Chapter 2). The phospholipid, PC 16:0_18:1 (11) was found to be less abundant than PC 16:0-18:1 (9) in both egg yolk and sheep brain extracts. However, the relative ratio of PC 16:0_18:1 (11) to PC 16:0_18:1 (9) was slightly higher in sheep brain extract than in egg yolk extract.

The analysis of mixtures of phospholipid *sn*-positional isomers alongside biological extracts containing mixtures of phospholipid *sn*-positional isomers using DESI-CID/OzID revealed that a wide degree of variation in phospholipid *sn*-positional isomeric composition. DESI-CID/OzID revealed differences in relative isomer

composition ranging from approximately 50% - 97% for some isomeric pairs across different organisms, different tissues and even different regions of the same tissue (see Chapter 4). One of the most interesting findings was discovered in lipid extracts from the cow eye lens. For these extracts, DESI-CID/OzID showed that PC 18:1/16:0 was at least as abundant, if not more abundant, than PC 16:0/18:1. This is interesting because, as discussed in Chapter 1, the contemporary scientific literature assumes that the unsaturated fatty acid is found predominately at the *sn*-2 position.[56] Another interesting finding is the fact that for the phospholipid *sn*-positional isomeric analysis of *m/z* 782 (PC 34:1), both egg yolk and sheep kidney medulla (but not cow kidney medulla) contained a higher purity of PC 16:0/18:1 than the synthetic phospholipid standard provided by a commercial vendor as PC 16:0/18:1 (9Z). Also interesting is the difference in phospholipid *sn*-positional isomeric purity for multiple micro-extractions of two different regions in the same tissue, white matter and grey matter of sheep brain. This was later confirmed by DESI-CID/OzID imaging of a sheep brain tissue section, showing the same trend of increased abundance of PC 16:0/18:1 over PC 18:1/16:0 in white matter than in grey matter.

It is important to remember that even though these biochemical findings are reproducible, the sample size used was relatively small consisting of only 1 – 6 biological replicates and 4 method/spot replicates.

5.2 Future Work

The continuation of this research can go in many directions. LC-OzID could be used to profile a wide array of phospholipid double bond positional isomers in complex biological extracts. In order to work towards profiling of biological extracts at a single structure level, LC-OzID could be used to simultaneously identify acyl chain double bond position and *sn*-position in a single experiment. These phospholipid profile datasets could be stored in a searchable, online database. These data could be added to a pre-existing online database like LIPID MAPS Lipidomics Gateway.[184] In order to facilitate doing so, future work to integrate automated mass spectral annotation, for instance to label ozonolysis peaks and their corresponding double bond position or acyl chain position, into pre-existing software platforms

would be very useful as currently mass spectra must be manually annotated. This automated annotation software or plug-in should be relatively straightforward as the neutral losses along with their corresponding double bond position or acyl chain position have already been tabulated in Chapter 3 and in a previous publication.[167]

To work towards this goal, a higher-throughput profiling method should be used. For instance, data-dependent LC-OzID and/or LC-CID/OzID scans could be used so that multiple phospholipid mass-to-charge ratios may be analyzed in a single chromatographic run. Using this approach, a full suite of phospholipid double bond positional and *sn*-positional isomers for a biological extract could be analyzed in a single chromatographic run. The limitation for this approach at present is software development.

Another approach that could be used for higher-throughput LC-OzID analysis of biological extracts that would allow for improved detection, quantification and analysis speed of phospholipid isomers during LC-OzID analysis would be to set up several successive MS scans followed by a single OzID scan. This approach allows for a larger number of MS data points across a peak, thereby allowing for the improved detection of subtle chromatographic peak features, like peak shouldering that could be indicative of partially-resolved phospholipid isomers. This would lead to improved LC optimization for use with OzID. This increase in MS data points across chromatographic peaks also renders quantification more accurate by the LC-MS scans, especially for fast-eluting or low-abundance phospholipids that result in sharper or smaller peaks, while using the more time-intensive OzID scans only sparingly for identification. If the current number of data points across a chromatographic peak is sufficient, using the LC-OzID method described herein, this approach could be used to shorten chromatographic run time while still maintaining an acceptable degree of resolution. This approach could also be used with lower flow rate chromatography, which typically make use of smaller diameter chromatographic columns and can result in sharper chromatographic peaks, which would require faster MS acquisition times to maintain the integrity of the apparent chromatographic resolution.

For improved structural identification, LC-CID/OzID could be combined with successive scan types so that double bond information can be obtained using the online ozonolysis set up on the single-stage ion trap mass spectrometer (Thermo Fisher Scientific, LTQ) as well. Double bond position assigned to fatty acids at specific *sn*-positions has been obtained using CID/OzID^2 and (CID/OzID)^2 with a similar instrumental setup.[102] However, these methods have not yet been combined with LC. This approach could also be used for detailed structural profiling of phospholipids in biological extracts.

The ability of DESI-CID/OzID to be used for high-throughput analysis of phospholipid *sn*-positional isomers would be most useful when applied to a large sample cohort and/or for which sample volume or availability is limited. In addition, not only does DESI save more analysis time the larger the sample size but sample carry-over is minimized and sample analysis is more automated when compared to using an approach like direct infusion (ESI). This is because DESI does not require repeated (manual) washing of a sample syringe between each sample analysis as with direct infusion. DESI-CID/OzID could also be used to analyze the phospholipid *sn*-positional isomeric distribution of samples that are present on a surface and cannot be easily extracted. Using DESI with CID/OzID, the extraction step may even be avoided altogether to save analysis time as well if the sample is already present on a flat surface. Along similar lines, liquid extraction surface analysis (LESA) could also be a viable alternative for use with CID/OzID. LESA-MS on arrays of lipid samples has previously been described.[185] Briefly, samples can be distributed on a surface or in 92-well plates. A robotic arm carrying a pipette tip can be directed to the location of the sample to deposit a droplet of solvent that remains in contact with the surface to extract analytes for a desired length of time. This droplet, now containing analytes of interest, is then aspirated into the syringe and introduced into the mass spectrometer by means of injection into one of many nanospray emitters on a chip. Alternatively, a liquid sample can be directly aspirated from a well in the 92-well plate into the pipette tip and introduced into a nanospray emitter. This would represent a small sacrifice in time but would allow for a greater number of scans to be averaged or summed, which could greatly improve the signal-to-noise ratio of

analyte ions, and their diagnostic ozonolysis ions, especially those present at low abundance.

DESI-CID/OzID imaging – demonstrated here for the first time - could in-principle be extended to three-dimensional imaging by acquisition of data from successive two-dimensional tissue sections.[186] Three-dimensional DESI-CID/OzID imaging may aid in understanding the roles of phospholipid isomers in biology as well as their associated mechanisms. However, this is not recommended as software limitations exist for 3D imaging using DESI as they do with 2D imaging. MALDI CID/OzID imaging could also be used to obtain mass spectral images of the distribution phospholipid *sn*-positional isomers with high spatial resolution as well as improved sensitivity. Because MALDI is also a soft ionization technique and because MALDI sample preparation, instrumental methods and data processing considerations have been researched in depth for imaging applications, and would make MALDI-CID/OzID analysis more amenable to 3D imaging applications than DESI-CID/OzID.[104, 186-188]

6 APPENDIX A: SUPPLEMENTARY MATERIALS FOR CHAPTER 2, COMBINING LIQUID CHROMATOGRAPHY WITH OZONE-INDUCED DISSOCIATION FOR THE SEPARATION AND IDENTIFICATION OF PHOSPHATIDYLCHOLINE DOUBLE BOND ISOMERS

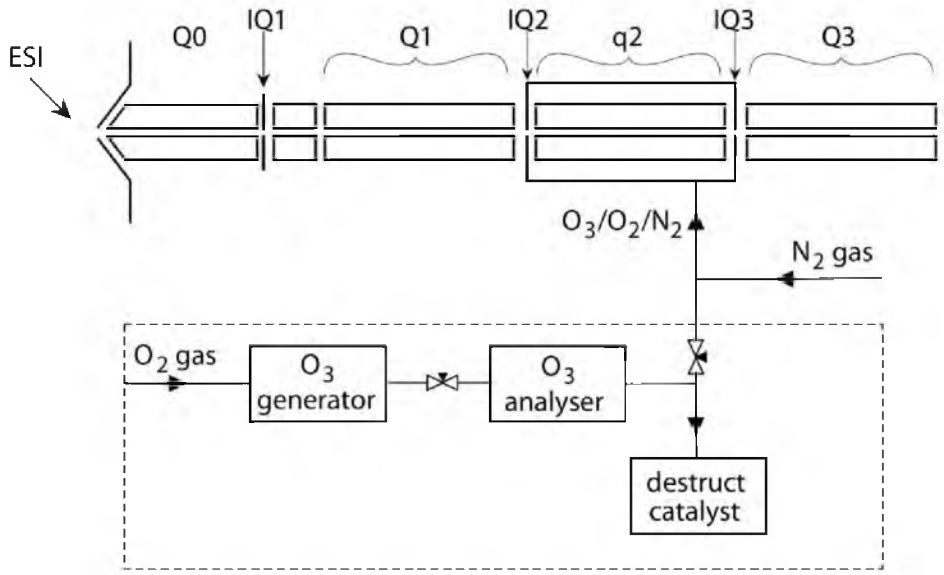

Figure 6.1 Schematic of the modified QTRAP 2000 mass spectrometer with online O3 generation used in these experiments.

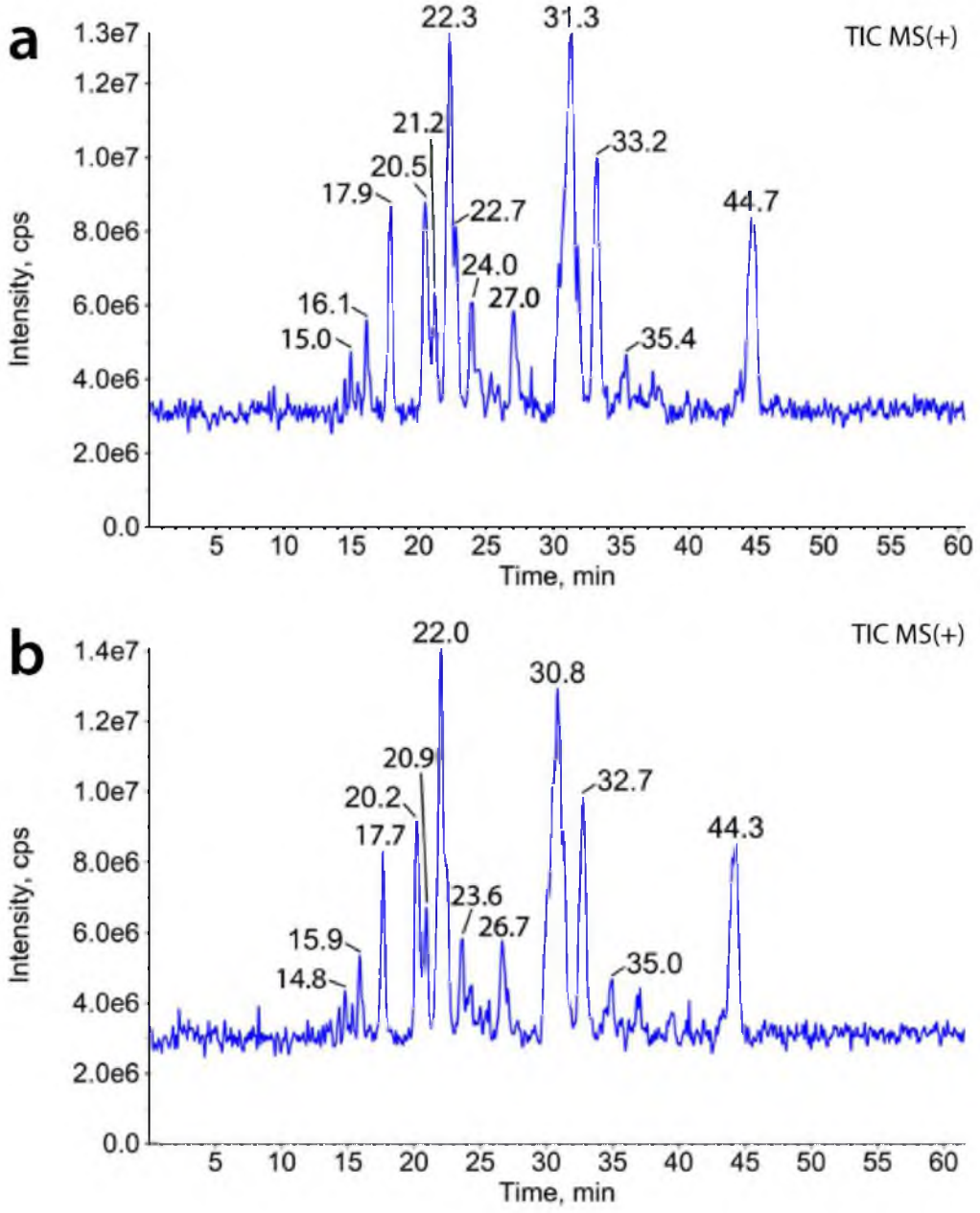

Figure 6.2 Results of LC-MS analysis for all detectable ions of a commercially available lipid extract from egg yolk.

Total ion chromatograms (TICs) extracted from the full scan mass spectra (*i.e.*, Q3 scans) are shown for two replicate injections (a and b) of egg yolk extract and highlight the repoducibility of the method and the complexity of the sample.

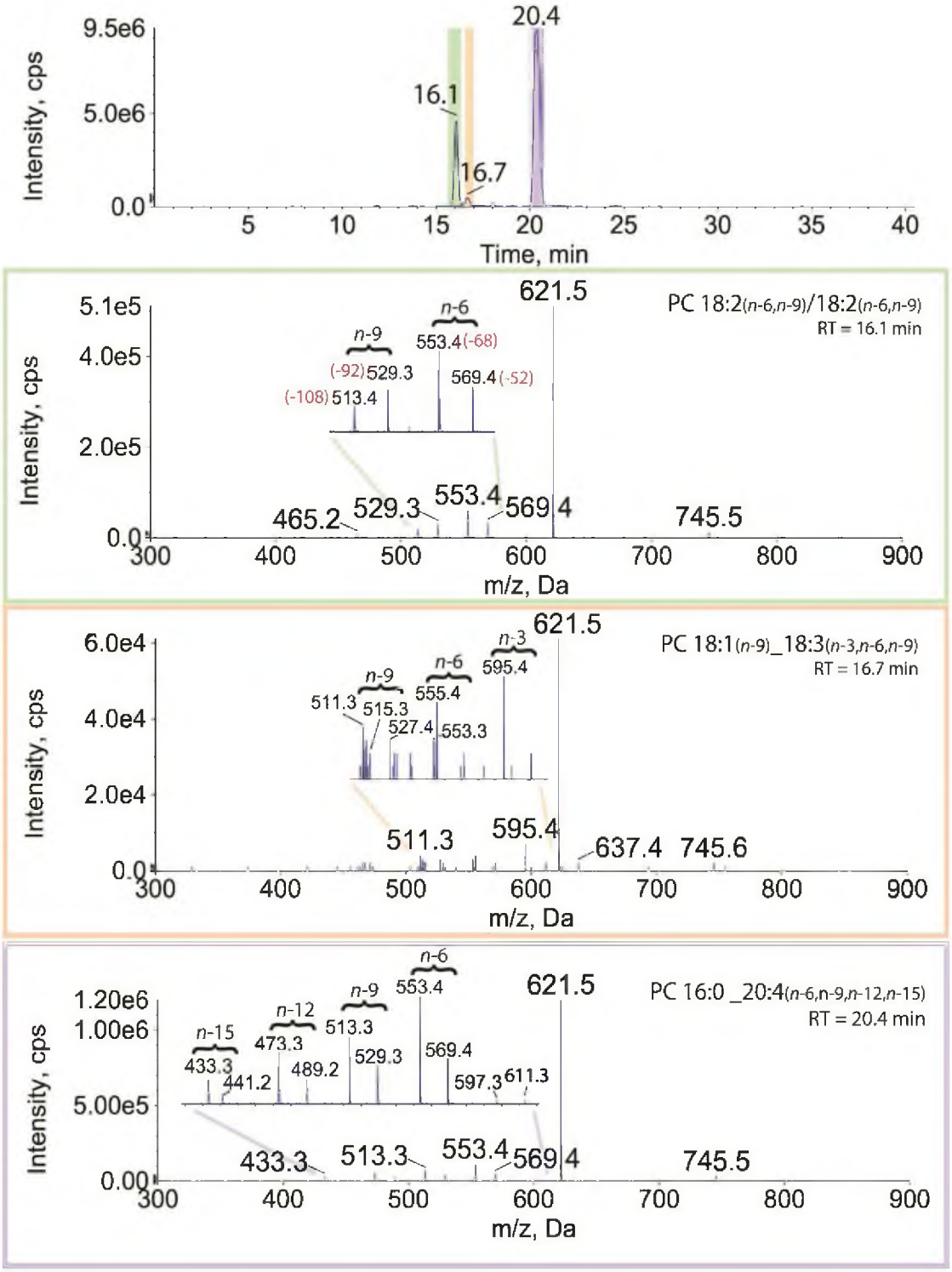

Figure 6.3 Results of LC-MS analysis of polyunsaturated phosphatidylcholines in a purified phosphatidylcholine extract from egg yolk.

Shown above is (a) the region of interest of the chromatogram constructed from total abundance of ions detected in OzID scans of mass-selected *m/z* 804. The OzID mass spectra obtained by integrating all scans between across the three chromatogtaphic peaks are shown as panels (b)-(d). OzID peaks (labelled with

brackets) indicate the presence of the isomeric polyunsaturated phosphatidylcholines (b) PC 18:2(*n*-6,*n*-9)_18:2(*n*-6,*n*-9) and (d) PC 16:0_20:4(*n*-6,*n*-9,*n*-12,*n*-15). The OzID spectrum obtained from the chromatographic peak eluting at 16.7 min (c) is consistent with the presence of PC 18:1(*n*-9)_18:3(*n*-3,*n*-6,*n*-9) but the lower signal-to-noise ratio prevents an unambiguous assignment under the current experimental conditions.

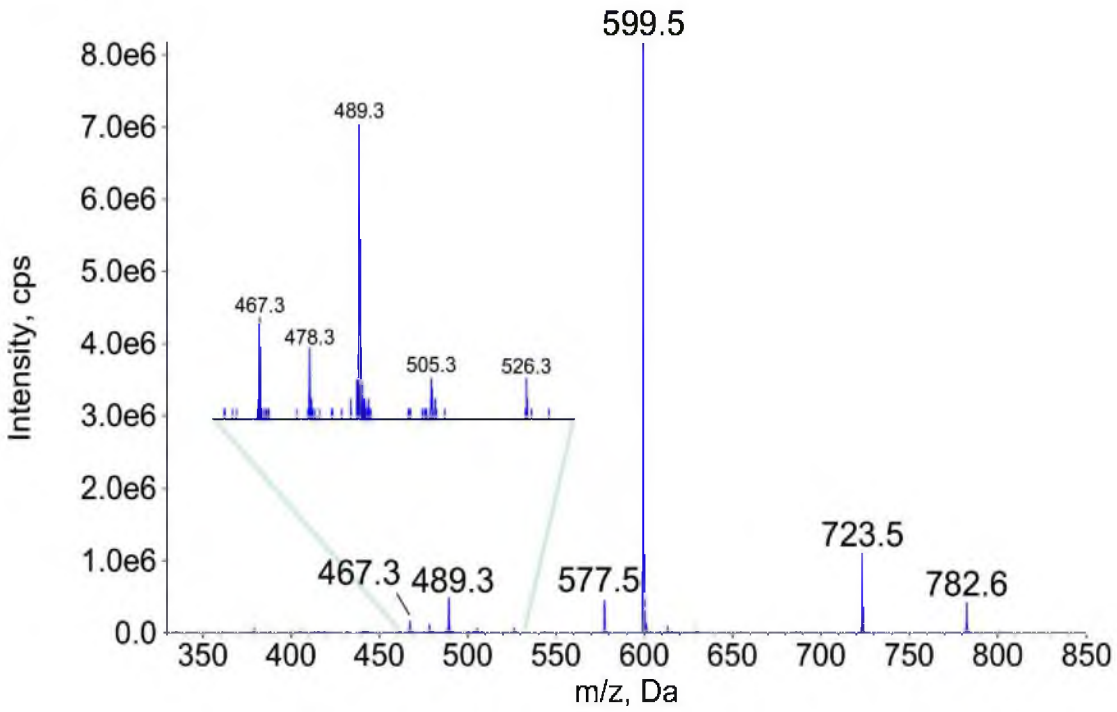

Figure 6.4 OzID spectrum obtained from a PC 16:0/18:1(n-9) standard using shorter reaction times.

OzID spectrum obtained from a PC 16:0/18:1(*n*-9) standard using reaction times of 300 ms (compared to 2000 ms used in the experiments reported herein, *cf.* Fig. 3). Despite the lower signal-to-noise the OzID peaks at m/z 489 and 505 allow the unambiguous assignment of the double bond position as *n*-9.

Table 6.1 Look-up table for characteristic neutral losses observed in OzID spectra for common carbon-carbon double bonds at positions "n-x" within mono-unsaturated acyl chains.[141, 167]

double bond position (*n*-x)*	**OzID neutral loss to form aldehyde ion** (Da)	**OzID neutral loss to form "Criegee ion"** (Da)
n-3	26	10
n-6	68	52
n-7	82	66
n-9	110	94
n-12	152	136

* where "x" provides the 1st carbon of the double bond as counted from the methyl terminus

7 APPENDIX B: SUPPLEMENTARY MATERIALS FOR CHAPTER 3, SEPARATION AND IDENTIFICATION OF PHOSPHATIDYLCHOLINE REGIOSOMERS BY COMBINING LIQUID CHROMATOGRAPHY WITH A FUSION OF COLLISION- AND OZONE-INDUCED DISSOCIATION

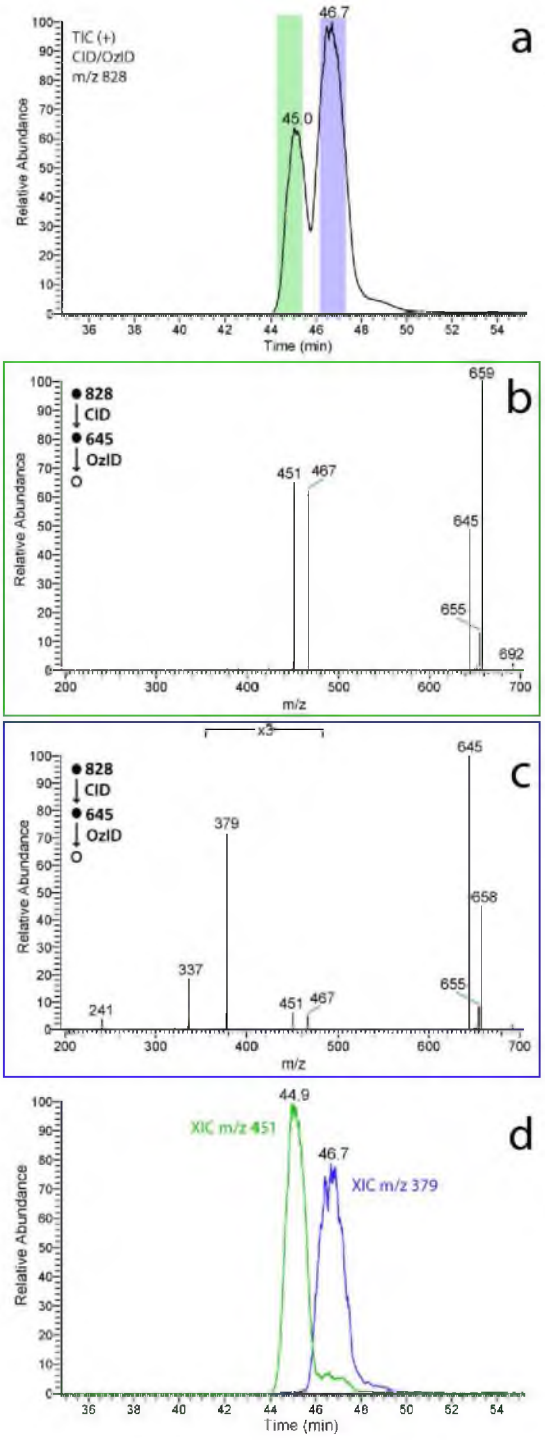

Figure 7.1 LC-MS analysis of a synthetic standard provided as PC 16:0/22:6.

These data were acquired with a much higher sample loading than those shown in Figure 2.2. (a) Total ion chromatogram for LC-CID/OzID of *m/z* 828. (b) The CID/OzID spectrum obtained from integrating across the chromatographic peak between 44.3-45.4 min. (c) The CID/OzID spectrum obtained from integrating across the chromatographic peak between 46.2-47.3 min. (d) The extracted ion chromatogram for CID/OzID product ions at *m/z* 451 (indicative of PC 22:6/16:0) is shown in green, while the extracted ion chromatogram for *m/z* 379 (indicative of PC 16:0/22:6) is shown in blue.

8 APPENDIX C: SUPPLEMENTARY MATERIALS FOR CHAPTER 4, A RAPID AMBIENT IONIZATION-MASS SPECTROMETRY APPROACH TO MONITORING THE RELATIVE ABUNDANCE OF ISOMERIC GLYCEROPHOSPHOLIPIDS

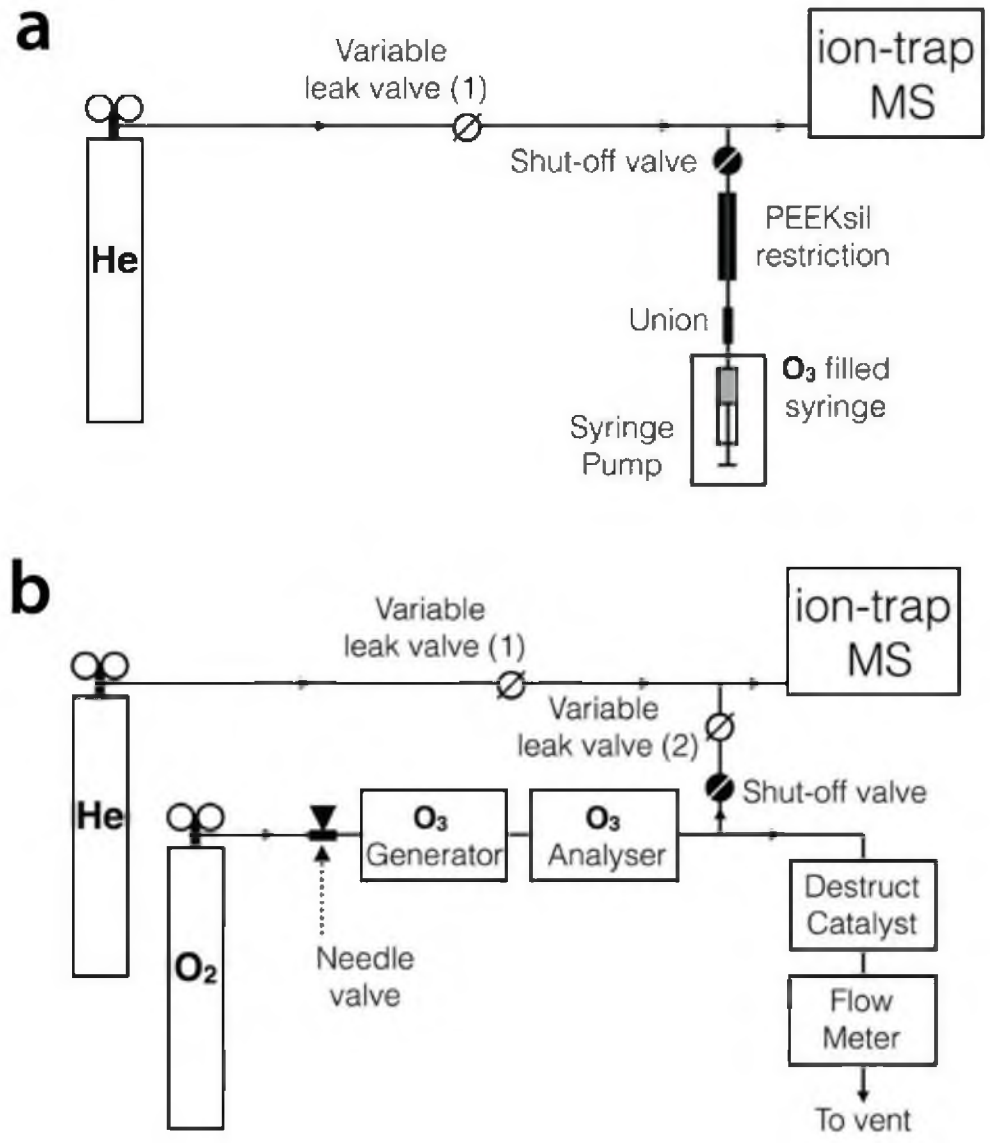

Figure 8.1 Schematic of the online and offline OzID setups.

Shown above is **(a)** the schematic illustrating the *offline* setup for delivery of ozone to a modified linear ion-trap mass spectrometer (LTQ Thermo Fisher Scientific, San Jose CA, USA). Ozone is generated offline using a HC-30 ozone generator (Ozone Solutions, Sioux Center, IA, USA) and collected in a suitable gas tight plastic syringe. Gas from the syringe is delivered to the helium buffer gas via a PEEKsil restriction (100 mm L × 1/16 in. OD × 0.025 mm ID, SGE Analytical Science, Ringwood, Vic, Australia). This method, including the safe generation and collection of ozone, is

described in detail in reference[167]. **(b)** the schematic illustrating the *online* ozone generation and delivery setup for the linear ion-trap mass spectrometer. Ozone is generated using a 0.2 L min^{-1} flow of industrial grade oxygen through an ozone generator (Titan 100 generator, Absolute Ozone, Edmonton Canada) and was measured at *ca.* 170 g m^{-3} (normal) using and inline ozone analyzer (Mini HiCon; InUSA Inc., Norwood, MA, USA). Thus formed, a low flow of ozone/oxygen was added to the ion trap supply helium buffer gas using a variable leak valve (VSE Vacuum, Lustenau, Austria). This method is based on previous developments for online ozone generation and delivery for ion-trap mass spectrometers as described in reference[140].

(a) PC 16:0/18:1

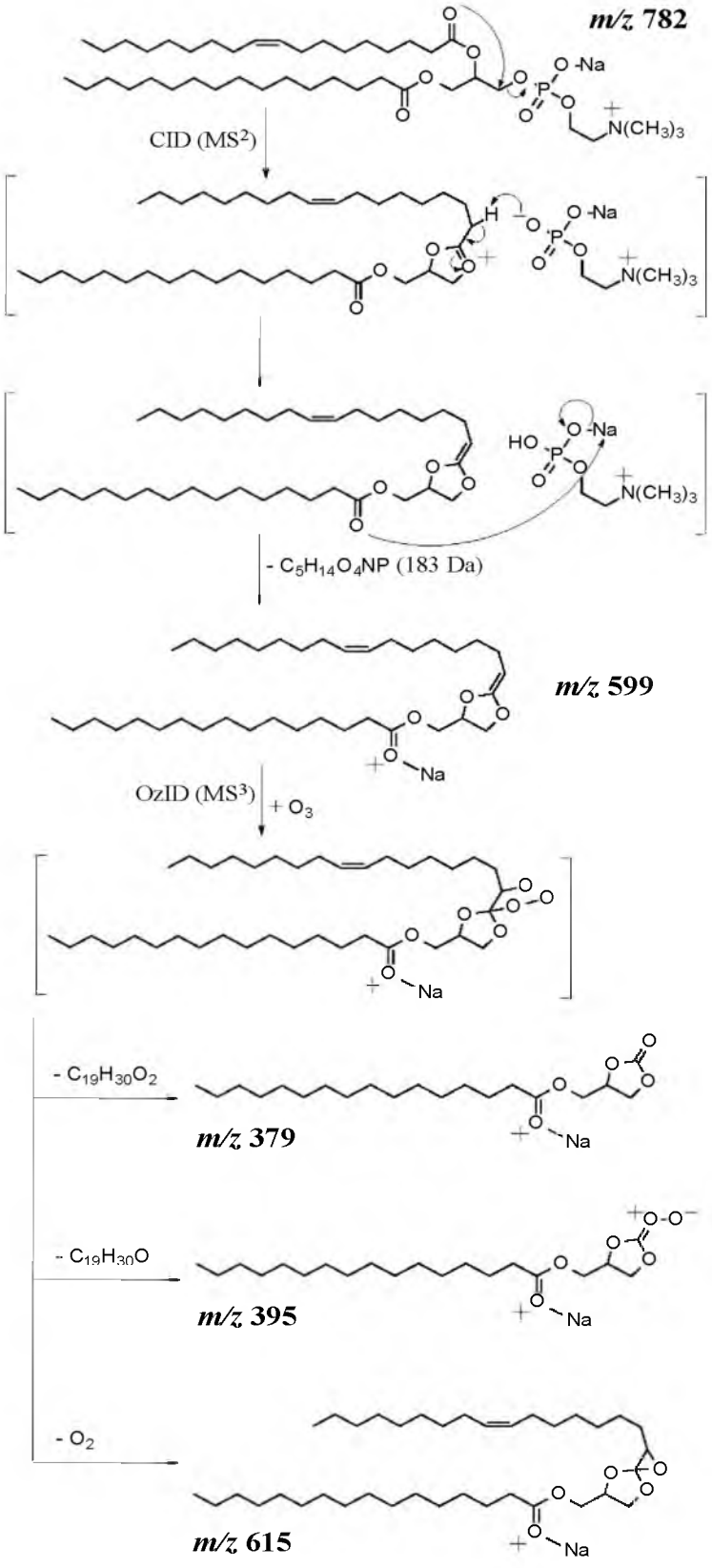

(In some spectra this ion appears as a broad, tailing peak centred at *m/z* 614)

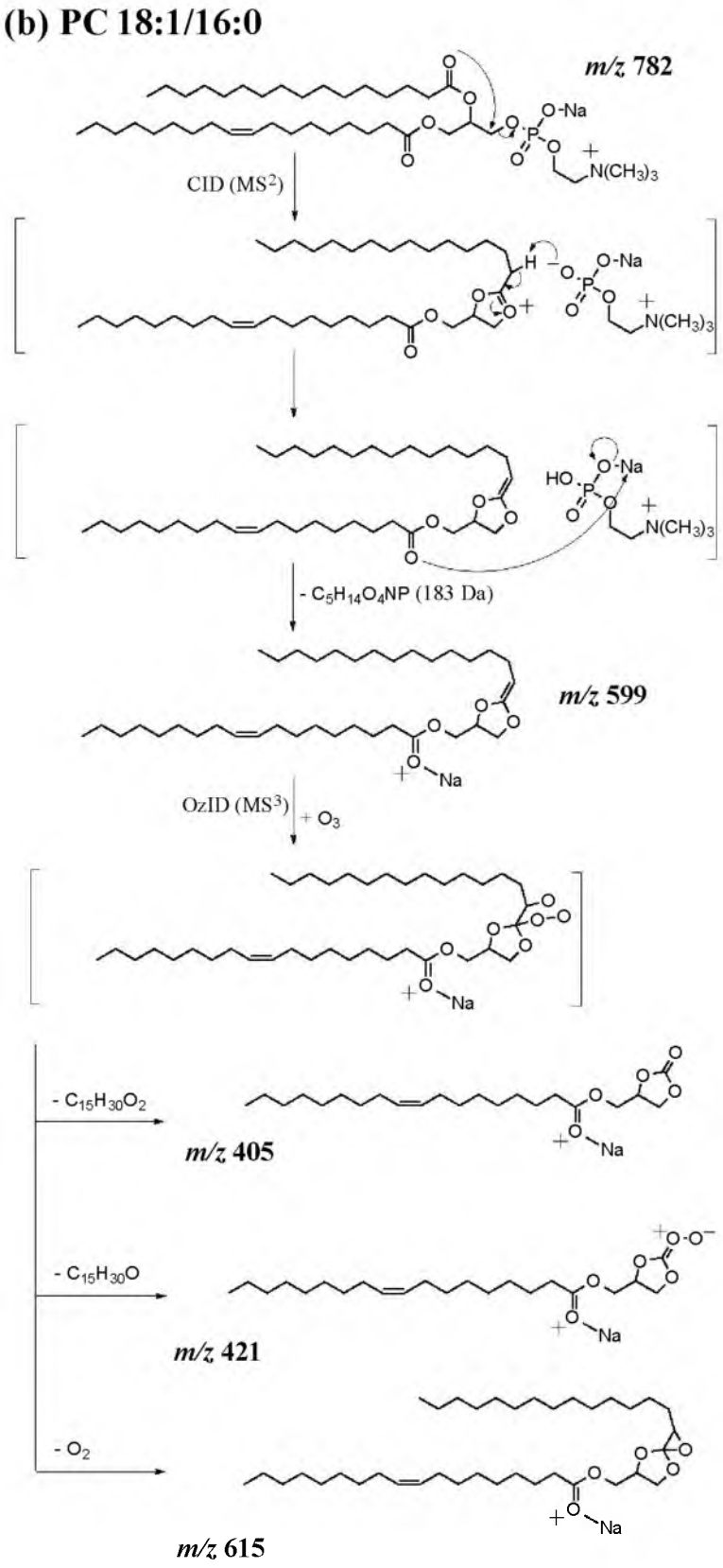

Scheme 8.1 Proposed CID/OzID mechanisms for PC 16:0/18:1 and PC 18:1/16:0.

Proposed mechanism to account for the CID/OzID product ions observed in the spectra shown in Figures 4.2 and 4.3 from **(a)** [PC 16:0/18:1 + Na]$^+$ and **(b)** [PC 18:1/16:0 + Na]$^+$. Mechanisms and product ion structures are based on proposals outlined in reference[102].

Day-to-day variation in abundance data when using offline ozone generation

Figure 8.2 displays the day-to-day variation for DESI-CID/OzID measurements of synthetic PC 18:1(9Z)/16:0 and PC 16:0/18:1(9Z), and a phosphatidylcholine extract from chicken egg yolk. Although the values for the % composition for analogous *sn*-positional isomers does not appear to vary from day to day, for all 3 samples, the values obtained on day 1 fall outside the error bars of those obtained on the second day. These data were acquired using "offline" ozone generation and so the variability observed likely arises from different ozone concentrations in the ion trap for the experiments conducted on different days. As noted in the main body of the manuscript, the two *sn*-positional isomers have slightly different rates of reaction at the OzID step in the sequence thus with different ozone concentrations the abundance of characteristic ions can vary accounting for the observed day-to-day variability in these data. Generating ozone "online" has been shown to provide reproducible ozone concentrations.[140, 147] Thus the experimental configuration was modified as shown in Figure 8.1 to provide a continuous, stable supply of ozone to the ion trap.

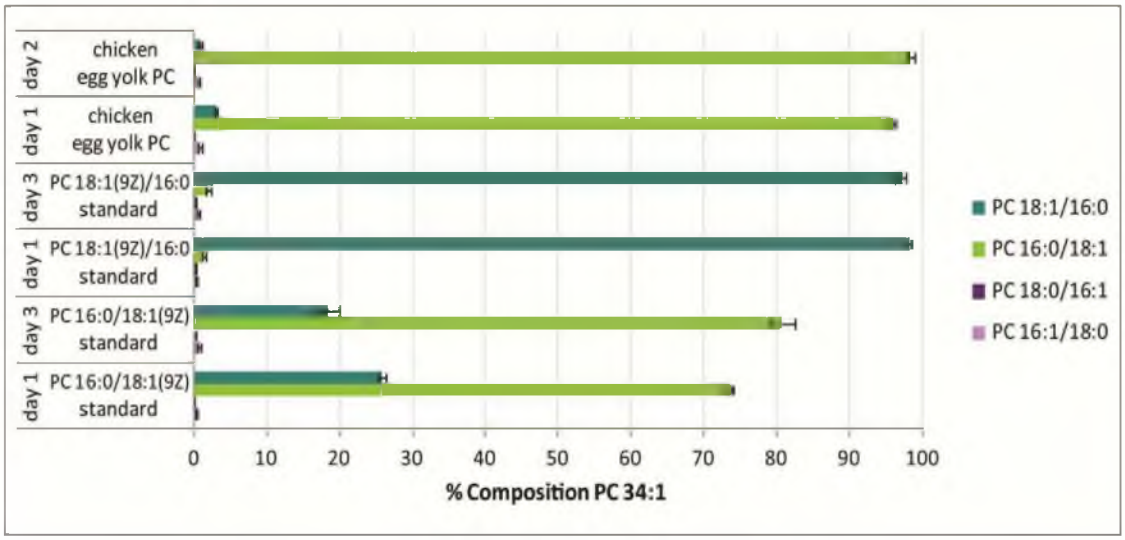

Figure 8.2 The abundance of PC 34:1 *sn*-positional isomers of composition in different phospholipid samples over multiple days.

The abundance of *sn*-positional isomers PC 18:1/16:0 and PC 16:0/18:1 as a percentage of phosphatidylcholines of composition PC 34:1 in different biological and synthetic samples. Isomer contributions are estimated from the normalised product ion abundances in DESI-CID/OzID mass spectra as described in the text. The inter-day comparison of composition of *sn*-positional isomers of PC 34:1 present in synthetic standards, PC 16:0/18:1 and PC 18:1/16:0, and an egg yolk phosphatidylcholine extract is shown. All data points represent an average of at least four technical replicates. Uncertainties shown represent standard deviation. Spectra acquired using offline ozone generation (see Methods).

Comparison of the relative rates of reaction of lipid isomers with ambient ozone

There are several opportunities during sample preparation and analysis for unsaturated lipids to be exposed to ambient ozone present in laboratory air. Previous studies have shown this reaction can be rapid.[179, 180] It was thus necessary to establish whether the *sn*-positional isomers would have similar or different rates of reaction under these conditions as this could alter the relative populations of isomers in the sample arrays.

To investigate this effect, the synthetic PC isomers - PC 16:0/18:1(9Z) and PC 18:1(9Z)/16:0 - were deposited onto PTFE spots in a sample array and were left on the bench for 15, 180 or 1440 mins. Following these intervals the arrays were analyzed using DESI-MS in positive ion mode (as described in the Methods section). The abundances of ions at *m/z* 830 corresponding to the lipid ozonide ions, $[M+Na+O_3]^+$, were compared to the abundances of the remaining un-reacted lipid at *m/z* 782. Under these conditions formation of ozonides on the surface was found to be minimal after an exposure of 15 mins. Given the procedures for sample preparation and storage used in this study (see Methods) this suggest a negligible effect on any results reported herein.

The data acquired at longer exposure times are summarized in Figure 8.3 and show the significant production of ozonides; consistent with prior reports. Importantly however, the ozonide production is comparable for the two isomers investigated suggesting that ambient ozonolysis will have a negligible impact of composition estimates based on DESI-CID/OzID analysis.

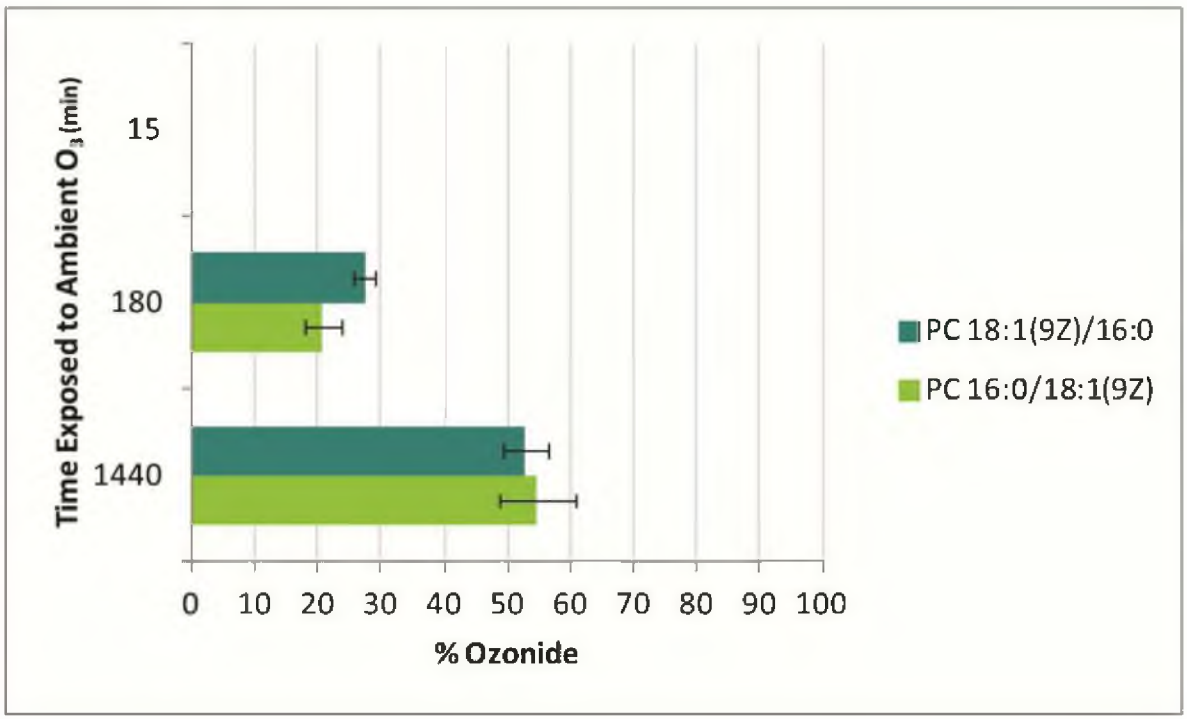

Figure 8.3 Ozonides formed from the reaction of unsaturated lipids deposited with ambient ozone.

The abundance of ozonides formed from the reaction of unsaturated lipids deposited on PTFE spots with ambient ozone present in laboratory air. Under positive ion DESI-MS analysis, ozonides were detected as $[M+Na+O_3]^+$ ions (*m/z* 830) and are shown as a percentage of the synthetic standards PC 18:1/16:0 or PC 16:0/18:1 detected as $[M+Na]^+$ ions (*m/z* 782). All data points represent an average of at least four technical replicates. Uncertainties shown represent the standard deviation.

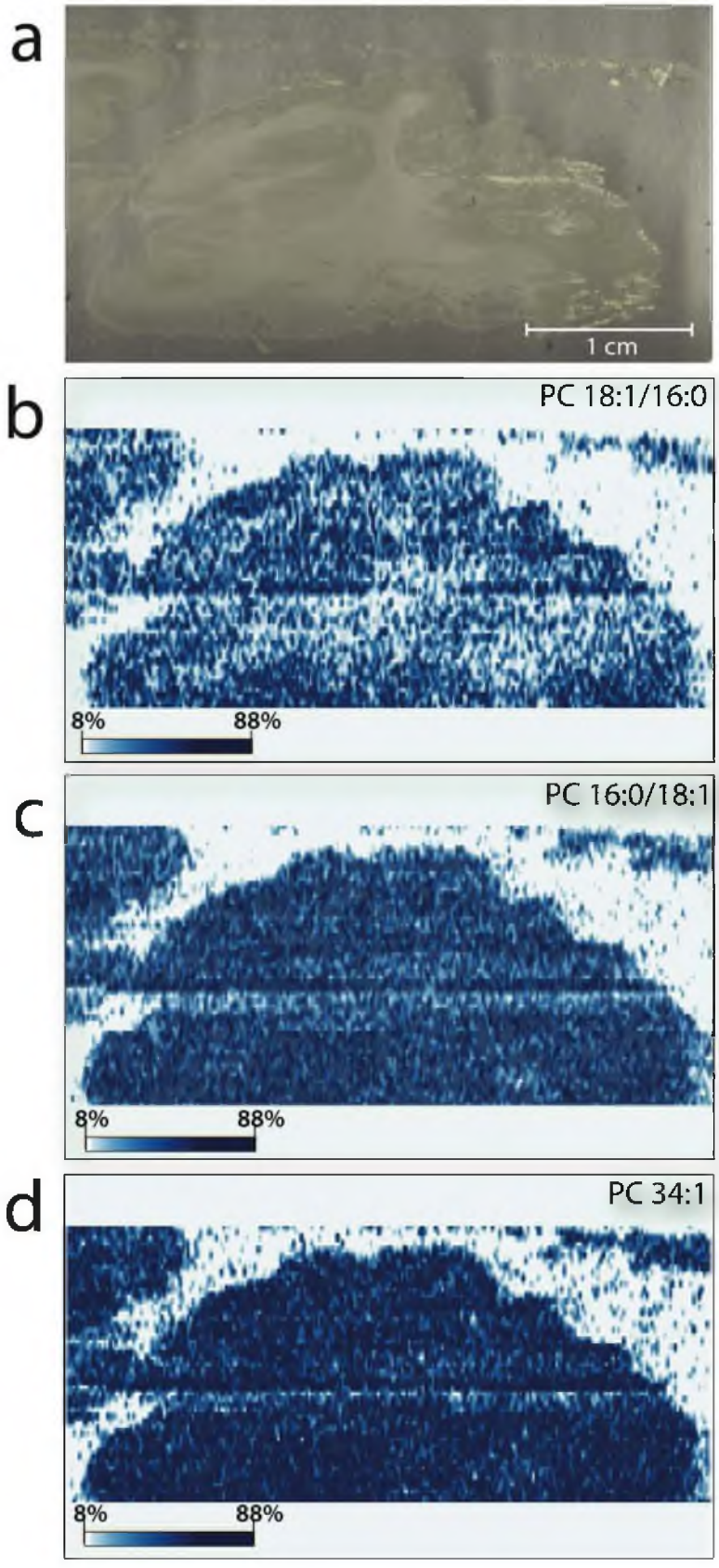

Figure 8.4 CID/OzID of m/z 782 conducted across a tissue section of a sheep brain.

A coronal section of the temporal lobe of the left hemisphere of a sheep brain was dissected and sliced to a thickness of 30 μm as described in the Methods. A small section of the slice was prepared for mounting onto a glass slide and was positioned with the sagittal face upwards for analysis and the outermost side of the left side of the brain was oriented at the top of the slide. (a) Photographic image of sheep brain section used for direct tissue analysis. Images reconstructed from DESI-MS analysis of the tissue. The abundance of diagnostic product ions observed in the DESI-CID/OzID (782 $\rightarrow$ 599 $\rightarrow$) spectra acquired at each position are illustrated for (b) *m/z* 405 and 421 indicative of the local abundance of PC 18:1/16:0; (c) *m/z* 379 and 395 indicative of the local abundance of PC 16:0/18:1; and (d) and *m/z* 599 and 615. All reconstructed ion images are normalized with the most abundant product ion signal detected as 100% and the intensity scale indicated by the darkness of the blue colour is shown under each image for all panels. Note that, the line across the sample image is due to a software communication error; the sample analysis was restarted from this point.

Table 8.1 Percent Composition for phosphatidylcholine *sn*-positional isomers in samples of different origin containing phospholipids.

Comparison of abundance of PC 36:1, PC 36:2 and PC 34:1 *sn*-positional isomers in biological tissues using DESI CID/OzID. The composition of PC *sn*-positional isomers present in synthetic standards are also included for comparison with tissue extracts. The composition of each *sn*-positional isomer as a % of total PC 36:1, 36:2 or 34:1 respectively for each tissue extract is shown ("average"). The standard deviation ("+/-") is shown directly below each corresponding average. To calculate the standard deviation, different types of replicate measurements were used. For all samples, a minimum of 4 sample spot replicates were analyzed. Biological replicates were as follows: 5 x sheep brain white matter of temporal lobe, 5 x sheep brain grey matter of temporal lobe, 3 x left lobe of sheep liver, 3 x medulla of sheep kidney, 3 x perinephric fat of sheep kidney, 3 x sheep heart ventricle, 6 x cow eye lens core (m/z 782 only, otherwise 1 biological replicate used), 1 x left lobe of cow liver, 1 x medulla of cow kidney and 1 x perinephric fat of cow kidney. Sheep brain extracts, cow ocular lens extracts and synthetic standards, PC 16:0/18:1(9Z) and PC 18:1(9Z)/16:0 were analyzed on 2 separate days.

		sheep						cow				chicken	synthetic standards				
		liver	kidney		brain		heart	liver	kidney		eye	egg	PC 36:1		PC 36:2	PC 34:1	
		left lobe	medulla	perinephric fat	grey matter	white matter	ventricle	left lobe	medulla	perinephric fat	lens core	yolk	PC 18:0/18:1(9Z)	PC 18:1(9Z)/18:0	PC 18:1(9Z)/18:1(9Z)	PC 16:0/18:1(9Z)	PC 18:1(9Z)/16:0
PC 36:1 (m/z 810)	PC 16:0/20:1 average	0.2	0.3	0.9	1.4	4.4	1.1	0.3	0.4	1.1	3.7	0.6	0.3	0.0			
	(m/z 379, 395) +/-	0.3	0.2	1.1	1.2	1.7	1.4	0.2	0.1	1.1	4.8	0.3	0.1	0.0			
	PC 20:1/16:0 average	0.1	0.2	1.1	5.6	2.4	0.5	0.2	0.8	0.1	39.6	0.0	0.0	0.0			
	(m/z 433, 449) +/-	0.3	0.2	1.3	2.2	2.0	3.8	0.2	0.5	0.3	25.4	0.1	0.0	0.0			
	PC 18:0/18:1 average	95.1	88.9	90.8	78.3	73.8	90.1	97.1	78.5	95.0	53.6	94.2	87.7	6.1			
	(m/z 407, 423) +/-	2.4	3.4	3.7	5.9	8.6	7.2	0.5	1.6	1.2	28.0	1.7	0.1	0.1			
	PC 18:1/18:0 average	4.7	10.6	7.3	14.7	19.5	8.4	2.5	20.3	3.8	3.1	5.2	12.0	93.9			
	(m/z 405, 421) +/-	2.1	3.3	2.9	6.8	9.0	5.4	0.5	2.0	1.6	4.7	1.6	0.2	0.2			
PC 36:2 (m/z 808)	PC 18:0/18:2 average	59.2	26.5	47.5	4.2	1.7	51.5	75.3	25.4	22.9	41.2	53.5			0.1		
	(m/z 407, 423) +/-	13.6	3.9	15.4	2.9	1.6	10.8	3.1	0.3	6.1	23.8	4.6			0.1		
	PC 18:2/18:0 average	1.7	1.7	1.9	0.6	0.9	3.7	1.6	2.0	0.0	4.1	1.8			0.4		
	(m/z 403, 419) +/-	0.8	1.0	2.2	0.7	0.8	1.1	0.8	0.4	0.0	9.2	0.7			0.1		
	PC 18:1/18:1 average	39.1	71.8	50.6	95.2	97.4	44.8	23.2	72.6	77.1	54.7	44.7			99.8		
	(m/z 405, 421) +/-	14.3	3.9	15.9	2.8	1.9	10.3	2.8	0.6	6.1	25.9	4.9			0.1		
PC 34:1 (m/z 782)	PC 16:0/18:1 average	96.8	93.4	81.9	60.3	83.9	94.9	95.5	82.3	96.4	39.1	97.2				79.28	1.85
	(m/z 379, 395) +/-	1.0	1.3	11.4	3.4	4.7	1.1	0.8	0.5	1.1	7.5	1.4				3.35	0.43
	PC 18:1/16:0 average	2.4	5.7	16.6	38.8	15.3	4.3	3.1	16.7	2.2	59.4	2.0				19.96	97.42
	(m/z 405, 421) +/-	0.9	1.2	11.0	3.4	4.8	1.1	0.7	0.4	0.8	7.1	1.2				3.42	0.54
	PC 16:1/18:0 average	0.6	0.6	0.9	0.5	0.6	0.6	0.8	0.8	0.7	0.9	0.7				0.65	0.52
	(m/z 377, 393) +/-	0.3	0.3	0.6	0.5	0.6	0.2	0.2	0.1	0.2	0.9	0.2				0.23	0.21
	PC 18:0/16:1 average	0.2	0.2	0.6	0.3	0.2	0.3	0.6	0.3	0.8	0.6	0.1				0.11	0.21
	(m/z 407, 423) +/-	0.2	0.1	0.4	0.2	0.2	0.2	0.1	0.1	0.3	1.0	0.1				0.16	0.10
PC 34:2 (m/z 780)	PC 16:0/18:2 average											85.4					
	(m/z 379, 395) +/-											1.5					
	PC 18:2/16:0 average											2.0					
	(m/z 403, 419) +/-											0.7					
	PC 16:1/18:1 average											12.3					
	(m/z 377, 393) +/-											1.8					
	PC 18:1/16:1 average											0.2					
	(m/z 405, 421) +/-											0.1					

Table 8.2 Comparison of reported % purities for synthetic standards PC 16:0/18:1 and PC 18:1/16:0.

Comparing the purity of commercially available synthetic phosphatidylcholines PC 16:0/18:1 and PC 18:1/16:0 measured in this study with other reports using alternative mass spectrometric methods. It should be noted that batch-to-batch variation in synthetic preparations may also give rise to some variation in these measurements.

Reference	**Citation**	**Method**	**% Alternate isomer in PC 16:0/18:1** (synthetic impurity)	**% Alternate isomer in PC 18:1/16:0** (synthetic impurity)
This study Ref[116]	Kozlowski *et al. Scientific Reports.* **2015**	DESI-CID/OzID	20%	2%
Ref[149]	Maccarone *et al. J. Lipid Res.* **2014**, *55*, 1668-1677	ion-mobility separation	13%	1%
Ref[149]	Maccarone *et al. J. Lipid Res.* **2014**, *55*, 1668-1677	PLA_2 enzyme assay	13%	3%
Ref[149]	Maccarone *et al. J. Lipid Res.* **2014**, *55*, 1668-1677	CID/OzID	17%	4%
Ref[102]	Pham *et al. Analyst.* **2014**, *139*, 204-214	CID/OzID	17%	3%
Ref[102]	Pham *et al. Analyst.* **2014**, *139*, 204-214	CID (+ve and -ve ion modes)	21-23%	10-16%
Ref[99]	Ekroos *et al. J. Lipid Res.* **2003**, *44*, 2181-2192	CID (-ve ion mode)	17%	7%

REFERENCES

1. Kozlowski, R.L., *Determination of a phospholipid signature for human Metabolic Syndrome using mass spectrometry-based metabolomic approaches* in *Biochemistry and Microbiology*. 2011, University of Victoria: Victoria.
2. Nagao, K. and T. Yanagita, *Bioactive lipids in metabolic syndrome.* Progress in Lipid Research, 2008. **47**(2): p. 127-46.
3. Spiegel, S. and A.H. Merrill, Jr., *Sphingolipid metabolism and cell growth regulation.* Faseb J, 1996. **10**(12): p. 1388-97.
4. Cui, Z. and M. Houweling, *Phosphatidylcholine and cell death.* Biochim Biophys Acta, 2002. **1585**(2-3): p. 87-96.
5. Poiichetti, E., A. Janisson, P.L. de la Porte, H. Portugal, J. Leonardi, A. Luna, P. La Droitte, and F. Chanussot, *Dietary polyenylphosphatidylcholine decreases cholesterolemia in hypercholesterolemic rabbits: role of the hepato-biliary axis.* Life Sci, 2000. **67**(21): p. 2563-76.
6. Jiang, Y., S.K. Noh, and S.I. Koo, *Egg phosphatidylcholine decreases the lymphatic absorption of cholesterol in rats.* J Nutr, 2001. **131**(9): p. 2358-63.
7. Buang, Y., Y.M. Wang, J.Y. Cha, K. Nagao, and T. Yanagita, *Dietary phosphatidylcholine alleviates fatty liver induced by orotic acid.* Nutrition, 2005. **21**(7-8): p. 867-73.
8. Murata, M., K. Imaizumi, and M. Sugano, *Effect of dietary phospholipids and their constituent bases on serum lipids and apolipoproteins in rats.* J Nutr, 1982. **112**(9): p. 1805-8.
9. Imaizumi, K., K. Mawatari, M. Murata, I. Ikeda, and M. Sugano, *The contrasting effect of dietary phosphatidylethanolamine and phosphatidylcholine on serum lipoproteins and liver lipids in rats.* J Nutr, 1983. **113**(12): p. 2403-11.
10. Stamler, C.J., D. Breznan, T.A. Neville, F.J. Viau, E. Camlioglu, and D.L. Sparks, *Phosphatidylinositol promotes cholesterol transport in vivo.* J Lipid Res, 2000. **41**(8): p. 1214-21.
11. Burgess, J.W., T.A. Neville, P. Rouillard, Z. Harder, D.S. Beanlands, and D.L. Sparks, *Phosphatidylinositol increases HDL-C levels in humans.* J Lipid Res, 2005. **46**(2): p. 350-5.
12. Liu, S., J.D. Brown, K.J. Stanya, E. Homan, M. Leidl, K. Inouye, P. Bhargava, M.R. Gangl, L. Dai, B. Hatano, G.S. Hotamisligil, A. Saghatelian, J. Plutzky, and C.H. Lee, *A diurnal serum lipid integrates hepatic lipogenesis and peripheral fatty acid use.* Nature, 2013. **502**(7472): p. 550-4.
13. Liebisch, G., J.A. Vizcaino, H. Kofeler, M. Trotzmuller, W.J. Griffiths, G. Schmitz, F. Spener, and M.J. Wakelam, *Shorthand notation for lipid structures derived from mass spectrometry.* J Lipid Res, 2013. **54**(6): p. 1523-30.
14. Hirschmann, H., P. Karlson, W. Stoffel, F. Snyder, S. Veibel, and F. Vogtle. *Nomenclature of Lipids.* Recommendations, 1976 1976; Available from: http://www.chem.qmul.ac.uk/iupac/lipid/.
15. *The nomenclature of lipids (Recommendations 1976) IUPAC-IUB Commission on Biochemical Nomenclature.* Biochem J, 1978. **171**(1): p. 21-35.

16. Ekroos, K., *Lipidomics Perspective: From Molecular Lipidomics to Validated Clinical Diagnostics*, in *Lipidomics*. 2012, Wiley-VCH Verlag GmbH & Co. KGaA. p. 1-19.
17. Shevchenko, A. and K. Simons, *Lipidomics: coming to grips with lipid diversity.* Nat Rev Mol Cell Biol, 2010. **11**(8): p. 593-8.
18. Bouley, H., *Nouveau dictionnaire lexicographique et descriptif des Sciences médicales et vétérinaires*. 1851, Paris, Labé.
19. Long, J.H., *A text-book of physiological chemistry for students of medicine*. 1909: P. Blakiston's Son.
20. MacLean, H., *Lecithin and allied substances, the lipins*. 1918: Longmans, Green.
21. Working, E.B. and A.C. Andrews, *The Structure of the Phospholipids.* Chemical Reviews, 1941. **29**(2): p. 245-256.
22. Folch, J. and H.A. Schneider, *An amino acid constituent of ox brain cephalin.* J Biol Chem, 1941. **137**(1): p. 51-62.
23. Hilditch, T.P., *The chemical constitution of natural fats*. 1956: Wiley.
24. Fischgold, H. and E. Chain, *The spontaneous decomposition of lecithin and its bearing on the determination of the isoelectric point.* Biochem J, 1934. **28**(6): p. 2044-51.
25. Grün, A. and R. Limpächer, *Synthese der Lecithine. (2. Mitteilung.).* Berichte der deutschen chemischen Gesellschaft (A and B Series), 1927. **60**(1): p. 147-150.
26. Baer, E., *On the Crystallization, Structure and Infrared Spectra of Saturated L-α-Lecithins.* Journal of the American Chemical Society, 1953. **75**(3): p. 621-623.
27. Baer, E. and M. Kates, *Synthesis of Enantiomeric α-Lecithins.* Journal of the American Chemical Society, 1950. **72**(2): p. 942-949.
28. Baer, E. and M. Kates, *Migration During Hydrolysis of Esters of Glycerophosphoric Acid II. The Acid and Alkaline Hydrolysis of l-α-Lecithins.* J Biol Chem, 1950. **185**(2): p. 615-623.
29. Baer, E. and N.Z. Stanacev, *Phosphonolipids I. Synthesis of a Phosphonic Acid Analogue of Cephalin.* J Biol Chem, 1964. **239**(10): p. 3209-3214.
30. Ansell, G.B., J.N. Hawthorne, and R.M.C. Dawson, *Form and function of phospholipids*. 1973: Elsevier Scientific Publishing Co.
31. Pearson, R.H. and I. Pascher, *The molecular structure of lecithin dihydrate.* Nature, 1979. **281**(5731): p. 499-501.
32. Levene, P. and I.P. Rolf, *Lysolecithins and lysocephalins.* J Biol Chem, 1923. **55**(4): p. 743-749.
33. Bloor, W.R., *Distribution of Unsaturated Fatty Acids in Tissues: I. Beef Heart Muscle.* J Biol Chem, 1926. **68**(1): p. 33-56.
34. Nunn, L.C.A. and I. Smedley-Maclean, *The nature of the fatty acids stored by the liver in the fat-deficiency disease of rats.* Biochem J, 1938. **32**(12): p. 2178.
35. Wesson, L.G., *The Isolation of Arachidonic Acid from Brain Tissue.* J Biol Chem, 1924. **60**(1): p. 183-187.
36. Kyes, P., *Uber die Lecithide des Schlangengiftes*, in *Biochemische Zeitschrift*. 1907, J. Springer.
37. Noguchi, H., *Snake Venoms: An investigation of venomous snakes with special reference to the phenomena of their venoms*. Vol. 111. 1909.

38. Willstätter, R. and K. Lüdecke, *Zur Kenntniss des Lecithins.* Berichte der deutschen chemischen Gesellschaft, 1904. **37**(3): p. 3753-3758.
39. Tattrie, N., *Positional distribution of saturated and unsaturated fatty acids on egg lecithin.* Journal of Lipid Research, 1959. **1**(1): p. 60-65.
40. de Haas, G.H., I. Mulder, and L.L.M. van Deenen, *On the specificity of phospholipase A.* Biochem Biophys Res Commun, 1960. **3**: p. 287-91.
41. van Deenen, L.L.M. and G.H. de Haas, *The Substrate Specificity of Phospholipase A.* Biochim Biophys Acta, 1963. **70**: p. 538-53.
42. Kuchmak, M. and L.R. Dugan, Jr., *Composition and Positional Distribution of Fatty Acids in Phospholipids Isolated from Pork Muscle Tissues.* Journal of the American Oil Chemists Society, 1965. **42**: p. 45-8.
43. Haverkate, F. and L.L. van Deenen, *Isolation and chemical characterization of phosphatidyl glycerol from spinach leaves.* Biochim Biophys Acta, 1965. **106**(1): p. 78-92.
44. Blomstrand, R., *The positional distribution of fatty acids in triglycerides and lecithins of human chylomicrons.* Acta Chem Scand, 1965. **19**(7): p. 1778-80.
45. Brockerhoff, H. and R.G. Ackman, *Positional distribution of isomers of monoenoic fatty acids in animal glycerolipids.* J Lipid Res, 1967. **8**(6): p. 661-6.
46. Hildebrand, J.G. and J.H. Law, *Fatty Acid Distribution in Bacterial Phospholipids. The Specificity of the Cyclopropane Synthetase Reaction.* Biochemistry, 1964. **3**: p. 1304-8.
47. van Golde, L.M., W.A. Pieterson, and L.L. van Deenen, *Alterations in the molecular species of rat liver lecithin by corn-oil feeding to essential fatty acid-deficient rats as a function of time.* Biochim Biophys Acta, 1968. **152**(1): p. 84-95.
48. Devor, K.A. and J.B. Mudd, *Structural analysis of phosphatidylcholine of plant tissue.* J Lipid Res, 1971. **12**(4): p. 396-402.
49. Vijayalakshmi, B. and S.V. Rao, *Positional distribution of fatty acids in oilseed lecithins.* Fette, Seifen, Anstrichmittel, 1972. **74**(7): p. 404-406.
50. Stern, W. and M. Pullman, *Acyl-CoA: sn-glycerol-3-phosphate acyltransferase and the positional distribution of fatty acids in phospholipids of cultured cells.* J Biol Chem, 1978. **253**(22): p. 8047-8055.
51. Rottem, S. and O. Markowitz, *Membrane lipids of Mycoplasma gallisepticum: a disaturated phosphatidylcholine and a phosphatidylglycerol with an unusual positional distribution of fatty acids.* Biochemistry, 1979. **18**(14): p. 2930-2935.
52. Moore, C.E. and G.A. Dhopeshwarkar, *Positional specificity of trans fatty acids in fetal lecithin.* Lipids, 1981. **16**(7): p. 479-84.
53. Murata, N., N. Sato, N. Takahashi, and Y. Hamazaki, *Compositions and positional distributions of fatty acids in phospholipids from leaves of chilling-sensitive and chilling-resistant plants.* Plant and Cell Physiology, 1982. **23**(6): p. 1071-1079.
54. Wiegand, R.D. and R.E. Anderson, *Phospholipid molecular species of frog rod outer segment membranes.* Exp Eye Res, 1983. **37**(2): p. 159-73.
55. Nelson, D.L., A.L. Lehninger, and M.M. Cox, *Lehninger Principles of Biochemistry.* 2008: W. H. Freeman.
56. Martinez-Seara, H., T. Róg, M. Karttunen, I. Vattulainen, and R. Reigada, *Why is the sn-2 Chain of Monounsaturated Glycerophospholipids Usually Unsaturated*

whereas the sn-1 Chain Is Saturated? Studies of 1-Stearoyl-2-oleoyl-sn-glycero-3-phosphatidylcholine (SOPC) and 1-Oleoyl-2-stearoyl-sn-glycero-3-phosphatidylcholine (OSPC) Membranes with and without Cholesterol. The Journal of Physical Chemistry B, 2009. **113**(24): p. 8347-8356.

57. Okuyama, H., T. Kankura, and S. Nojima, *Positional distribution of fatty acids in phospholipids from Mycobacteria.* J Biochem, 1967. **61**(6): p. 732-7.
58. Mukhamedova, K.S. and A.I. Glushenkova, *Molecular composition of soybean phospholipids.* Chemistry of Natural Compounds, 1997. **33**(6): p. 693-694.
59. Connor, W.E., D.S. Lin, G. Thomas, F. Ey, T. DeLoughery, and N. Zhu, *Abnormal phospholipid molecular species of erythrocytes in sickle cell anemia.* J Lipid Res, 1997. **38**(12): p. 2516-28.
60. Subbaiah, P.V., I.G. Gould, S. Lal, and B. Aizezi, *Incorporation profiles of conjugated linoleic acid isomers in cell membranes and their positional distribution in phospholipids.* Biochim Biophys Acta, 2011. **1811**(1): p. 17-24.
61. Kuksis, A. and L. Marai, *Determination of the complete structure of natural lecithins.* Lipids, 1967. **2**(3): p. 217-224.
62. Takamura, H., H. Kasai, H. Arita, and M. Kito, *Phospholipid molecular species in human umbilical artery and vein endothelial cells.* J Lipid Res, 1990. **31**(4): p. 709-17.
63. Kerwin, J.L., A.R. Tuininga, and L.H. Ericsson, *Identification of molecular species of glycerophospholipids and sphingomyelin using electrospray mass spectrometry.* J Lipid Res, 1994. **35**(6): p. 1102-14.
64. Wang, D.Y., Y.Z. Zhu, and W.M. Xu, *Comparative study of intramuscular phospholipid molecular species in tradition Chinese duck meat products.* Asian-Australasian journal of animal sciences, 2009. **22**(10): p. 1441-1446.
65. Bernhard, W., A.D. Postle, M. Linck, and K.F. Sewing, *Composition of phospholipid classes and phosphatidylcholine molecular species of gastric mucosa and mucus.* Biochim Biophys Acta, 1995. **1255**(2): p. 99-104.
66. Postle, A.D., M.D. Al, G.C. Burdge, and G. Hornstra, *The composition of individual molecular species of plasma phosphatidylcholine in human pregnancy.* Early Hum Dev, 1995. **43**(1): p. 47-58.
67. Salas, J.J., E. Martinez-Force, and R. Garces, *Phospholipid molecular profiles in the seed kernel from different sunflower (Helianthus annuus) mutants.* Lipids, 2006. **41**(8): p. 805-11.
68. Delton-Vandenbroucke, I., M.B. Maude, H. Chen, G.D. Aguirre, G.M. Acland, and R.E. Anderson, *Effect of diet on the fatty acid and molecular species composition of dog retina phospholipids.* Lipids, 1998. **33**(12): p. 1187-93.
69. Cherian, G., *Egg yolk conjugated linoleic acid alters phospholipid molecular species in chick tissues.* European Journal of Lipid Science and Technology, 2009. **111**(6): p. 546-552.
70. Pacetti, D., P. Lucci, E. Boselli, and N.G. Frega, *Effect of antioxidant-enriched foods on plasma: Phospholipid molecular species composition.* European Journal of Lipid Science and Technology, 2009. **111**(12): p. 1201-1211.
71. Han, X., R.A. Gubitosi-Klug, B.J. Collins, and R.W. Gross, *Alterations in individual molecular species of human platelet phospholipids during thrombin stimulation: electrospray ionization mass spectrometry-facilitated identification of the*

boundary conditions for the magnitude and selectivity of thrombin-induced platelet phospholipid hydrolysis. Biochemistry, 1996. **35**(18): p. 5822-32.
72. de Kroon, A.I., *Metabolism of phosphatidylcholine and its implications for lipid acyl chain composition in Saccharomyces cerevisiae.* Biochim Biophys Acta, 2007. **1771**(3): p. 343-52.
73. Wagner, S. and F. Paltauf, *Generation of glycerophospholipid molecular species in the yeast Saccharomyces cerevisiae. Fatty acid pattern of phospholipid classes and selective acyl turnover at sn-1 and sn-2 positions.* Yeast, 1994. **10**(11): p. 1429-1437.
74. Ansell, G.G.B. and J.J.N. Hawthorne, *Phospholipids.* Vol. 4. 1982: Access Online via Elsevier.
75. Moser, M., D. Marsh, P. Meier, K.H. Wassmer, and G. Kothe, *Chain configuration and flexibility gradient in phospholipid membranes. Comparison between spin-label electron spin resonance and deuteron nuclear magnetic resonance, and identification of new conformations.* Biophysical Journal, 1989. **55**(1): p. 111-123.
76. Salnikov, E.S., A.J. Mason, and B. Bechinger, *Membrane order perturbation in the presence of antimicrobial peptides by< sup> 2</sup> H solid-state NMR spectroscopy.* Biochimie, 2009. **91**(6): p. 734-743.
77. Leftin, A. and M.F. Brown, *An NMR database for simulations of membrane dynamics.* Biochim Biophys Acta, 2011. **1808**(3): p. 818-839.
78. Huang, C.-h., *Mixed-chain phospholipids: structures and chain-melting behavior.* Lipids, 2001. **36**(10): p. 1077-1097.
79. Pulfer, M. and R.C. Murphy, *Electrospray mass spectrometry of phospholipids.* Mass Spectrometry Reviews, 2003. **22**(5): p. 332-364.
80. Blanksby, S.J. and T.W. Mitchell, *Advances in mass spectrometry for lipidomics.* Annu Rev Anal Chem (Palo Alto Calif), 2010. **3**: p. 433-65.
81. Cui, Z. and M.J. Thomas, *Phospholipid profiling by tandem mass spectrometry.* Journal of Chromatography B, 2009. **877**(26): p. 2709-2715.
82. Ecker, J., *Profiling eicosanoids and phospholipids using LC-MS/MS: Principles and recent applications.* J Sep Sci, 2012. **35**(10-11): p. 1227-1235.
83. Guo, X. and E. Lankmayr, *Multidimensional approaches in LC and MS for phospholipid bioanalysis.* Bioanalysis, 2010. **2**(6): p. 1109-1123.
84. Postle, A.D., D.C. Wilton, A.N. Hunt, and G.S. Attard, *Probing phospholipid dynamics by electrospray ionisation mass spectrometry.* Progress in Lipid Research, 2007. **46**(3–4): p. 200-224.
85. Hunt, A.N. and A.D. Postle, *Mass spectrometry determination of endonuclear phospholipid composition and dynamics.* Methods, 2006. **39**(2): p. 104-111.
86. Sparvero, L.J., A.A. Amoscato, C.E. Dixon, J.B. Long, P.M. Kochanek, B.R. Pitt, H. Bayır, and V.E. Kagan, *Mapping of phospholipids by MALDI imaging (MALDI-MSI): realities and expectations.* Chemistry and Physics of Lipids, 2012. **165**(5): p. 545-562.
87. Schiller, J., R. Süß, J. Arnhold, B. Fuchs, J. Leßig, M. Müller, M. Petković, H. Spalteholz, O. Zschörnig, and K. Arnold, *Matrix-assisted laser desorption and ionization time-of-flight (MALDI-TOF) mass spectrometry in lipid and phospholipid research.* Progress in Lipid Research, 2004. **43**(5): p. 449-488.

88. Murphy, R.C. and S.J. Gaskell, *New Applications of Mass Spectrometry in Lipid Analysis.* J Biol Chem, 2011. **286**(29): p. 25427-25433.
89. Ivanova, P.T., S.B. Milne, D.S. Myers, and H.A. Brown, *Lipidomics: a mass spectrometry based systems level analysis of cellular lipids.* Curr Opin Chem Biol, 2009. **13**(5): p. 526-531.
90. Han, X., K. Yang, and R.W. Gross, *Multi-dimensional mass spectrometry-based shotgun lipidomics and novel strategies for lipidomic analyses.* Mass Spectrometry Reviews, 2012. **31**(1): p. 134-178.
91. Isaac, G., R. Jeannotte, S.W. Esch, and R. Welti, *New mass-spectrometry-based strategies for lipids*, in *Genetic engineering*. 2007, Springer. p. 129-157.
92. Byrdwell, W.C., *Atmospheric pressure chemical ionization mass spectrometry for analysis of lipids.* Lipids, 2001. **36**(4): p. 327-346.
93. Fuchs, B. and J. Schiller, *MALDI-TOF MS analysis of lipids from cells, tissues and body fluids*, in *Lipids in Health and Disease*. 2008, Springer. p. 541-565.
94. Fuchs, B., R. Süß, and J. Schiller, *An update of MALDI-TOF mass spectrometry in lipid research.* Progress in Lipid Research, 2010. **49**(4): p. 450-475.
95. Holčapek, M., R. Jirásko, and M. Lísa, *Recent developments in liquid chromatography–mass spectrometry and related techniques.* Journal of Chromatography A, 2012. **1259**: p. 3-15.
96. Patton, G.M. and S.J. Robins, *Separation and Quantitation of Phospholipid Classes by HPLC*, in *Lipoprotein Protocols*, J. Ordovas, Editor. 1998, Humana Press. p. 193-215.
97. Clejan, S., *HPLC Analytical Methods for the Separation of Molecular Species of Fatty Acids in Diacylglycerol and Cellular Phospholipids*, in *Phospholipid Signaling Protocols*, I. Bird, Editor. 1998, Humana Press. p. 255-274.
98. Ketola, R.A. and T. Mauriala, *Mass spectrometric tools for cell and tissue studies.* European Journal of Pharmaceutical Sciences, 2012. **46**(5): p. 293-314.
99. Ekroos, K., C.S. Ejsing, U. Bahr, M. Karas, K. Simons, and A. Shevchenko, *Charting molecular composition of phosphatidylcholines by fatty acid scanning and ion trap MS3 fragmentation.* J Lipid Res, 2003. **44**(11): p. 2181-92.
100. Huang, L.Q., A. Paiva, H. Tong, S.J. Monson, and M.L. Gross, *Application of gas chromatography high-resolution mass spectrometry to the determination of trace monobromopolychlorodibenzo-p-dioxins in environmental samples.* J Am Soc Mass Spectrom, 1992. **3**(3): p. 248-59.
101. Smith, J.C., W. Hou, S.N. Whitehead, M. Ethier, S.A. Bennett, and D. Figeys, *Identification of lysophosphatidylcholine (LPC) and platelet activating factor (PAF) from PC12 cells and mouse cortex using liquid chromatography/multi-stage mass spectrometry (LC/MS3).* Rapid Commun Mass Spectrom, 2008. **22**(22): p. 3579-87.
102. Pham, H.T., A. Maccarone, M.C. Thomas, J.L. Campbell, T.W. Mitchell, and S. Blanksby, *Structural characterization of glycerophospholipids by combinations of ozone- and collision-induced dissociation mass spectrometry: The next step towards "top-down" lipidomics.* Analyst, 2014.
103. Mitchell, T.W., S.H.J. Brown, and S.J. Blanksby, *Structural Lipidomics*, in *Lipidomics*. 2012, Wiley-VCH Verlag GmbH & Co. KGaA. p. 99-128.

104. Chughtai, K. and R.M. Heeren, *Mass spectrometric imaging for biomedical tissue analysis.* Chemical Reviews, 2010. **110**(5): p. 3237-3277.
105. Svatoš, A., *Mass spectrometric imaging of small molecules.* Trends in biotechnology, 2010. **28**(8): p. 425-434.
106. Ellis, S.R., S.H. Brown, M. in het Panhuis, S.J. Blanksby, and T.W. Mitchell, *Surface analysis of lipids by mass spectrometry: More than just imaging.* Progress in Lipid Research, 2013. **52**(4): p. 329-353.
107. Amstalden van Hove, E.R., D.F. Smith, and R.M.A. Heeren, *A concise review of mass spectrometry imaging.* Journal of Chromatography A, 2010. **1217**(25): p. 3946-3954.
108. Lanni, E.J., S.S. Rubakhin, and J.V. Sweedler, *Mass spectrometry imaging and profiling of single cells.* Journal of Proteomics, 2012. **75**(16): p. 5036-5051.
109. Horn, P.J. and K.D. Chapman, *Lipidomics in situ: Insights into plant lipid metabolism from high resolution spatial maps of metabolites.* Progress in Lipid Research, 2014. **54**(0): p. 32-52.
110. Eberlin, L.S., C.R. Ferreira, A.L. Dill, D.R. Ifa, and R.G. Cooks, *Desorption electrospray ionization mass spectrometry for lipid characterization and biological tissue imaging.* Biochim Biophys Acta, 2011. **1811**(11): p. 946-960.
111. Passarelli, M.K. and N. Winograd, *Lipid imaging with time-of-flight secondary ion mass spectrometry (ToF-SIMS).* Biochim Biophys Acta, 2011. **1811**(11): p. 976-990.
112. Goto-Inoue, N., T. Hayasaka, N. Zaima, and M. Setou, *Imaging mass spectrometry for lipidomics.* Biochim Biophys Acta, 2011. **1811**(11): p. 961-969.
113. Ye, H., T. Greer, and L. Li, *From pixel to voxel: a deeper view of biological tissue by 3D mass spectral imaging.* Bioanalysis, 2011. **3**(3): p. 313-332.
114. Kozlowski, R.L., J.L. Campbell, T.W. Mitchell, and S.J. Blanksby, *Combining liquid chromatography with ozone-induced dissociation for the separation and identification of phosphatidylcholine double bond isomers.* Analytical and Bioanalytical Chemistry, 2015: p. 1-12.
115. Kozlowski, R.L., T.W. Mitchell, and S.J. Blanksby, *Separation and identification of phosphatidylcholine regioisomers by combining liquid chromatography with a fusion of collision and ozone-induced dissociation.* European Journal of Mass Spectrometry, 2015. **21**: p. 0-0.
116. Kozlowski, R.L., T.W. Mitchell, and S.J. Blanksby, *A rapid ambient ionization-mass spectrometric method to elucidate variations in the relative abundance of isomeric glycerophospholipids.* Scientific Reports, Forthcoming 2015.
117. Minakami, R., Y. Maehara, S. Kamakura, O. Kumano, K. Miyano, and H. Sumimoto, *Membrane phospholipid metabolism during phagocytosis in human neutrophils.* Genes Cells, 2010. **15**(5): p. 409-24.
118. Hughes, P.J. and R.H. Michell, *Novel inositol containing phospholipids and phosphates: their synthesis and possible new roles in cellular signalling.* Curr Opin Neurobiol, 1993. **3**(3): p. 383-400.
119. Bo, T. and J. Pawliszyn, *Protein thermal stability and phospholipid-protein interaction investigated by capillary isoelectric focusing with whole column imaging detection.* J Sep Sci, 2006. **29**(7): p. 1018-25.

120. Berkowitz, M.L. and R. Vacha, *Aqueous solutions at the interface with phospholipid bilayers.* Acc Chem Res, 2012. **45**(1): p. 74-82.
121. Schroit, A.J. and R. Gallily, *Macrophage fatty acid composition and phagocytosis: effect of unsaturation on cellular phagocytic activity.* Immunology, 1979. **36**(2): p. 199-205.
122. de Jonge, H.W., D.H. Dekkers, E.M. Bastiaanse, K. Bezstarosti, A. van der Laarse, and J.M. Lamers, *Eicosapentaenoic acid incorporation in membrane phospholipids modulates receptor-mediated phospholipase C and membrane fluidity in rat ventricular myocytes in culture.* J Mol Cell Cardiol, 1996. **28**(5): p. 1097-108.
123. Zeng, Y., X. Han, and R.W. Gross, *Phospholipid subclass specific alterations in the passive ion permeability of membrane bilayers: separation of enthalpic and entropic contributions to transbilayer ion flux.* Biochemistry, 1998. **37**(8): p. 2346-55.
124. Brouwers, J.F., *Liquid chromatographic-mass spectrometric analysis of phospholipids. Chromatography, ionization and quantification.* Biochim Biophys Acta, 2011. **1811**(11): p. 763-75.
125. Sandra, K. and P. Sandra, *Lipidomics from an analytical perspective.* Curr Opin Chem Biol, 2013. **17**(5): p. 847-53.
126. Nikolova-Damyanova, B., *Retention of lipids in silver ion high-performance liquid chromatography: facts and assumptions.* Journal of Chromatography A, 2009. **1216**(10): p. 1815-24.
127. Dobson, G., W.W. Christie, and B. Nikolova-Damyanova, *Silver ion chromatography of lipids and fatty acids.* Journal of Chromatography B, 1995. **671**(1–2): p. 197-222.
128. Marmer, W.N., T.A. Foglia, and P.D. Vail, *HPLC of plasmalogen-containing phosphatidylcholine under reverse-phase or argentation conditions.* Lipids, 1984. **19**(5): p. 353-8.
129. Beckman, B.S., C. Mallia, and S. Clejan, *Molecular species of phospholipids in a murine stem-cell line responsive to erythropoietin.* Biochem J, 1996. **314 (Pt 3)**: p. 861-7.
130. Chen, S., N.A. Belikova, and P.V. Subbaiah, *Structural elucidation of molecular species of pacific oyster ether amino phospholipids by normal-phase liquid chromatography/negative-ion electrospray ionization and quadrupole/multiple-stage linear ion-trap mass spectrometry.* Analytica Chimica Acta, 2012. **735**(0): p. 76-89.
131. Retra, K., O.B. Bleijerveld, R.A. van Gestel, A.G. Tielens, J.J. van Hellemond, and J.F. Brouwers, *A simple and universal method for the separation and identification of phospholipid molecular species.* Rapid Commun Mass Spectrom, 2008. **22**(12): p. 1853-62.
132. Zahradnickova, H., A. Tomcala, P. Berkova, I. Schneedorferova, J. Okrouhlik, P. Simek, and M. Hodkova, *Cost effective, robust, and reliable coupled separation techniques for the identification and quantification of phospholipids in complex biological matrices: application to insects.* J Sep Sci, 2014. **37**(15): p. 2062-8.
133. Lin, J.-T., T.A. McKeon, C.L. Woodruff, and J.A. Singleton, *Separation of synthetic phosphatidylcholine molecular species by high-performance liquid*

chromatography on a C8 column. Journal of Chromatography A, 1998. **824**(2): p. 169-174.
134. Damen, C.W., G. Isaac, J. Langridge, T. Hankemeier, and R.J. Vreeken, *Enhanced lipid isomer separation in human plasma using reversed-phase UPLC with ion-mobility/high-resolution MS detection.* J Lipid Res, 2014. **55**(8): p. 1772-1783.
135. Brouwers, J.F., C. Versluis, L.M. van Golde, and A.G. Tielens, *5-Octadecenoic acid: evidence for a novel type of fatty acid modification in schistosomes.* Biochem J, 1998. **334**(2): p. 315-319.
136. Mitchell, T.W., H. Pham, M.C. Thomas, and S.J. Blanksby, *Identification of double bond position in lipids: from GC to OzID.* Journal of Chromatography B 2009. **877**(26): p. 2722-35.
137. Sun, C., Y.Y. Zhao, and J.M. Curtis, *The direct determination of double bond positions in lipid mixtures by liquid chromatography/in-line ozonolysis/mass spectrometry.* Anal Chim Acta, 2013. **762**: p. 68-75.
138. Sun, C., Y.-Y. Zhao, and J.M. Curtis, *Elucidation of phosphatidylcholine isomers using two dimensional liquid chromatography coupled in-line with ozonolysis mass spectrometry.* Journal of Chromatography A, 2014. **1351**(0): p. 37-45.
139. Thomas, M.C., T.W. Mitchell, D.G. Harman, J.M. Deeley, J.R. Nealon, and S.J. Blanksby, *Ozone-Induced Dissociation: Elucidation of Double Bond Position within Mass-Selected Lipid Ions.* Analytical Chemistry, 2008. **80**(1): p. 303-311.
140. Poad, B.L.J., H.T. Pham, M.C. Thomas, J.R. Nealon, L.J. Campbell, T.W. Mitchell, and S.J. Blanksby, *Ozone-Induced Dissociation on a Modified Tandem Linear Ion-Trap: Observations of Different Reactivity for Isomeric Lipids.* J Am Soc Mass Spectrom, 2010. **21**(12): p. 1989-1999.
141. Brown, S.H., T.W. Mitchell, and S.J. Blanksby, *Analysis of unsaturated lipids by ozone-induced dissociation.* Biochim Biophys Acta, 2011. **1811**(11): p. 807-17.
142. Deeley, J.M., T.W. Mitchell, X. Wei, J. Korth, J.R. Nealon, S.J. Blanksby, and R.J. Truscott, *Human lens lipids differ markedly from those of commonly used experimental animals.* Biochim Biophys Acta, 2009. **1781**(6-7): p. 288-98.
143. Chin, J.S., S.R. Ellis, H.T. Pham, S.J. Blanksby, K. Mori, Q.L. Koh, W.J. Etges, and J.Y. Yew, *Sex-specific triacylglycerides are widely conserved in Drosophila and mediate mating behavior.* Elife, 2014. **3**: p. e01751.
144. Stahlman, M., H.T. Pham, M. Adiels, T.W. Mitchell, S.J. Blanksby, B. Fagerberg, K. Ekroos, and J. Boren, *Clinical dyslipidaemia is associated with changes in the lipid composition and inflammatory properties of apolipoprotein-B-containing lipoproteins from women with type 2 diabetes.* Diabetologia, 2012. **55**(4): p. 1156-66.
145. Folch, J., M. Lees, and G.H. Sloane Stanley, *A simple method for the isolation and purification of total lipides from animal tissues.* J Biol Chem, 1957. **226**(1): p. 497-509.
146. Fahy, E., S. Subramaniam, R.C. Murphy, M. Nishijima, C.R. Raetz, T. Shimizu, F. Spener, G. van Meer, M.J. Wakelam, and E.A. Dennis, *Update of the LIPID MAPS comprehensive classification system for lipids.* Journal of Lipid Research, 2009. **50**(Supplement): p. S9-S14.
147. Pham, H.T., A.T. Maccarone, J.L. Campbell, T.W. Mitchell, and S.J. Blanksby, *Ozone-induced dissociation of conjugated lipids reveals significant reaction rate*

enhancements and characteristic odd-electron product ions. J Am Soc Mass Spectrom, 2013. **24**(2): p. 286-296.
148. Hsu, F.F. and J. Turk, *Electrospray ionization/tandem quadrupole mass spectrometric studies on phosphatidylcholines: the fragmentation processes.* J Am Soc Mass Spectrom, 2003. **14**(4): p. 352-63.
149. Maccarone, A., J. Duldig, T. Mitchell, S. Blanksby, E. Duchoslav, and J. Campbell, *Characterization of acyl chain position in unsaturated phosphatidylcholines using differential mobility-mass spectrometry.* Journal of Lipid Research, 2014. **55**(8): p. 1668.
150. Le Grandois, J., E. Marchioni, M. Zhao, F. Giuffrida, S. Ennahar, and F. Bindler, *Investigation of natural phosphatidylcholine sources: separation and identification by liquid chromatography-electrospray ionization-tandem mass spectrometry (LC-ESI-MS2) of molecular species.* J Agric Food Chem, 2009. **57**(14): p. 6014-20.
151. Nealon, J.R., S.J. Blanksby, T.W. Mitchell, and P.L. Else, *Systematic differences in membrane acyl composition associated with varying body mass in mammals occur in all phospholipid classes: an analysis of kidney and brain.* J Exp Biol, 2008. **211**(Pt 19): p. 3195-204.
152. Bird, S.S., V.R. Marur, I.G. Stavrovskaya, and B.S. Kristal, *Separation of cis-trans phospholipid isomers using reversed phase LC with high resolution MS detection.* Anal Chem, 2012. **84**(13): p. 5509-17.
153. Nakanishi, H., Y. Iida, T. Shimizu, and R. Taguchi, *Separation and quantification of sn-1 and sn-2 fatty acid positional isomers in phosphatidylcholine by RPLC-ESIMS/MS.* J Biochem, 2010. **147**(2): p. 245-56.
154. Kliman, M., J.C. May, and J.A. McLean, *Lipid analysis and lipidomics by structurally selective ion mobility-mass spectrometry.* Biochim Biophys Acta, 2011. **1811**(11): p. 935-45.
155. Lintonen, T.P., P.R. Baker, M. Suoniemi, B.K. Ubhi, K.M. Koistinen, E. Duchoslav, J.L. Campbell, and K. Ekroos, *Differential mobility spectrometry-driven shotgun lipidomics.* Anal Chem, 2014. **86**(19): p. 9662-9.
156. Wenk, M.R., *Lipidomics: new tools and applications.* Cell, 2010. **143**(6): p. 888-95.
157. Murphy, R.C. and P.H. Axelsen, *Mass spectrometric analysis of long-chain lipids.* Mass Spectrom Rev, 2011. **30**(4): p. 579-99.
158. Larsen, Å., E. Mokastet, E. Lundanes, and E. Hvattum, *Separation and identification of phosphatidylserine molecular species using reversed-phase high-performance liquid chromatography with evaporative light scattering and mass spectrometric detection.* Journal of Chromatography B, 2002. **774**(1): p. 115-120.
159. Uran, S., Å. Larsen, P.B. Jacobsen, and T. Skotland, *Analysis of phospholipid species in human blood using normal-phase liquid chromatography coupled with electrospray ionization ion-trap tandem mass spectrometry.* Journal of Chromatography B, 2001. **758**(2): p. 265-275.
160. Berdeaux, O., P. Juaneda, L. Martine, S. Cabaret, L. Bretillon, and N. Acar, *Identification and quantification of phosphatidylcholines containing very-long-chain polyunsaturated fatty acid in bovine and human retina using liquid*

chromatography/tandem mass spectrometry. Journal of Chromatography A, 2010. **1217**(49): p. 7738-7748.
161. Jungalwala, F.B., J.E. Evans, and R.H. McCluer, *Compositional and molecular species analysis of phospholipids by high performance liquid chromatography coupled with chemical ionization mass spectrometry.* Journal of Lipid Research, 1984. **25**(7): p. 738-49.
162. Takamura, H. and M. Kito, *A Highly Sensitive Method for Quantitative Analysis of Phospholipid Molecular Species by High-Performance Liquid Chromatography.* The Journal of Biochemistry, 1991. **109**(3): p. 436-439.
163. Taguchi, R., J. Hayakawa, Y. Takeuchi, and M. Ishida, *Two-dimensional analysis of phospholipids by capillary liquid chromatography/electrospray ionization mass spectrometry.* Journal of Mass Spectrometry, 2000. **35**(8): p. 953-966.
164. Ma, Y.C. and H.Y. Kim, *Development of the On-Line High-Performance Liquid-Chromatography Thermospray Mass Spectrometry Method for the Analysis of Phospholipid Molecular Species in Rat Brain.* Analytical Biochemistry, 1995. **226**(2): p. 293-301.
165. Castro-Perez, J., T. Roddy, N.M. Nibbering, V. Shah, D. McLaren, S. Previs, A. Attygalle, K. Herath, Z. Chen, S.-P. Wang, L. Mitnaul, B. Hubbard, R. Vreeken, D. Johns, and T. Hankemeier, *Localization of Fatty Acyl and Double Bond Positions in Phosphatidylcholines Using a Dual Stage CID Fragmentation Coupled with Ion Mobility Mass Spectrometry.* J Am Soc Mass Spectrom, 2011. **22**(9): p. 1552-1567.
166. Huang, Z.H., D.A. Gage, and C.C. Sweeley, *Characterization of Diacylglycerylphosphocholine Molecular Species by FAB-CAD-MS/MS: A General Method Not Sensitive to the Nature of the Fatty Acyl Groups.* J Am Soc Mass Spectrom, 1992. **3**(1): p. 71-8.
167. Thomas, M.C., T.W. Mitchell, and S.J. Blanksby, *OnLine ozonolysis methods for the determination of double bond position in unsaturated lipids.* Methods Mol Biol, 2009. **579**: p. 413-41.
168. Pluckthun, A. and E.A. Dennis, *Acyl and phosphoryl migration in lysophospholipids: importance in phospholipid synthesis and phospholipase specificity.* Biochemistry, 1982. **21**(8): p. 1743-1750.
169. Murphy, J.P., 3rd and R.A. Yost, *Origin of mass shifts in the quadrupole ion trap: dissociation of fragile ions observed with a hybrid ion trap/mass filter instrument.* Rapid Commun Mass Spectrom, 2000. **14**(4): p. 270-3.
170. Renaud, J.B., S. Overton, and P.M. Mayer, *Energy and entropy at play in competitive dissociations: The case of uneven positional dissociation of ionized triacylglycerides.* International Journal of Mass Spectrometry, 2013. **352**(0): p. 77-86.
171. Gurr, M.I., J.L. Harwood, and K.N. Frayn, *Lipid biochemistry.* 2002: Springer.
172. Durvasula, R.V. and C.H. Huang, *Thermotropic phase behavior of mixed-chain phosphatidylglycerols: implications for acyl chain packing in fully hydrated bilayers.* Biochim Biophys Acta, 1999. **1417**(1): p. 111-21.
173. Lin, H.N., Z.Q. Wang, and C.H. Huang, *Differential scanning calorimetry study of mixed-chain phosphatidylcholines with a common molecular weight identical*

with diheptadecanoylphosphatidylcholine. Biochemistry, 1990. **29**(30): p. 7063-72.
174. Mazari, A., S. Iwamoto, and R. Yamauchi, *Effects of Linoleic Acid Position in Phosphatidylcholines and Cholesterol Addition on Their Rates of Peroxidation in Unilamellar Liposomes.* Bioscience, Biotechnology, and Biochemistry, 2010. **74**(5): p. 1013-1017.
175. Subbaiah, P.V., M. Liu, and F. Paltauf, *Role of sn-2 acyl group of phosphatidylcholine in determining the positional specificity of lecithin-cholesterol acyltransferase.* Biochemistry, 1994. **33**(45): p. 13259-66.
176. Lambeau, G. and M.H. Gelb, *Biochemistry and physiology of mammalian secreted phospholipases A2.* Annu Rev Biochem, 2008. **77**: p. 495-520.
177. Hou, W., H. Zhou, M. Bou Khalil, D. Seebun, S.A. Bennett, and D. Figeys, *Lyso-form fragment ions facilitate the determination of stereospecificity of diacyl glycerophospholipids.* Rapid Commun Mass Spectrom, 2011. **25**(1): p. 205-17.
178. Brown, S.H., T.W. Mitchell, A.J. Oakley, H.T. Pham, and S.J. Blanksby, *Time to face the fats: what can mass spectrometry reveal about the structure of lipids and their interactions with proteins?* J Am Soc Mass Spectrom, 2012. **23**(9): p. 1441-9.
179. Cohen, S.L., *Ozone in Ambient Air as a Source of Adventitious Oxidation. A Mass Spectrometric Study.* Analytical Chemistry, 2006. **78**(13): p. 4352-4362.
180. Ellis, S.R., J.R. Hughes, T.W. Mitchell, M.i.h. Panhuis, and S.J. Blanksby, *Using ambient ozone for assignment of double bond position in unsaturated lipids.* Analyst, 2012. **137**(5): p. 1100-1110.
181. Harman, D.G. and S.J. Blanksby, *Investigation of the gas phase reactivity of the 1-adamantyl radical using a distonic radical anion approach.* Organic & Biomolecular Chemistry, 2007. **5**(21): p. 3495-3503.
182. McClellan, J.E., J.P. Murphy, 3rd, J.J. Mulholland, and R.A. Yost, *Effects of fragile ions on mass resolution and on isolation for tandem mass spectrometry in the quadrupole ion trap mass spectrometer.* Anal Chem, 2002. **74**(2): p. 402-12.
183. Lee, Y.J., D.C. Perdian, Z. Song, E.S. Yeung, and B.J. Nikolau, *Use of mass spectrometry for imaging metabolites in plants.* The Plant Journal, 2012. **70**(1): p. 81-95.
184. Sud, M., E. Fahy, D. Cotter, A. Brown, E.A. Dennis, C.K. Glass, A.H. Merrill, Jr., R.C. Murphy, C.R. Raetz, D.W. Russell, and S. Subramaniam, *LMSD: LIPID MAPS structure database.* Nucleic Acids Res, 2007. **35**(Database issue): p. D527-32.
185. Eikel, D., M. Vavrek, S. Smith, C. Bason, S. Yeh, W.A. Korfmacher, and J.D. Henion, *Liquid extraction surface analysis mass spectrometry (LESA-MS) as a novel profiling tool for drug distribution and metabolism analysis: the terfenadine example.* Rapid Commun Mass Spectrom, 2011. **25**(23): p. 3587-3596.
186. Seeley, E.H. and R.M. Caprioli, *3D Imaging by Mass Spectrometry: A New Frontier.* Analytical Chemistry, 2012. **84**(5): p. 2105-2110.
187. Gode, D. and D.A. Volmer, *Lipid imaging by mass spectrometry - a review.* Analyst, 2013. **138**(5): p. 1289-1315.
188. Römpp, A. and B. Spengler, *Mass spectrometry imaging with high resolution in mass and space.* Histochemistry and Cell Biology, 2013. **139**(6): p. 759-783.